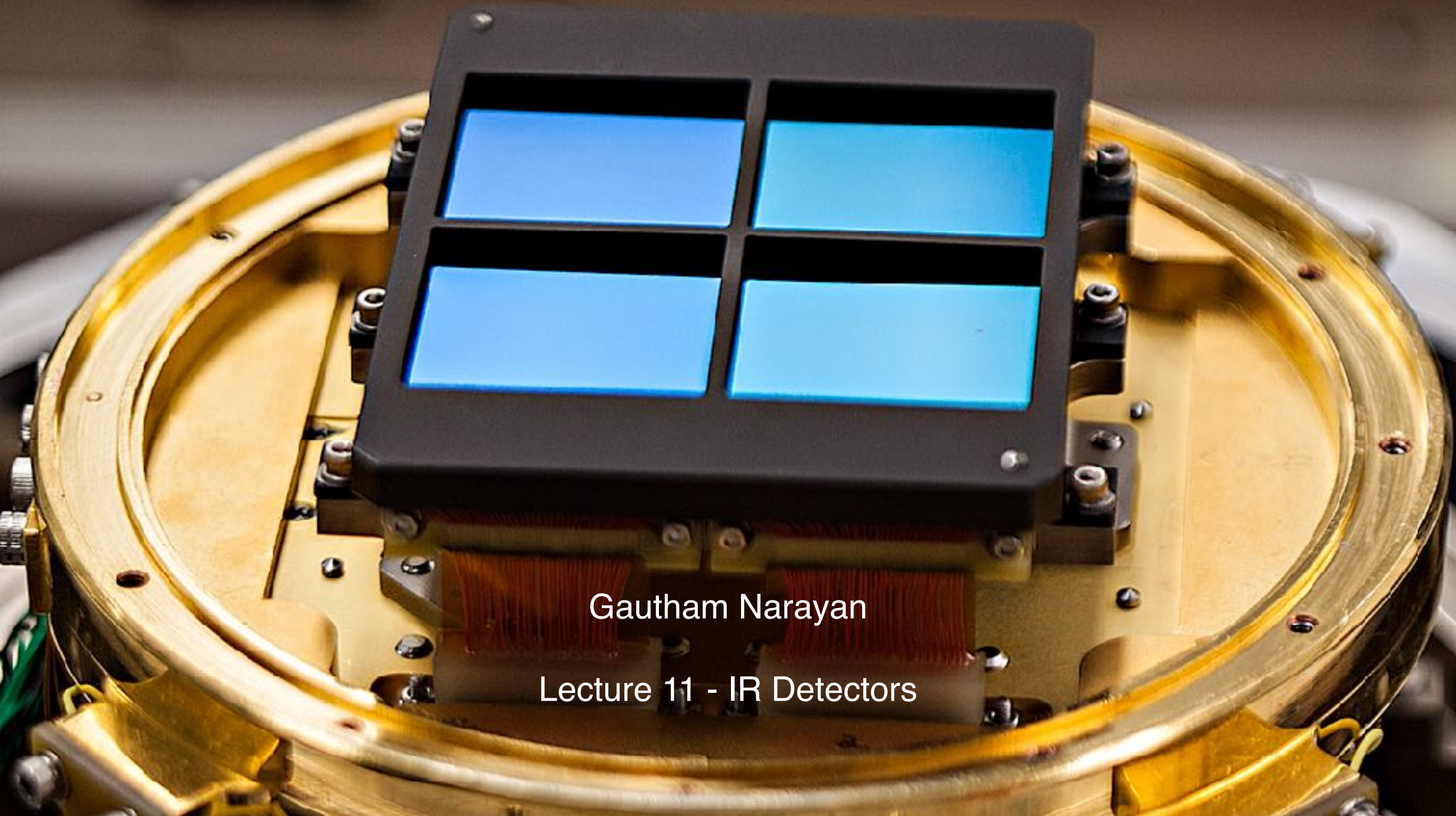


Astronomy 503

Observational Astronomy



Gautham Narayan

Lecture 11 - IR Detectors

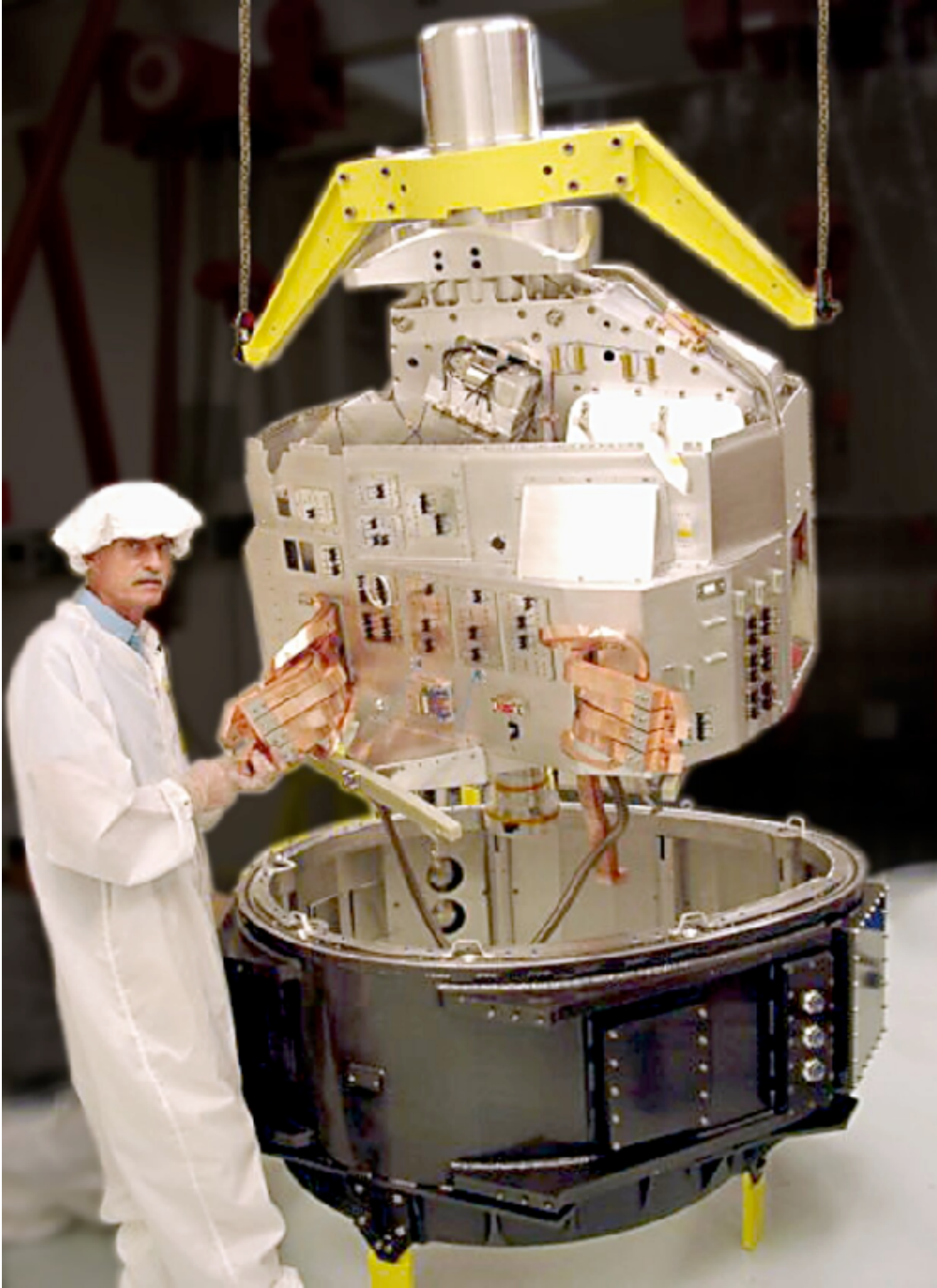
If you are planning to write a HST/WFC3/IR or JWST proposal, or anything using IR detectors, you should read G. Rieke (2006)

<https://www.annualreviews.org/content/journals/10.1146/annurev.astro.44.051905.092436>

Among other contributions, Rieke and his group discovered [ultraluminous infrared galaxies](#), the [starburst](#) phenomenon, studies of the [Galactic Center](#) as a prototypical [active galactic nucleus](#), the physical origin of the infrared emission of active galactic nuclei, planetary [debris disks](#), as well as Solar System astronomy at infrared wavelengths.^[3]

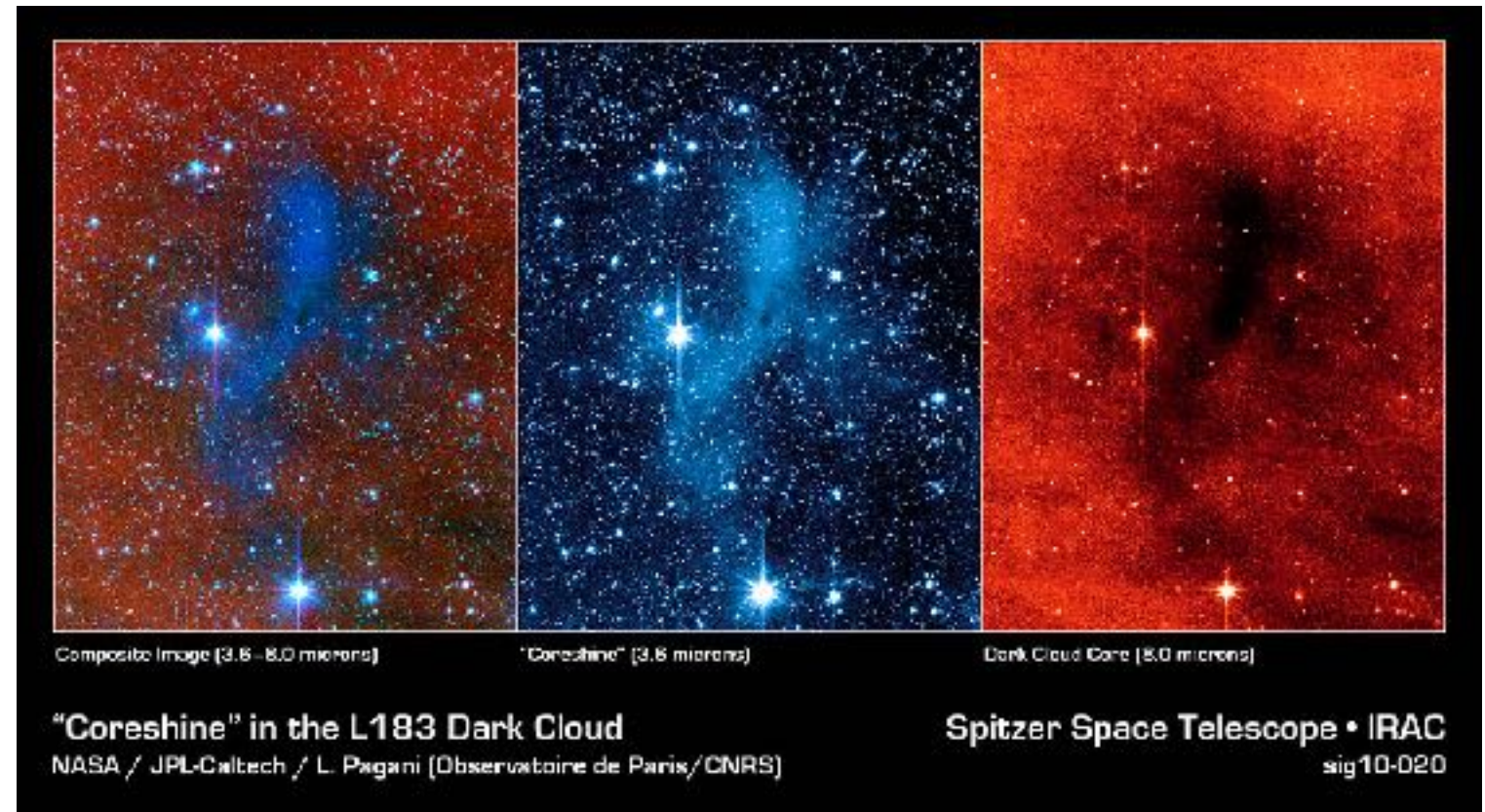
Rieke helped develop the first infrared-optimized telescope and constructed a series of state-of-the-art focal plane instruments. Rieke was involved with the [Spacelab 2 infrared telescope](#), a pioneering infrared space mission. He led the MIPS instrument team for Spitzer. The highly sensitive MIPS camera was built at [Ball Aerospace](#) under Rieke's leadership. Also, Rieke is the lead scientist on a team to produce a [Mid-Infrared Instrument](#) (MIRI) for the James Webb Space Telescope.

Also owes to an old tutorial
from Dick Joyce
at NOAO from when
I was a postdoc



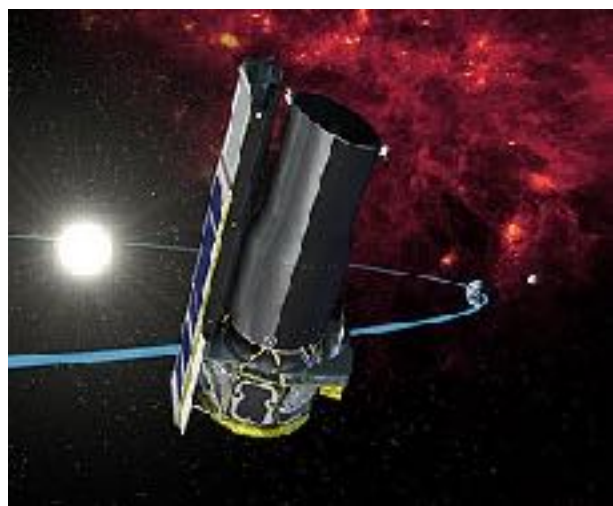
Importance of infrared astronomy

- Science applications of IR astronomy:
 - ▣ High redshift galaxies
 - ▣ Dust- and gas-enshrouded star-forming regions.
 - ▣ Sgr A* and galactic center
 - ▣ Cold interstellar matter emits in the FIR
 - ▣ Rotational and vibrational molecular transitions:
 - ISM
 - Late-type, evolved stars



Beginnings

- **1979:** 3-4 meter class telescopes dedicated to infrared astronomy, the 3.8-m United Kingdom Infrared Telescope (UKIRT) and the NASA's 3-m Infrared Telescope Facility (IRTF).
- Located on 4.2 km (14,000 ft) summit of Mauna Kea, Hawaii, an exceptional site for IR work.
- **1983:** The Anglo-American-Dutch Infrared Astronomical Satellite (IRAS) mission gave astronomers the first deep all-sky survey in IR at wavelengths of 12, 25, 60 and 100 μm , produced a point source catalog of over 245,000 sources (>100 times the number known previously).
- European project, called ISO (Infrared Space Observatory), was launched successfully in late 1995 and operated until 1998
- American project, called SIRTF (Space Infrared Telescope Facility) was delayed and then finally launched in 2003, at which time it was renamed the **Spitzer Space Telescope**.
- In the interim an infrared instrument (NICMOS) was placed into service on Hubble.

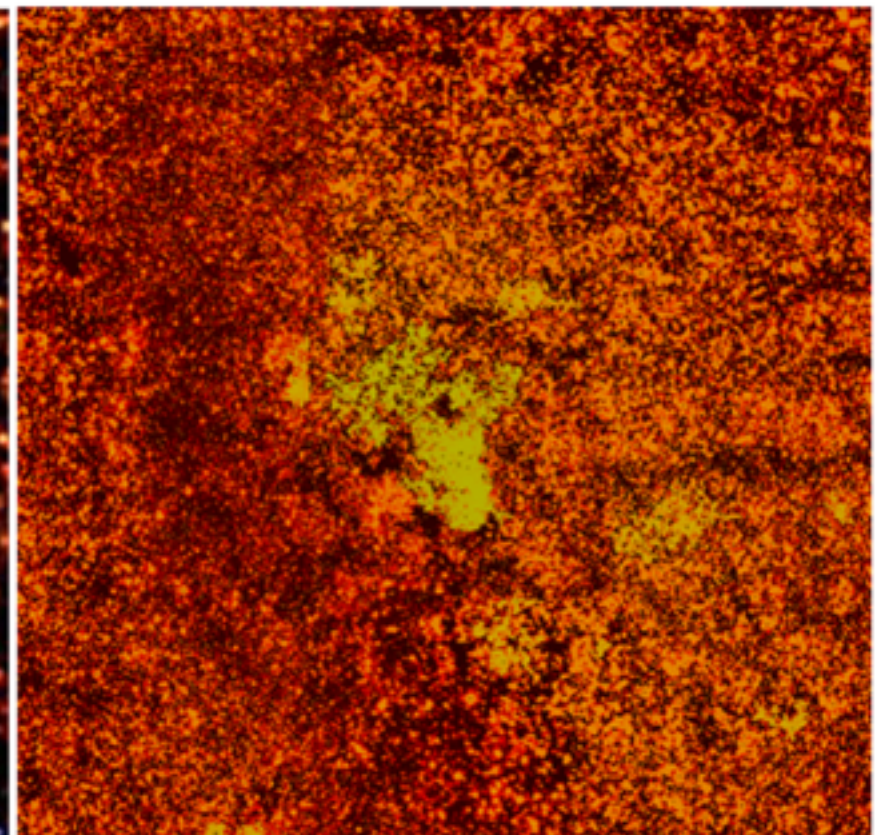
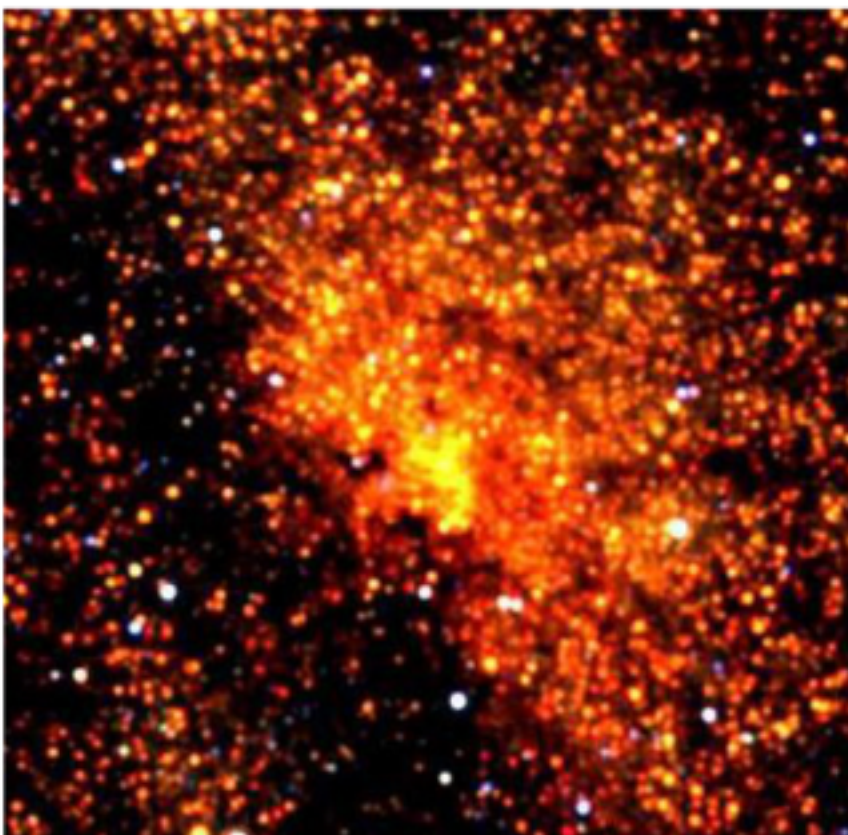
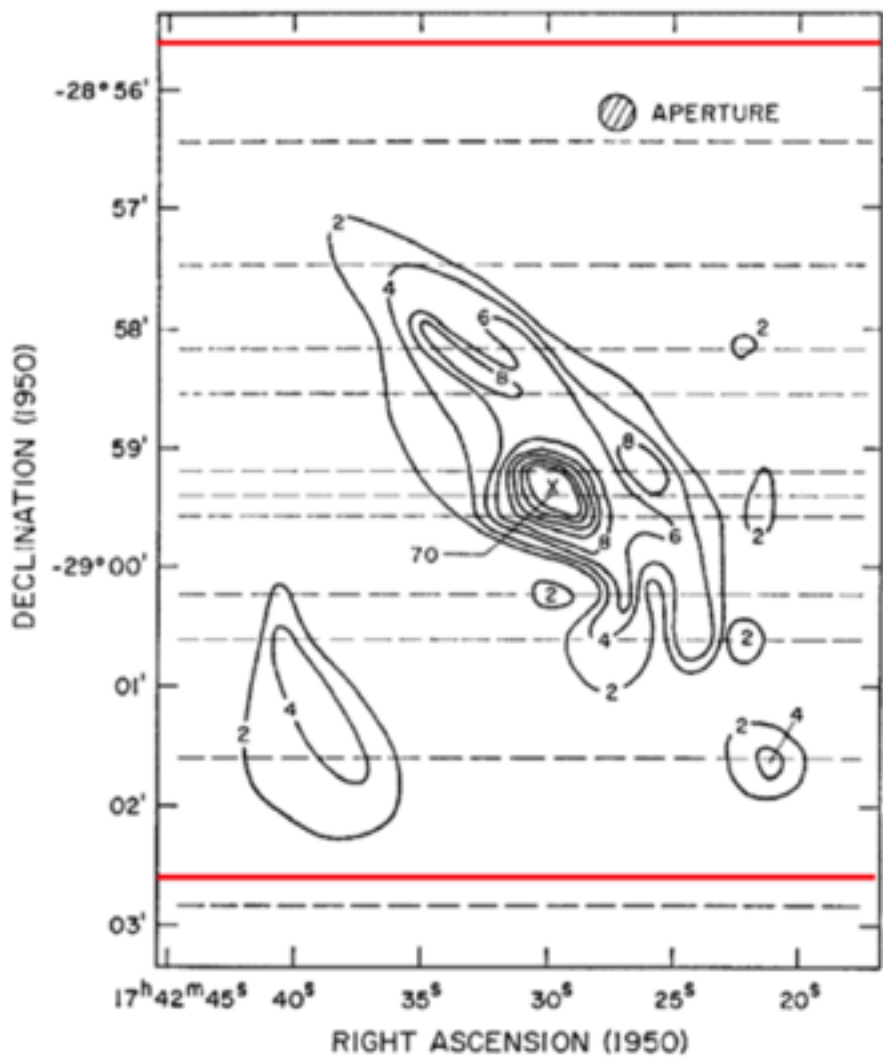


The Array Revolution in Infrared Astronomy

1968, 5-m telescope,
3 nights, single detector

~ 2000, 1.3-m
telescope, 8
seconds, 256 X 256

~ 2006, 6.5-m
telescope, 1 hour,
1024 X 1024
(would be 4 minutes
with the 2x2 2048 X
2048 NIRCam
mosaic)



Images of the Galactic Center region at 2 μm. (a) The original map by Becklin & Neugebauer (1968), using a single detector with an aperture of 15 arcsec (reproduced by permission of the American Astronomical Society). The dashed lines show the actual scans across the region; the data were taken over three nights with the Palomar 200-in (5-m) telescope. The red lines delineate the roughly 7 × 7 arcmin field shown in panels b and c. (b) The 2MASS image of the same region, using a 256 × 256 detector array on a 1.3-m telescope and with integrations of 8 s per point. The image includes data at 1.25 μm, which identifies foreground stars as blue in the false color image (courtesy of 2MASS/UMass/IPAC-Caltech/NASA/NSF). (c) A mosaic obtained by Laycock et al. (private communication) on the 6.5-m Magellan Telescope with a 1 K × 1 K array. The typical resolution is 0.5 arcsec and the total time for the area shown was about an hour. At the depth of this image, Olber's Paradox comes to mind—nearly every line of sight seems to intersect a star.

Infrared regime

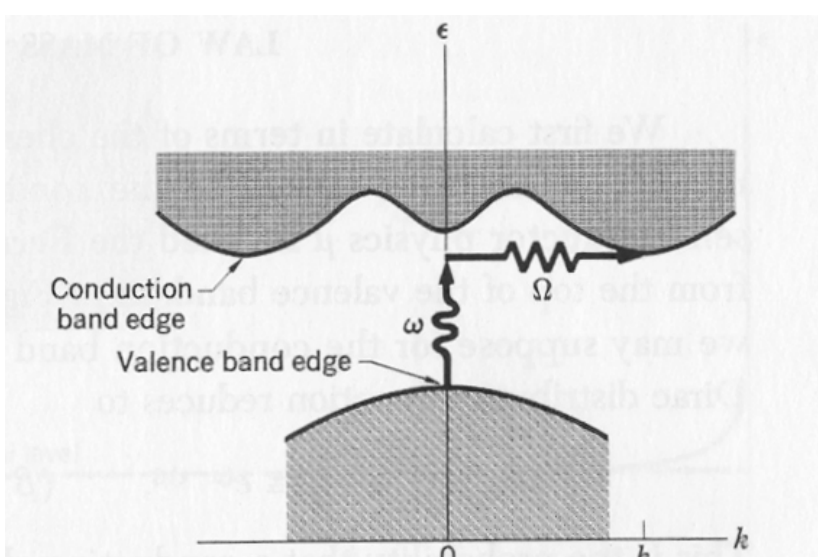
- The red limit of sensitivity of the human eye is ~ 720 nm (or 0.72 μm).
- With the advent of CCDs, “optical” astronomy extended its territorial claims to about 1.1 μm , the cut-off wavelength for detection of light imposed by the fundamental band-gap of silicon ($\lambda_c = 1.24/E_G$; for $E_G = 1.13$ eV, $\lambda_c = 1.1$ μm).
- Where is the “real” optical-IR boundary for ground-based astronomy?
- A reasonable response is “ 2.2 - 2.4 μm ” because at these wavelengths there is a marked and fundamental change in the nature of the “background” light entering the telescope/detector.
- There is a practical change in observing methods and instrument too.
- For wavelengths shorter than ~ 2.2 μm , the background comes mainly from OH emission in Earth's upper atmosphere, whereas at longer wavelengths the dominant source of background radiation is thermal (heat) emission from the atmosphere and telescope components.

CCD, IR Detectors: same physics

II III IV V VI

	5	6	7	8
II	B	C	N	O
III	A	Si	P	S
IV	Zn	Ga	Ge	As
V	Cd	In	Sn	Sb
VI	Hg	Ti	Pb	Bi
	30	31	32	33
	48	49	50	51
	80	81	82	83
				84

- Silicon is type IV element
- Electrons shared covalently in crystalline material
 - Acts as insulator
 - But electrons can be excited to conduction band with relatively small energy ($1.0 \text{ eV} = 1.24 \mu\text{m}$), depending on temperature
- Internal photoelectric effect
- Collect electrons, read out

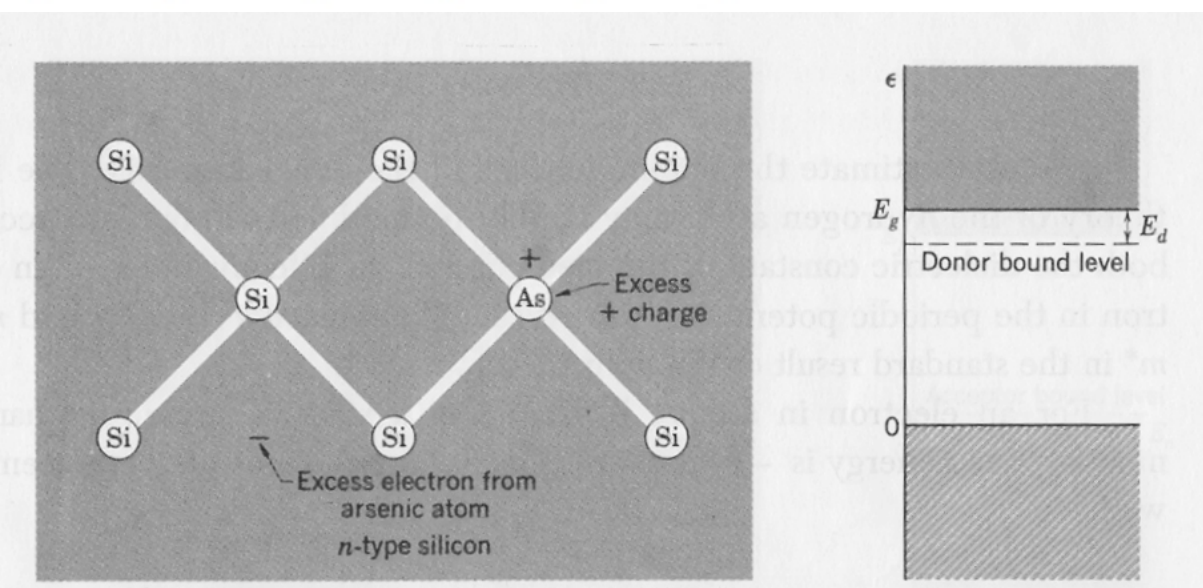


C. Kittel, *Intro. to Solid State Physics*

Extrinsic Photoconductor

II	III	IV	V	VI
		B 5	C 6	N 7
		Al 13	Si 14	P 15
Zn 30	Ga 31	Ge 32	As 33	Se 34
Cd 48	In 49	Sn 50	Sb 51	Te 52
Hg 80	Ti 81	Pb 82	Bi 83	Po 84

- Silicon is type IV element
- Add small amount of type V (As)
- Similar to H atom within Si crystal
 - Extra electron bound to As nucleus
 - Very small energy required for excitation ($48 \text{ meV} = 26 \mu\text{m}$)
- Sensitive through mid-IR
 - Spitzer MIPS, WISE



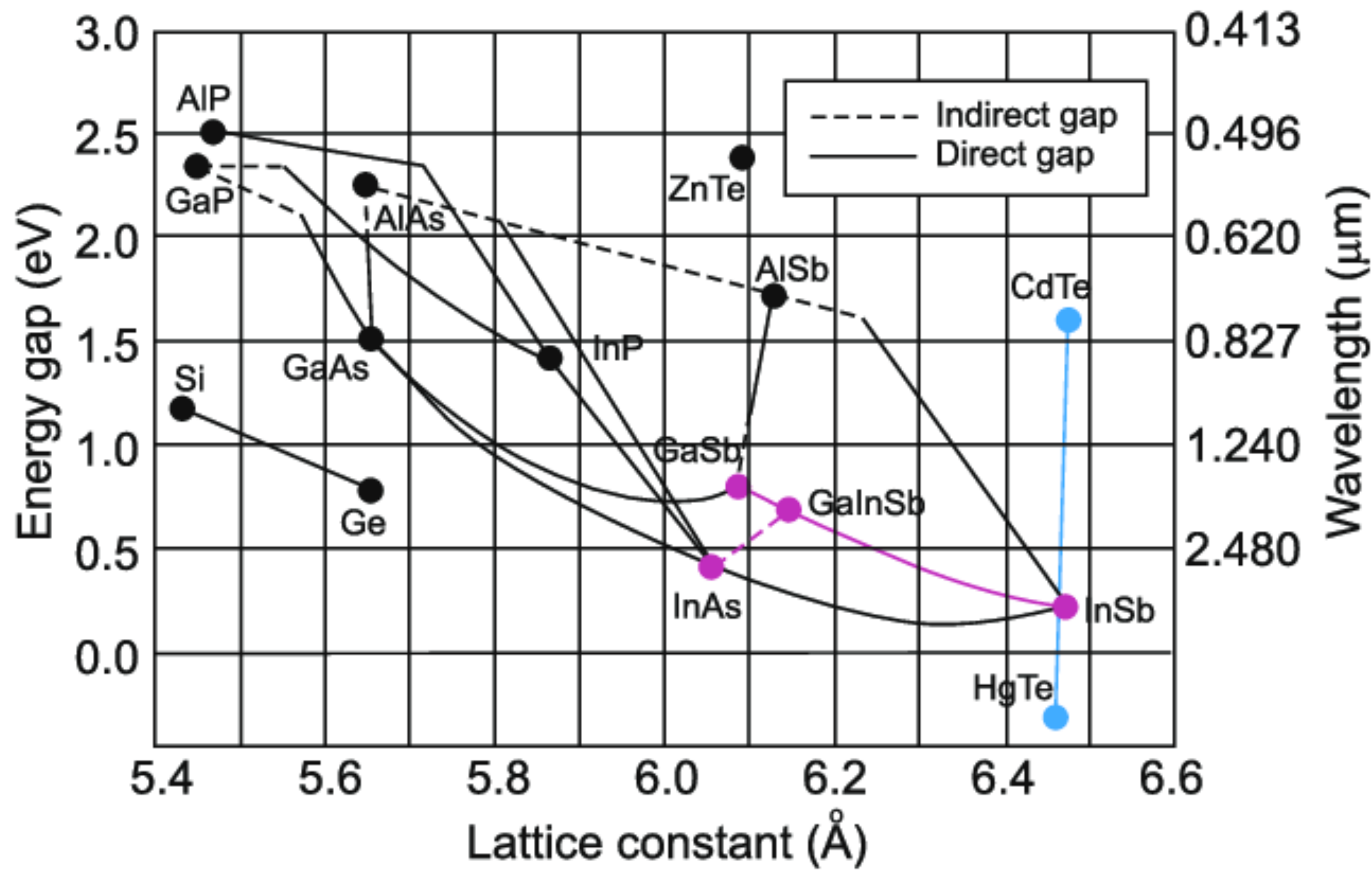
Intermetallic Photoconductor

II III IV V VI

	5	6	7	8	
II	B	C	N	O	
III	Al	Si	P	S	
IV	Zn	Ga	Ge	As	
V	Cd	In	Sn	Sb	
VI	Hg	Ti	Pb	Bi	
	30	31	32	33	34
	48	49	50	51	52
	80	81	82	83	84

- Make Si-like compound
 - III-V (InSb, GaAs)
 - II-VI ($\text{Hg}_x\text{Cd}_{1-x}\text{Te}$)
 - Semiconductors like Si, but with different energy gap for photoexcitation
 - InSb 0.23 eV = 5.4 μm
 - HgCdTe 0.73 eV = 1.75 μm
 0.48 eV = 2.55 μm
 0.24 eV = 5.3 μm
- (Hg/Cd ratio can change energy gap)

But, can excite electrons by other means.....



The good, bad, and ~~ugly~~

- Good electrons, bad electrons
 - Electrons have thermal energy $\sim kT$, can be thermally excited into conduction band (dark current)
 - Solution is to operate detector at low temperature
 - Si CCD 0.3 – 1 μm 170 K **GMOS**
 - HgCdTe 0.5 – 2.5 μm 75 – 80 K **NIFS, NICI, FLAMINGOS2**
 - InSb 0.5 – 5.4 μm 30 K **NIRI, GNIRS, PHOENIX**
 - Si:As 5 – 28 μm 12 K **TReCS, TEXES**
- Good photons, bad photons
 - Only want photons coming through telescope
 - Eliminate thermal photons from surroundings
 - IR instrumentation, optics are in cold vacuum environment

Subject for separate presentation!

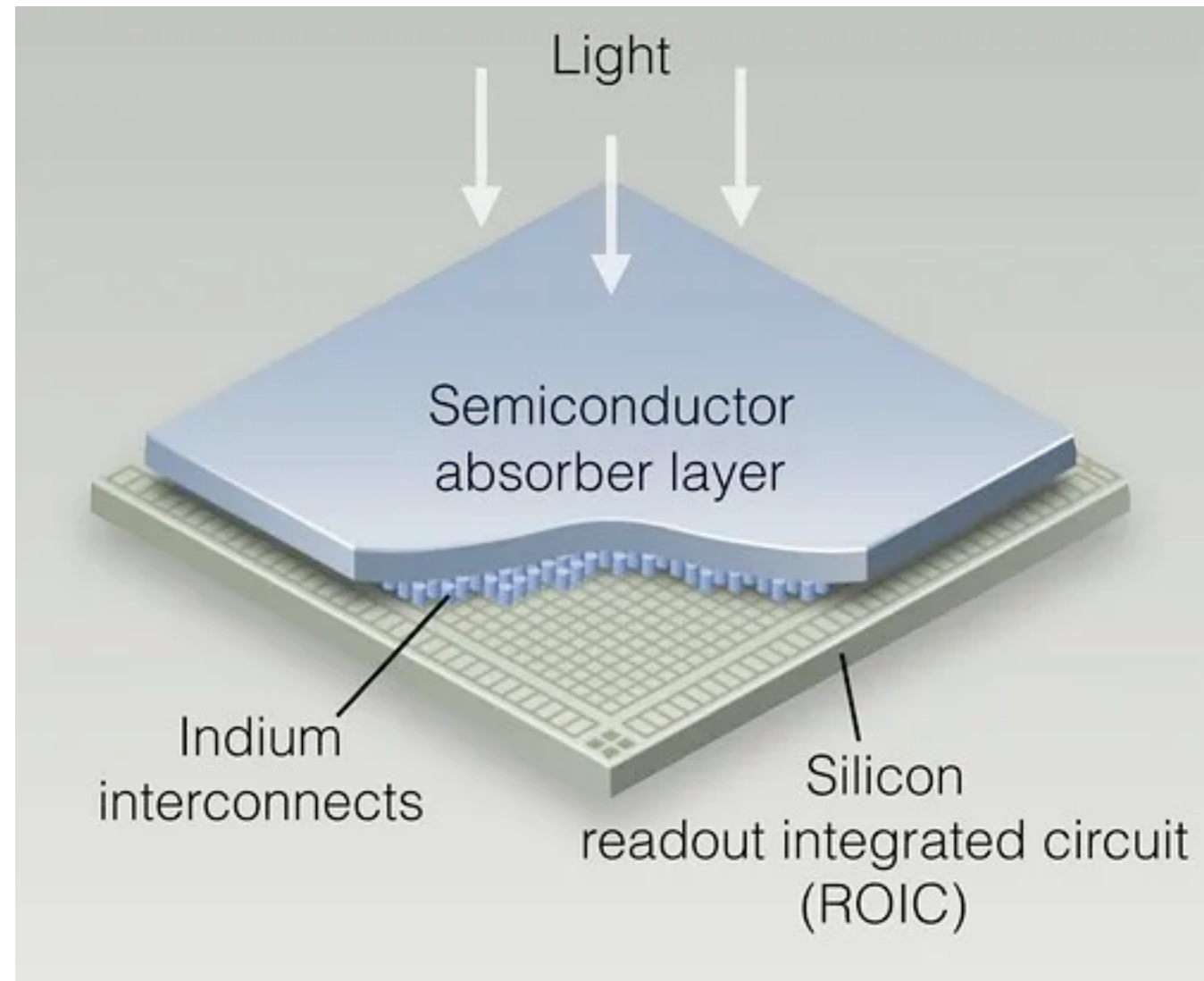
The “hybrid” structure for IR arrays

An IR array must meet same requirements on CCD: convert radiation to electrical charge by the internal photoelectric effect (or bolometer) and:

- store the charge at the site (pixel) of generation
- transfer the charge on each pixel to a single (or a small number of) outlets (the multiplexing task)
- enable the charges to be removed sequentially as a voltage which can be digitized

Initially tried to make CCD from non-silicon semiconductor – manufacturing challenges too steep. Instead adopted “hybrid” design:

IR detector + Silicon ROIC



ROIC: readout-integrated circuit (silicon)

- Best performance with silicon integrated circuit readout
 - Cannot manufacture high quality electronics in other semiconductors
 - **CCD-type readout has charge transfer problems at cold temperatures**
- ... but silicon has a large band gap - and IR photons don't have much energy
- Direct hybrid construction
 - Fields of indium bumps evaporated on detector array, readout amplifiers
 - Aligned and squeezed together - very carefully
 - **Detector and readout can be separately tested (improve yield)**

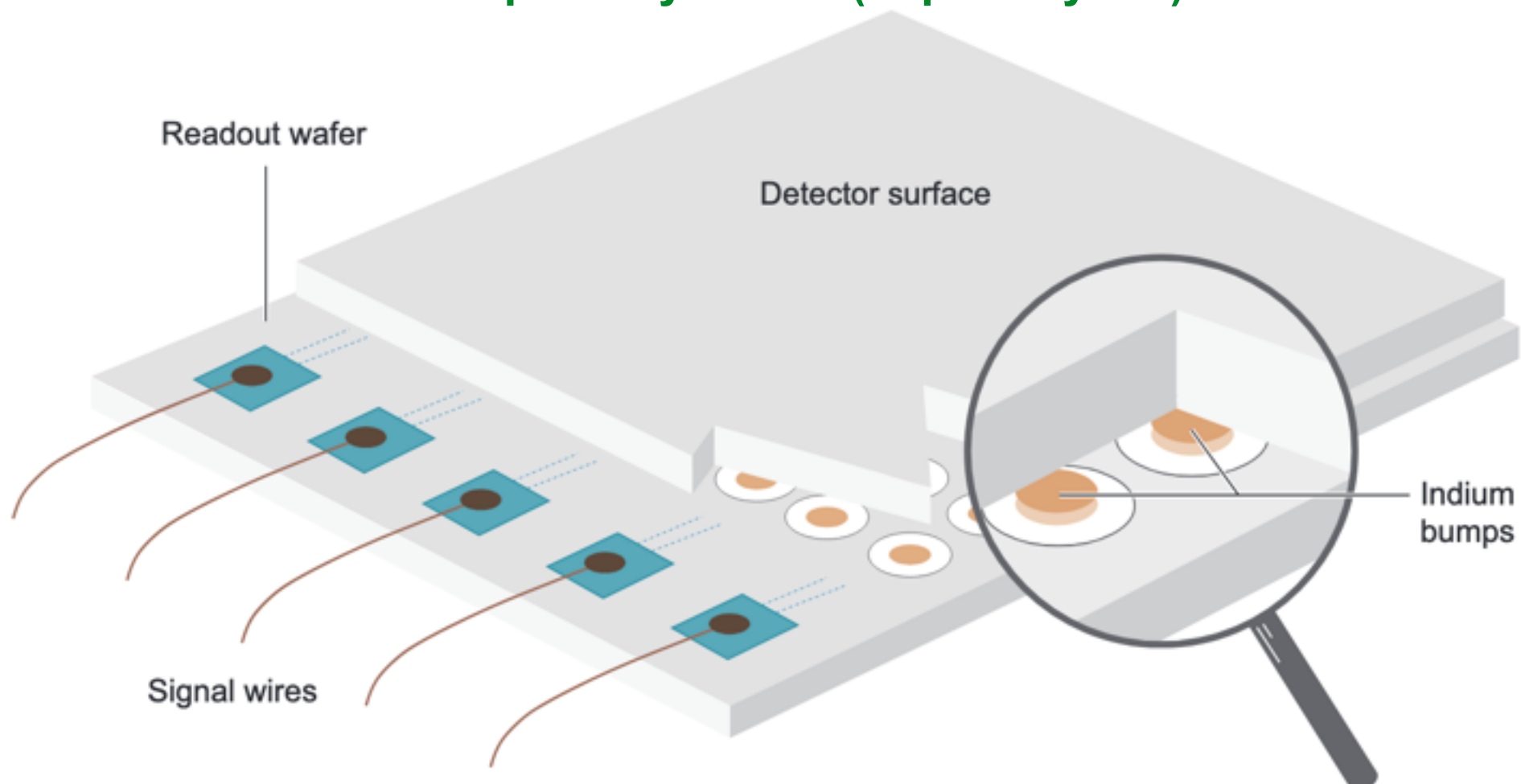


Figure 4

In direct hybrid construction, a wafer of detectors is attached to a silicon wafer (carrying the readout amplifiers and associated circuitry) through matching grids of indium bumps. When the wafers are aligned and pressed together, the bumps distort, their indium oxide skins crack, and the exposed indium metal welds the detector outputs to their individual amplifier inputs to complete the array. Figure from Rieke (2006), reprinted by permission of the University of Arizona Press.

Reminder: CMOS (complementary metal oxide semiconductor) detectors

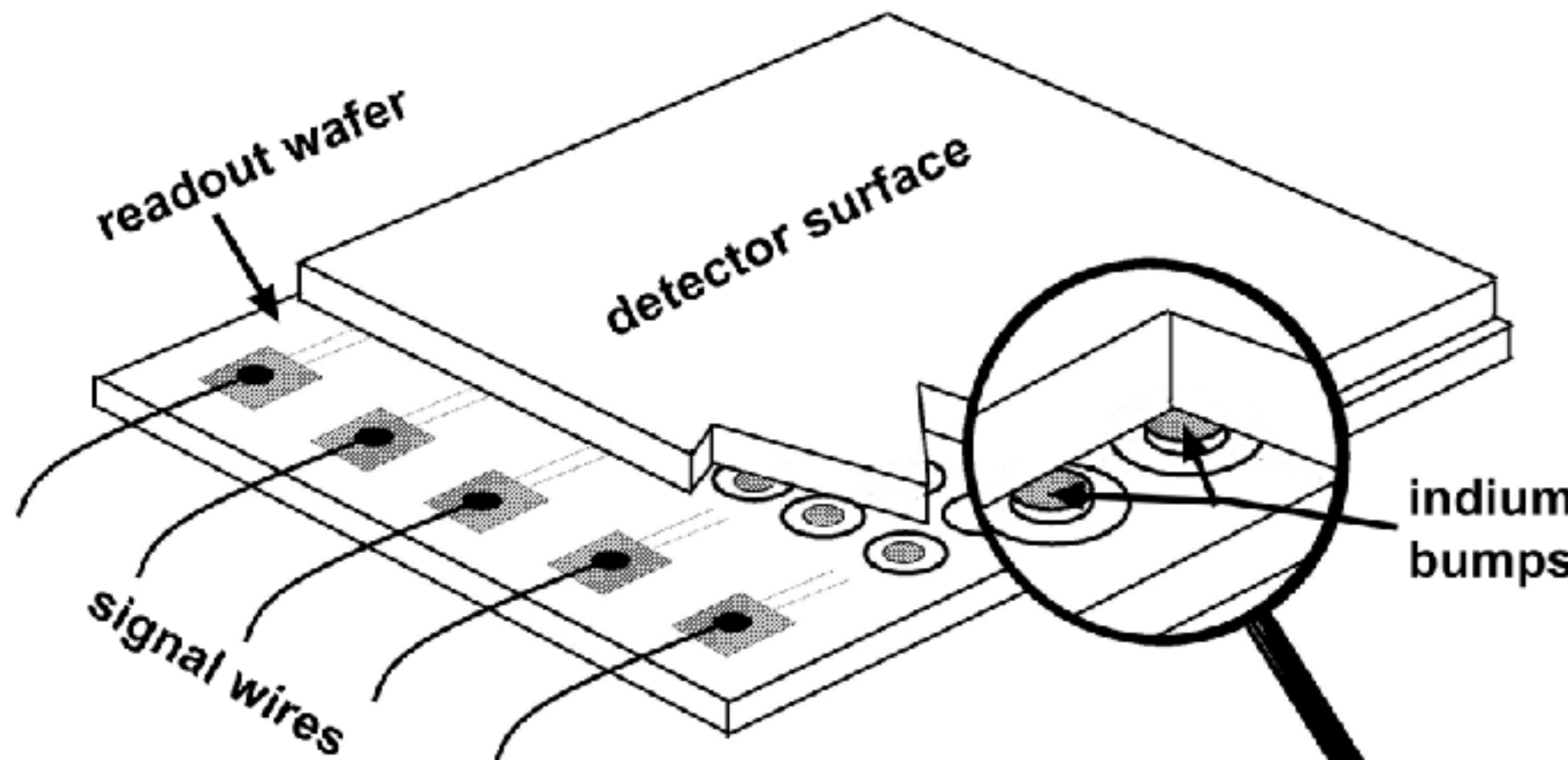
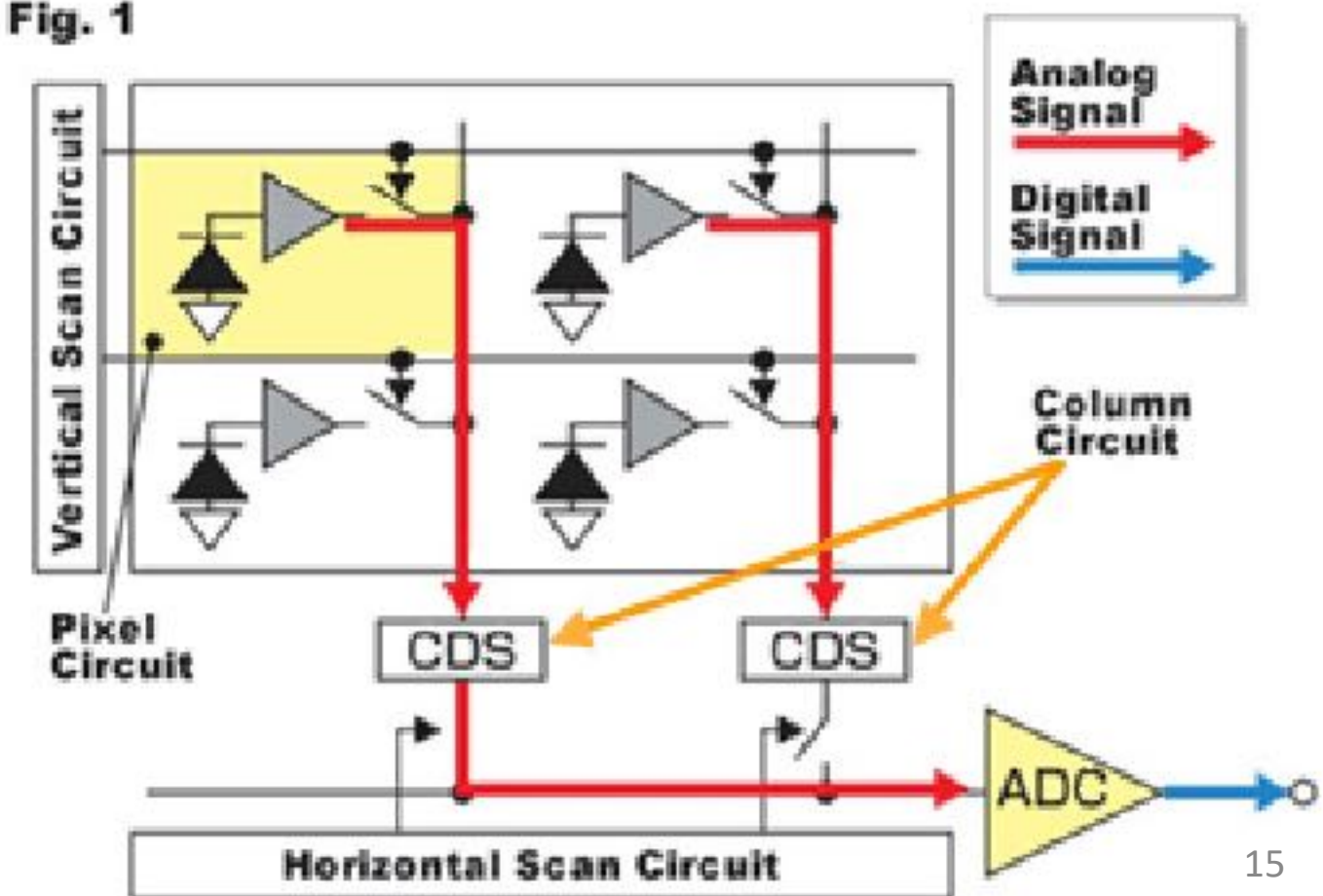


Fig. 1

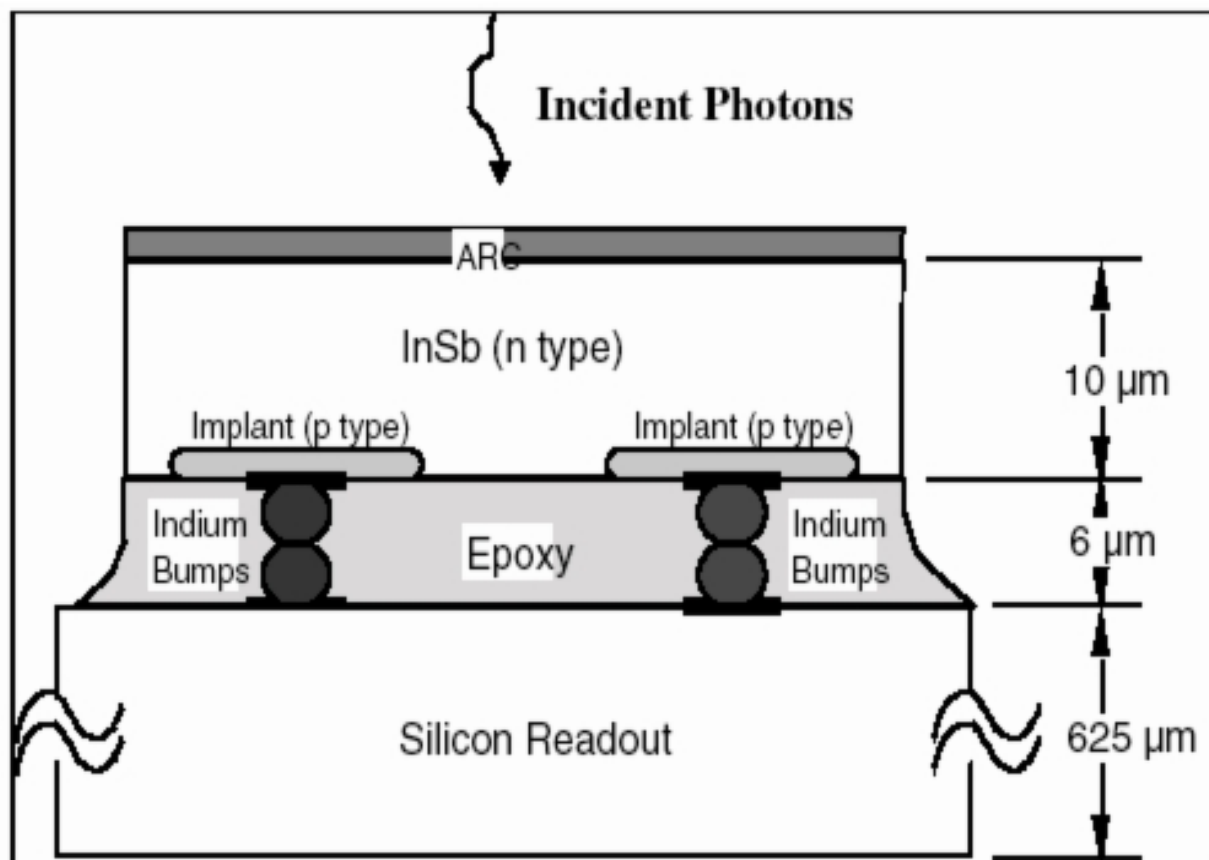
Because they can be made in standard integrated circuit foundries, they are relatively cheap. They can also be made with a lot of the support electronics on the same silicon chip. To the right is Sony's diagram of how one works.

CMOS detectors are like taking just the readout for an infrared array and placing photodiodes on the inputs of the amplifiers.



Hybrid array construction

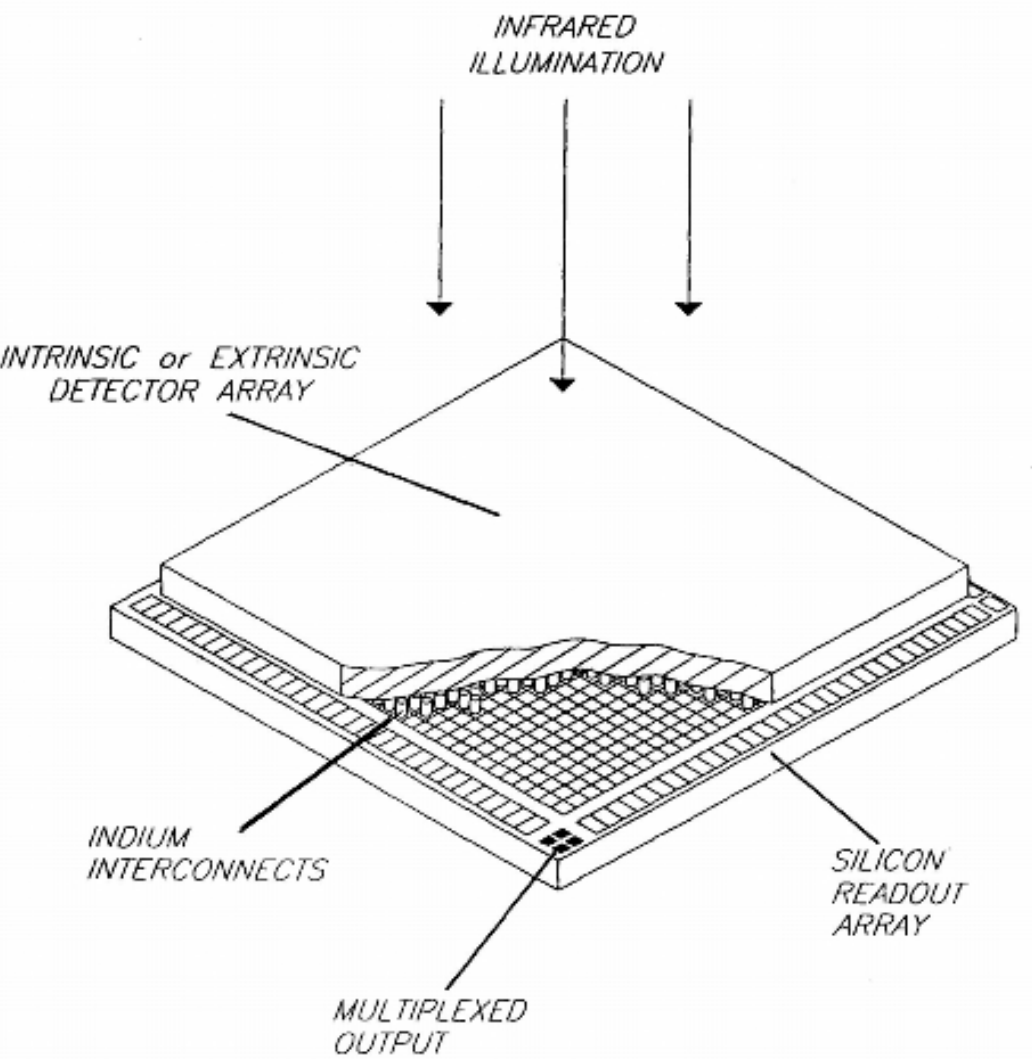
- IR detector array, Si readout separately fabricated and tested
- Indium bumps grown on each pixel of array and readout
- Two arrays are carefully aligned and pressed together – indium acts as electrical connection between detector material and readout
- Epoxy fill to support detector material
- Detector must be thinned to $\sim 10 \mu\text{m}$ (backside illuminated)
 - Too thin, detector is transparent to photons
 - Too thick, photoelectrons recombine before making it to readout



- Apply antireflection coating on detector to optimize quantum efficiency (high index material)

Complex construction
Yield issues
\$\$!!

Hybrid architecture -- different readout



- Pixels utilize “unit cell” architecture
 - Separate readout amplifier for each pixel
- Addressed by row, column independently
 - No charge transfer, no charge transfer effects (charge trails, etc.)
 - Bad pixels are independent of others
- **Readout is nondestructive**
 - Address row/column enable, read voltage on pixel during an integration

Nondestructive readout makes it possible to read out a portion of the array or to read out the array multiple times

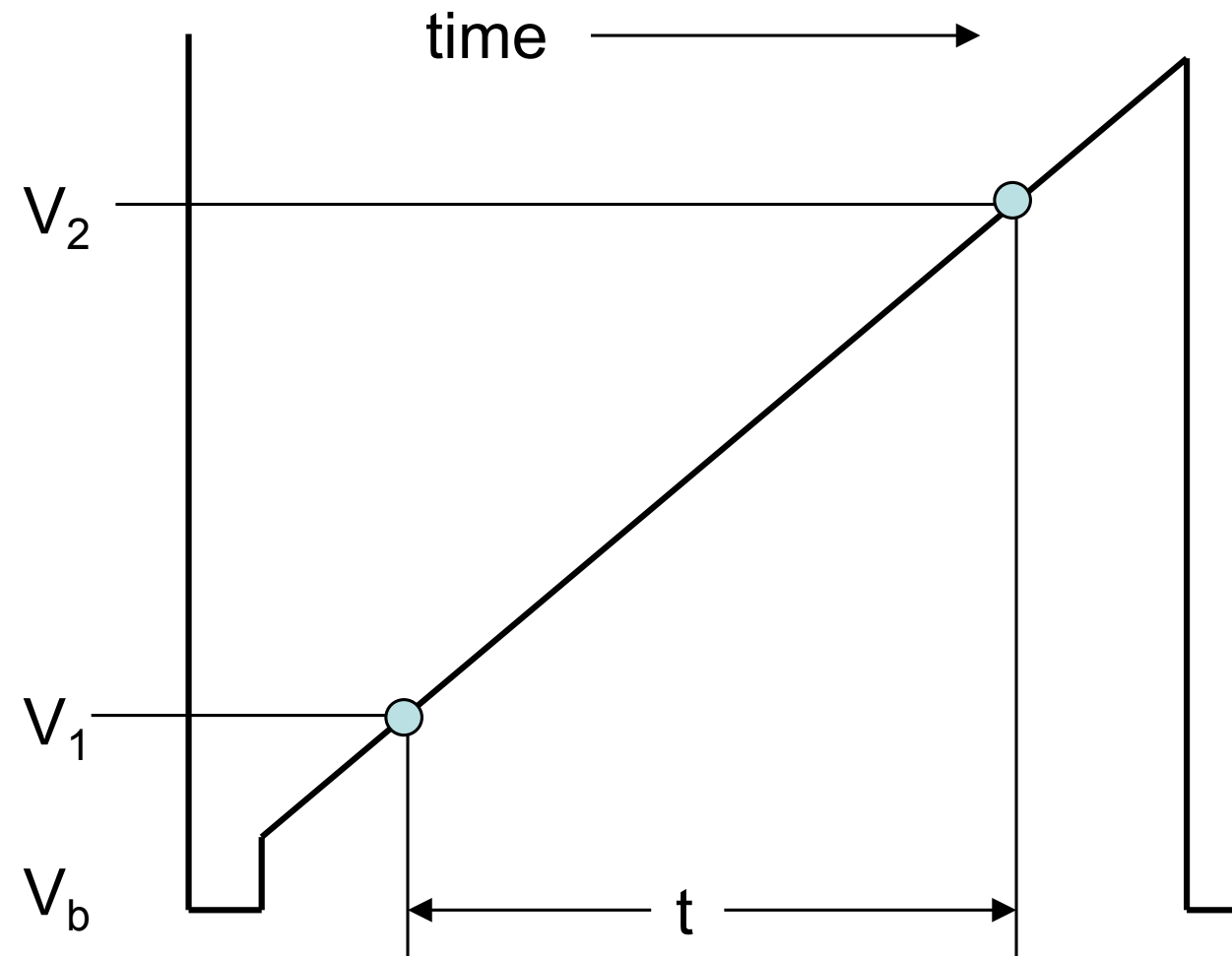
Differences with CCDs

10

- No charge-coupling:
 - ▣ pixels accessed directly and their voltage fed to the output bus.
- A single voltage pulse is required to reset the charge collection node at each pixel.
- Can perform a “**non-destructive**” readout.
- Even at the shortest infrared wavelengths the pixels can fill up in a few tens of seconds in broad band imaging applications and the maximum integration time drops to milli-seconds in the thermal IR.
- In fact, it is customary to sum many short on-chip exposures in a “co-adder” before writing a data frame to disk. **Thus the integration time is the product of the on-chip exposure time and the number of “coadds” used.**
- Readout times for a full frame are much faster than with CCDs.

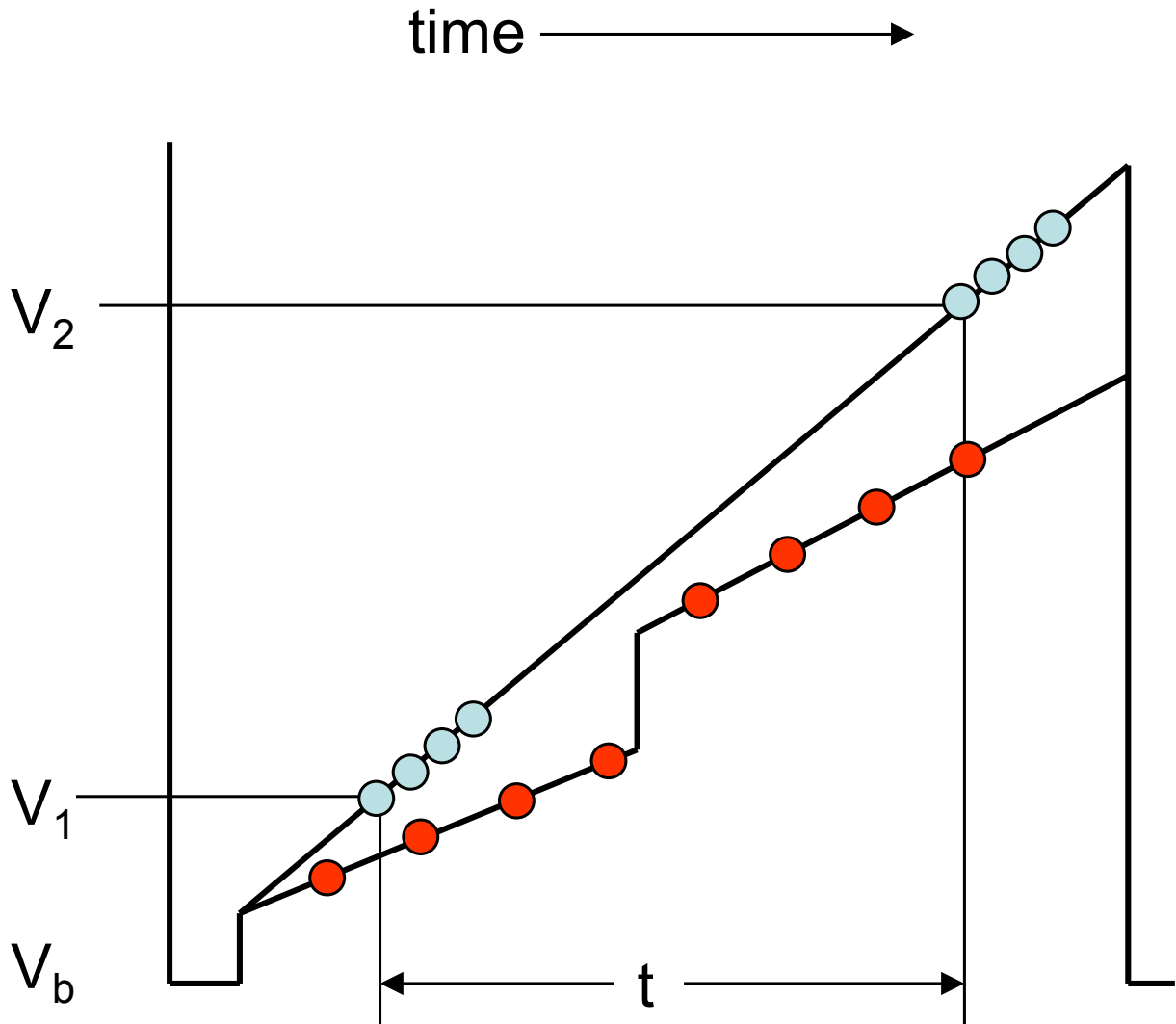
Nondestructive readout is versatile

[Hypothetical voltage on a pixel as a function of time]



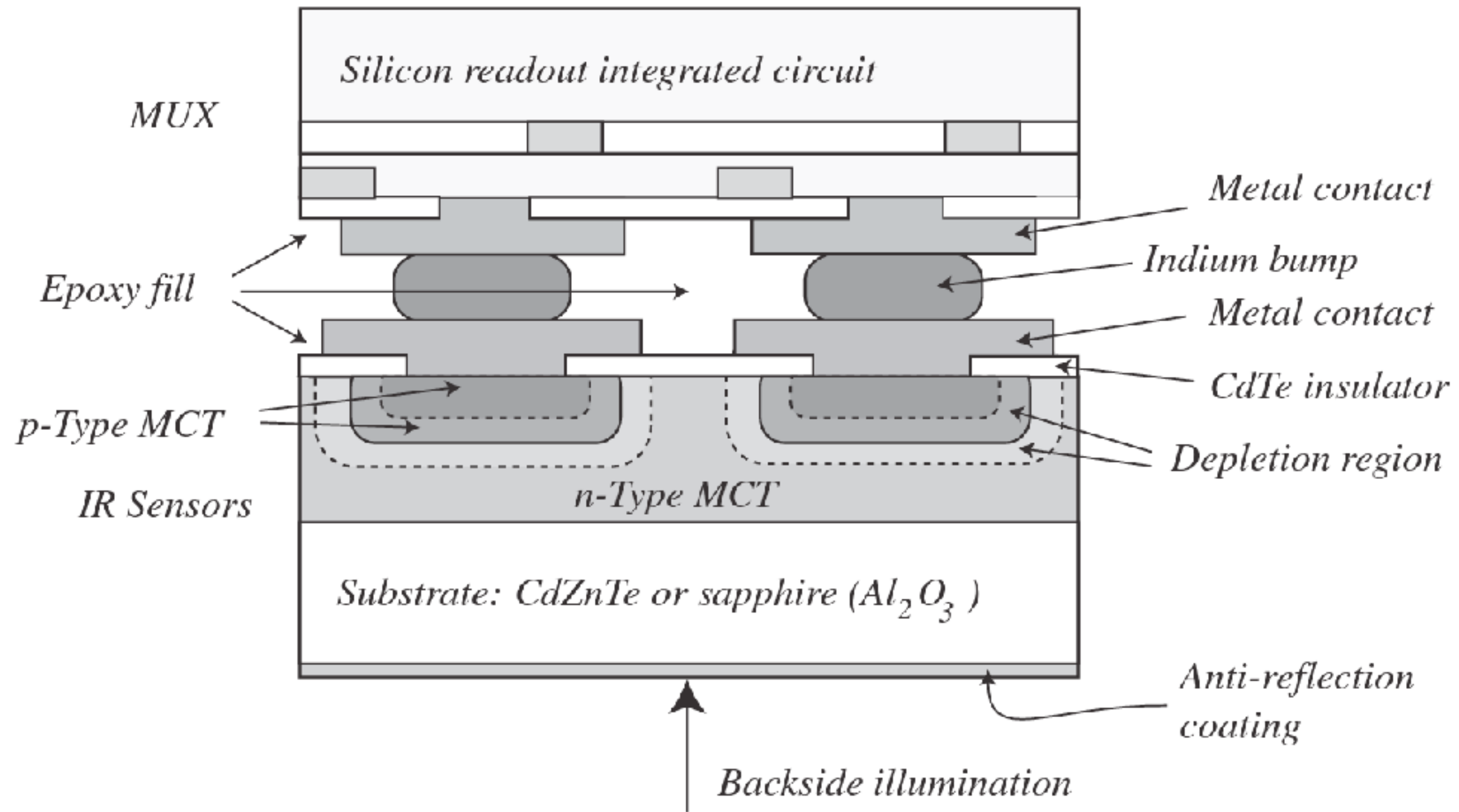
- Integration defined electronically (no shutter; ambient shutter gives background!)
- Initially, bias pixel to V_b
 - Creates potential well (capacitor)
 - Release, get jump (kTC jump)
 - Photoelectrons accumulate
- After bias, sample voltage V_1
- After time t , sample voltage V_2
- Subtract two readouts—difference is the final image
- Double Correlated Sampling (DCS) – removes bias
- But, minimum integration time is array readout time
 - Multiple readout amplifiers → readout time \sim seconds
- Two reads increases read noise by $\sqrt{2}$

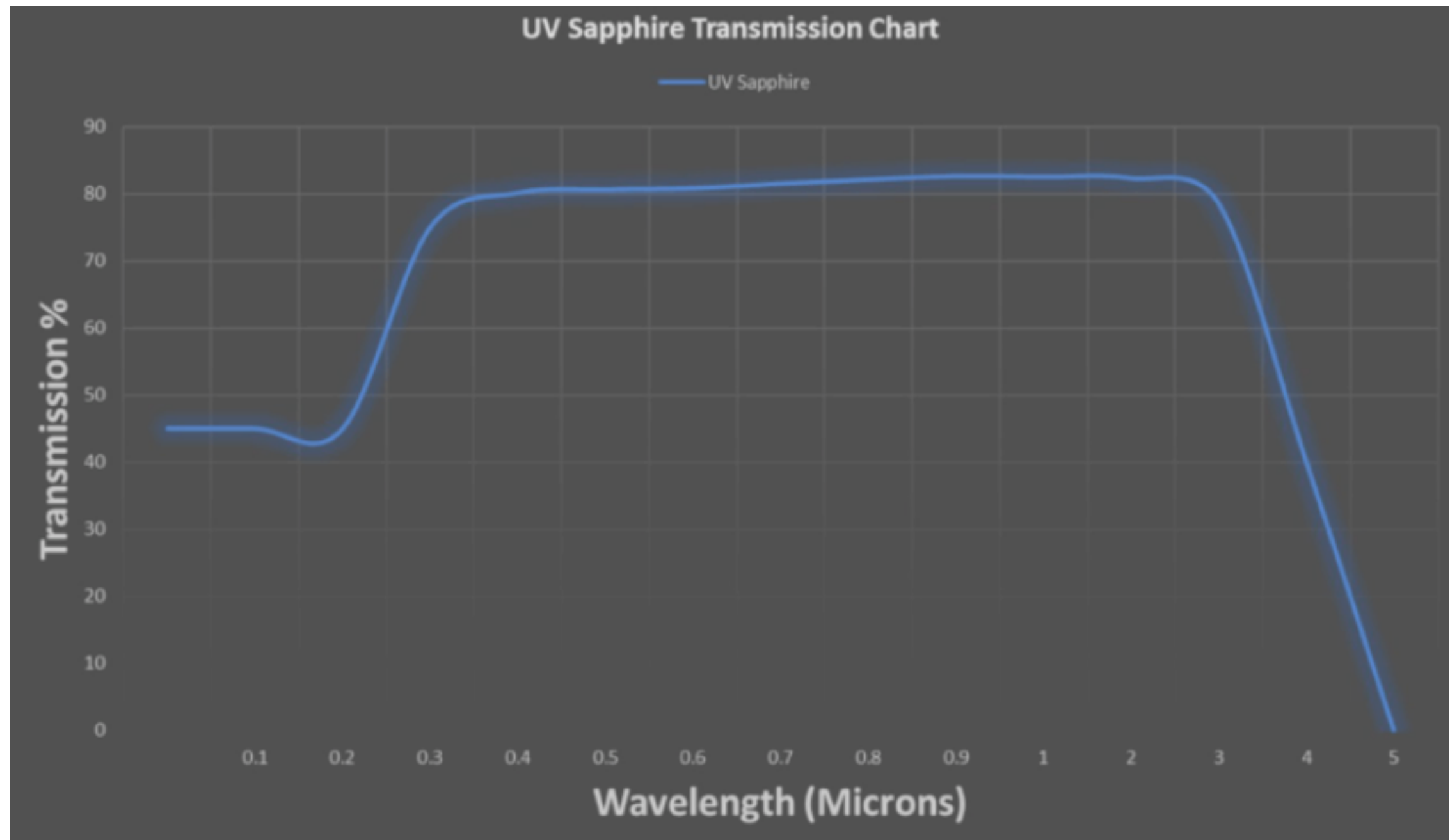
Nondestructive readout is versatile (2)



- IR arrays have higher read noise than CCD
 - 15 – 35 e vs 4-6 e
 - Higher capacitance
 - Surface channel readout
 - DCS readout
- Al Fowler (NOAO detector engineer) pioneered multiple readouts at beginning and end of readout cycle
 - “Fowler” sampling (LNRs)
 - Can reduce read noise by almost $N^{1/2}$
 - FLAMINGOS2 achieves 5 e with $N=8$

- Other readout mode is to sample during entire integration
 - Fit slope to samples, can achieve similar read noise reduction
 - More applicable to space instrumentation in removing discontinuities due to particle events





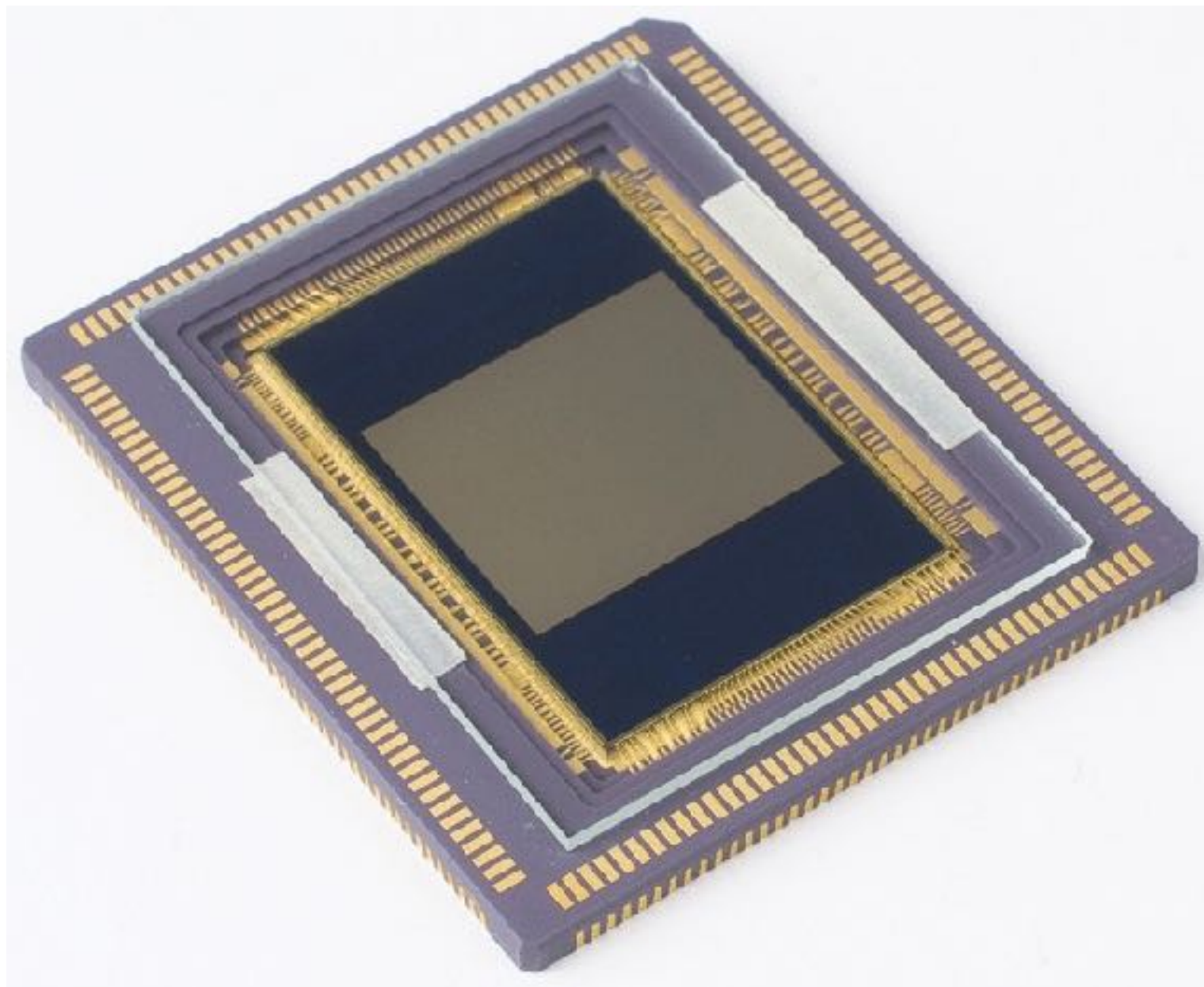
Reminder: CMOS detectors can be really big!

To the left, an X-ray detector; to the right a garden variety 18 Mpix camera detector.



An example: Fairchild CIS2521F

- 2560 X 2160 pixels
- $6.5 \mu\text{m} \times 6.5 \mu\text{m}$ pixel pitch
- Readout speed maximum: 100 frames per second
- Read noise < 1.5 electrons rms
- Peak quantum efficiency > 52%

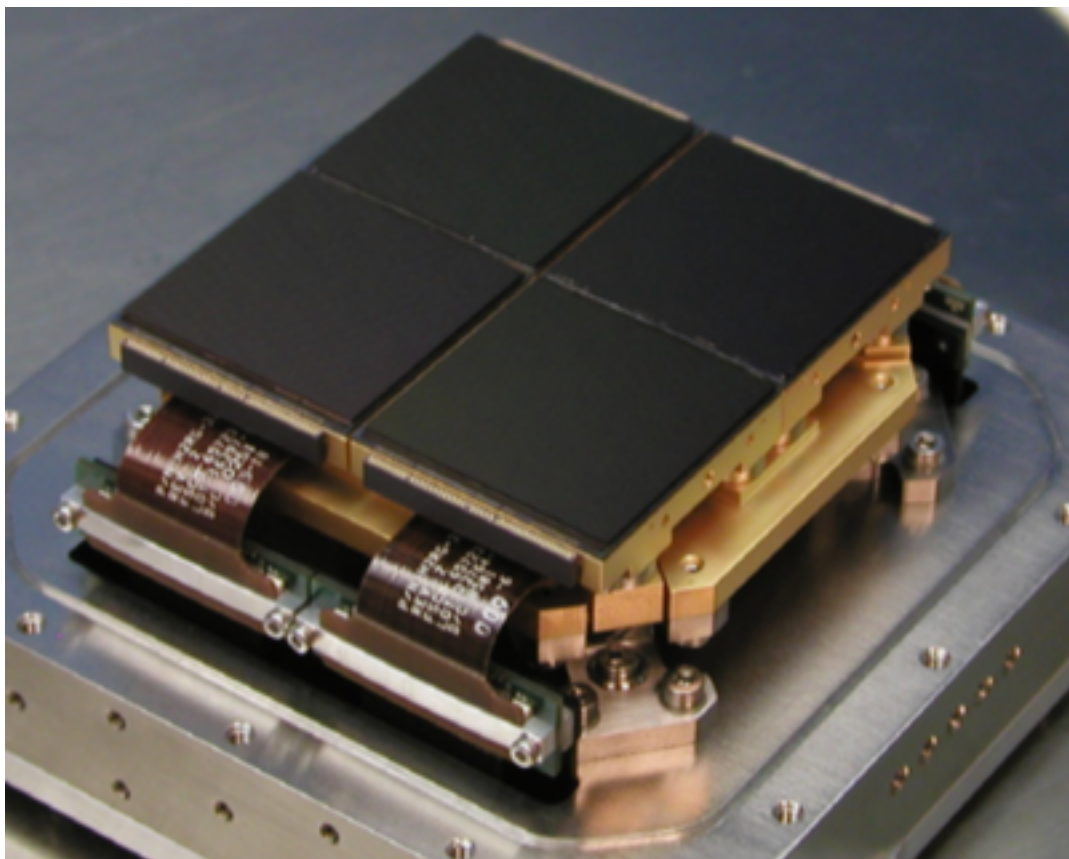
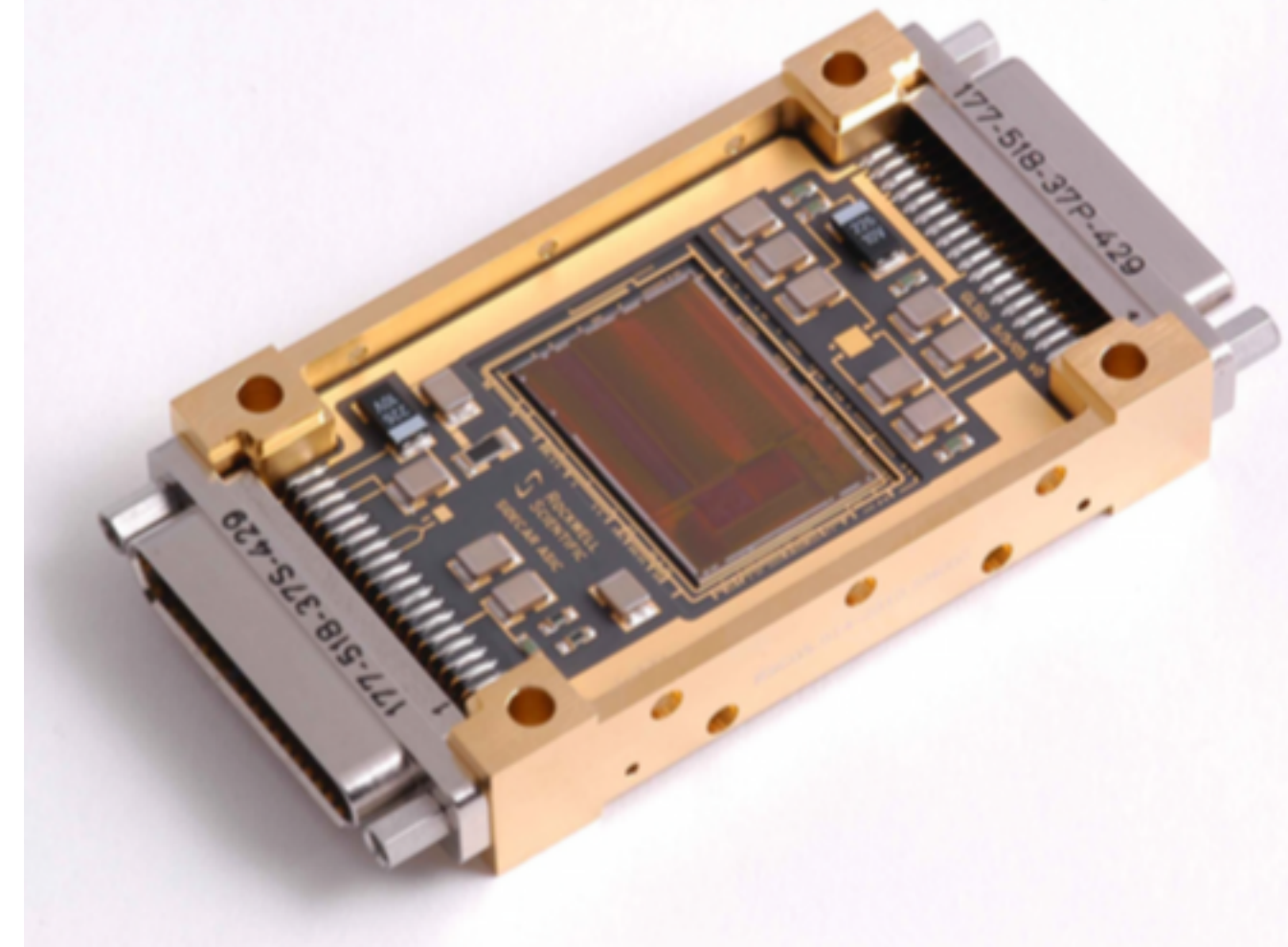


Types of IR arrays

- **Mercury-Cadmium-Telluride (HgCdTe) arrays:**
 - Light enters from back through sapphire substrate; transmits to $6.5 \mu\text{m}$.
 - Percentage of Hg to Cd determines cut-off wavelength. For example, with $\text{Hg}_{1-x}\text{Cd}_x\text{Te}$ then for $x = 0.196$ $E_G = 0.09 \text{ eV}$ and $\lambda_c = 14 \mu\text{m}$. Similarly, $x = 0.295$ yields $E_G = 0.25 \text{ eV}$ and $\lambda_c = 5 \mu\text{m}$, and $x = 0.55$ gives $E_G = 0.73 \text{ eV}$ and $\lambda_c = 1.7 \mu\text{m}$.
 - Newer devices are “substrate removed” somewhat like thinned, back-illuminated CCDs, and it is this process that not only provides response down to visible wavelengths but also improves resistance to particle damage for space applications.
 - Substrate removal - Crucial for minimizing the impact of ionizing radiation on the detector's performance by eliminating the unwanted signal generated within the substrate when struck by radiation particles like cosmic rays; essentially, removing the substrate significantly reduces background noise caused by radiation interaction with the supporting material
- **Indium-antimonide (InSb) arrays:**
 - Indium antimonide photodiode arrays.
 - The pn junctions are diffused into the InSb substrate.

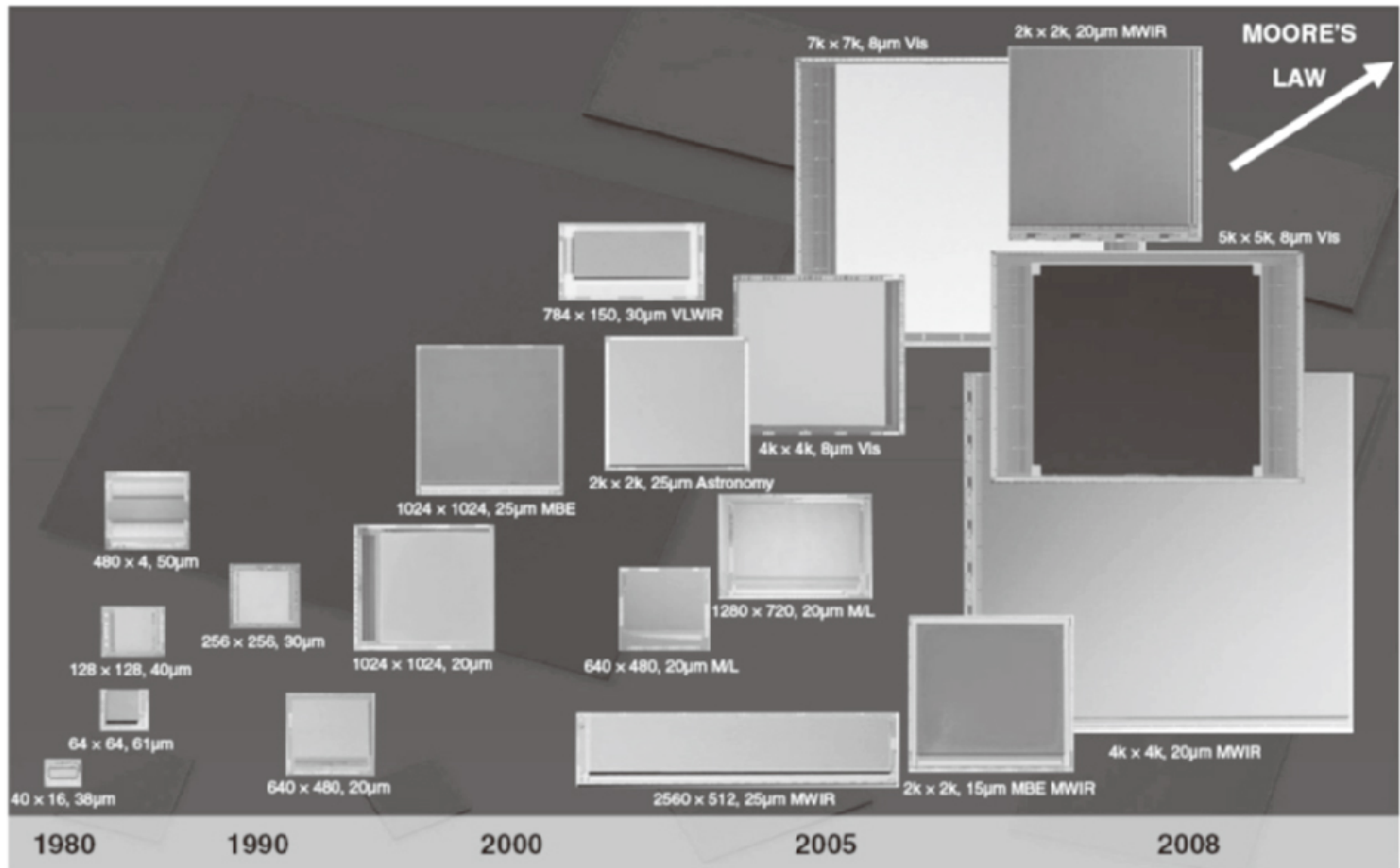
Teledyne Hawaii Chips

- hybrid CMOS arrays
- HgCdTe (“mircad”)
- Hawaii 2k (2048x2048) 18 μm pixel pitch
- 80-90% QE

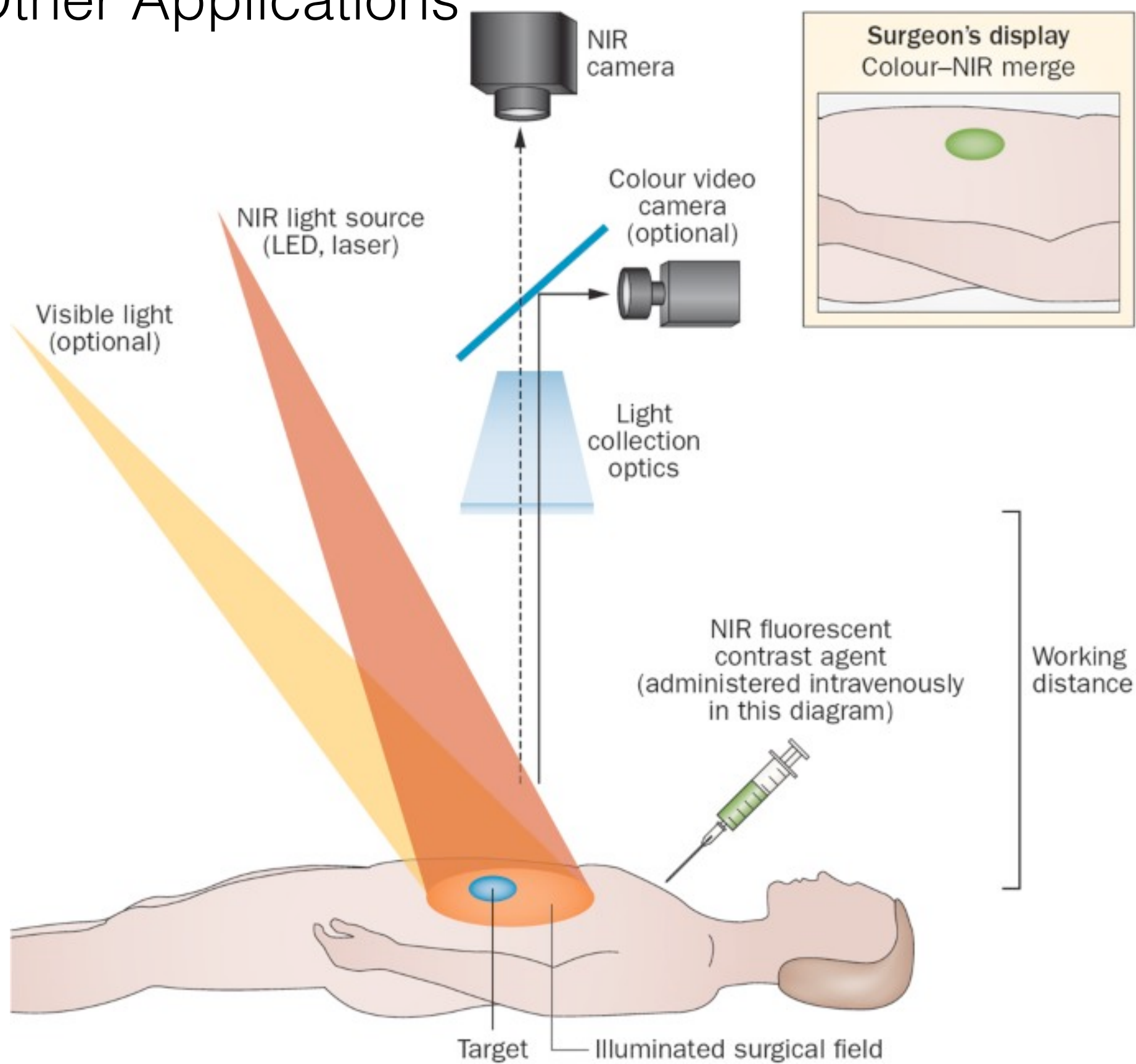


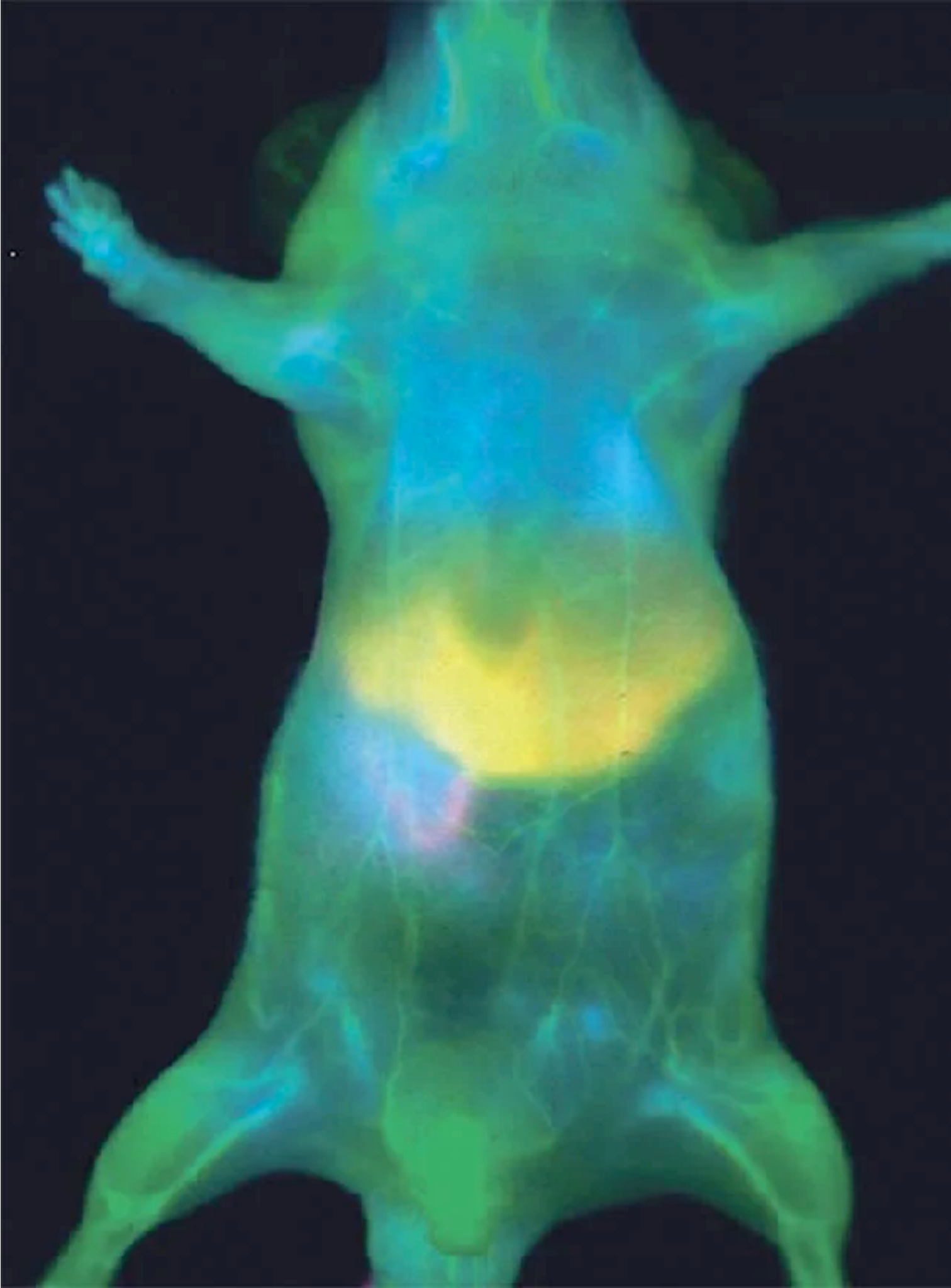
- WISE — Hawaii 1K
- HST/WFC3 — Hawaii 1k
- JWST/NIRCam — Hawaii 2k
- Roman — Hawaii 4k

Raytheon Detectors



Lots of Other Applications

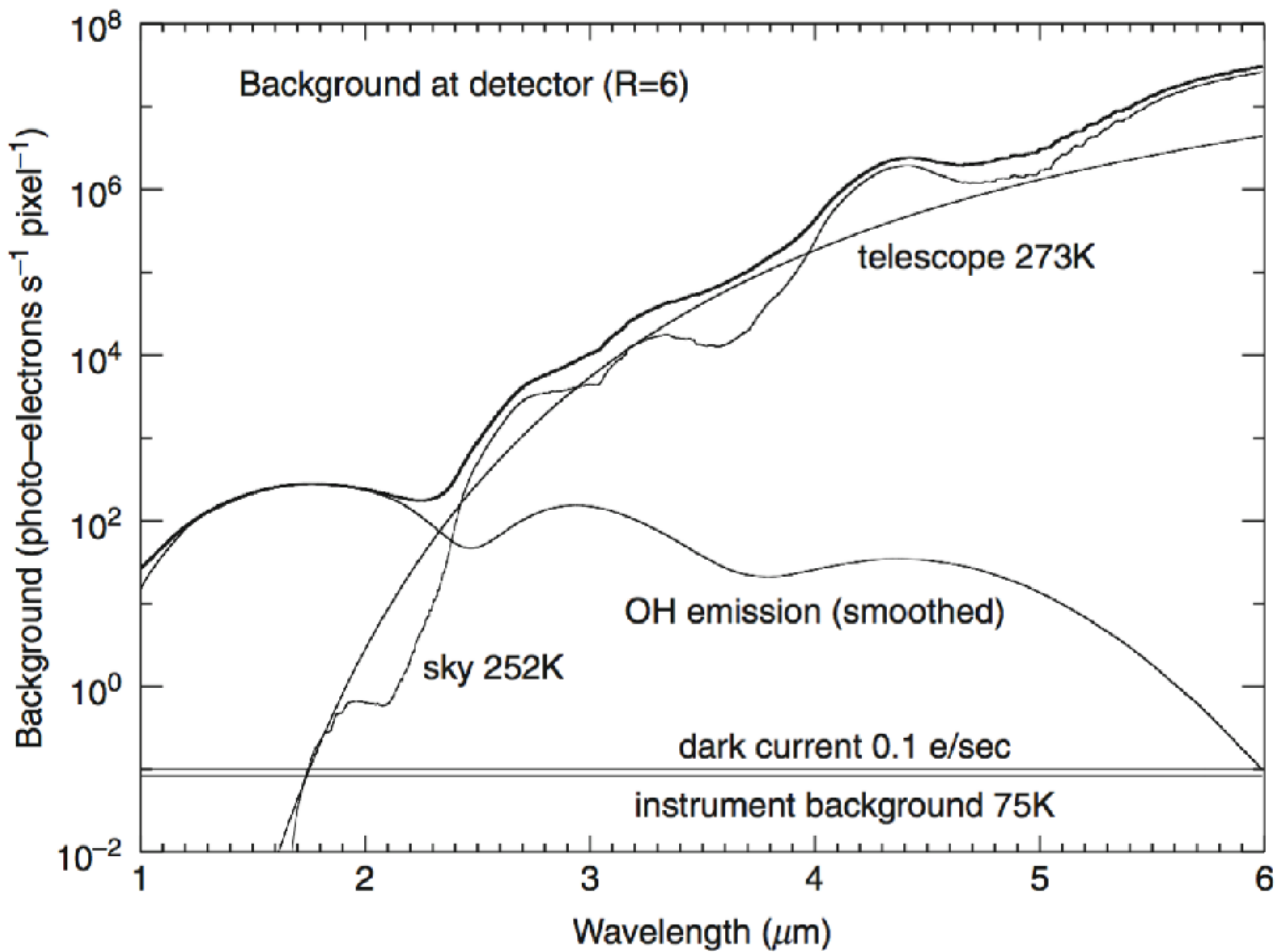




Fluorescence *in vivo* imaging of an anesthetized mouse injected with ICG. The real-time signal is acquired in the NIR-II (\sim 900-1700 nm) window.

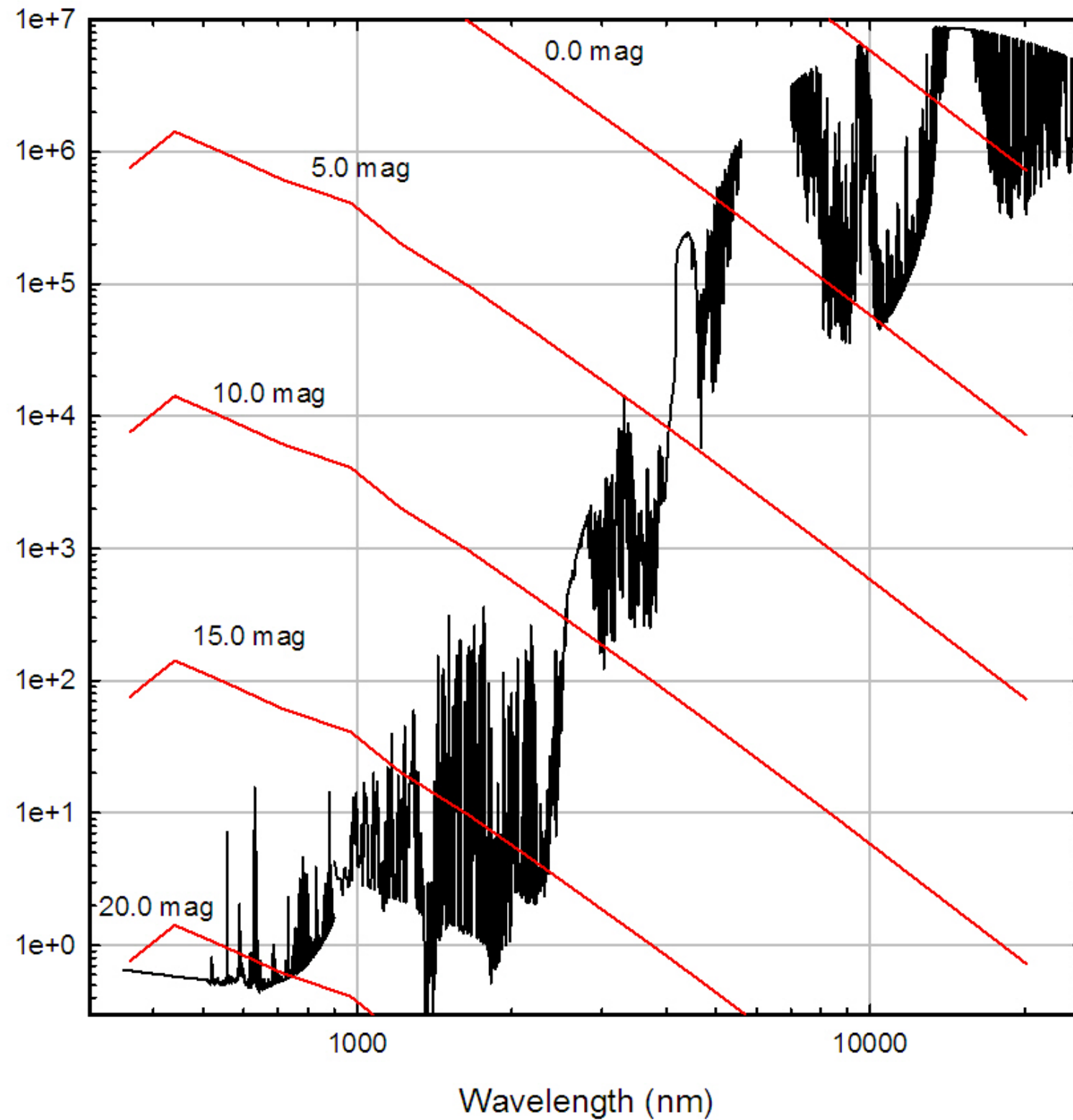
The enhanced depth and contrast allow for clear vasculature imaging, organs delineation, and metabolism.

Backgrounds



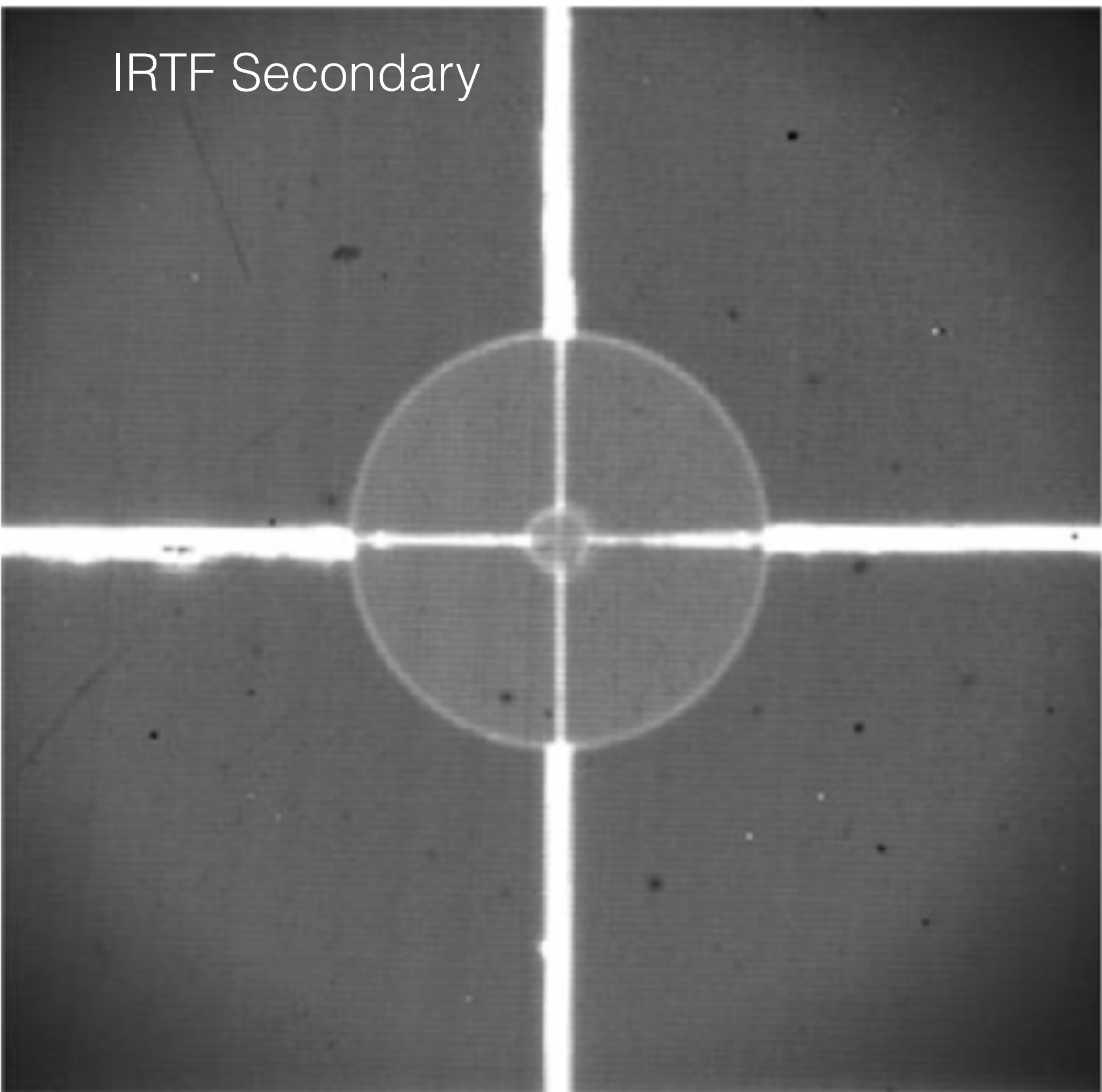
The good, bad, and ugly (continued)

Sky Background – Mauna Kea



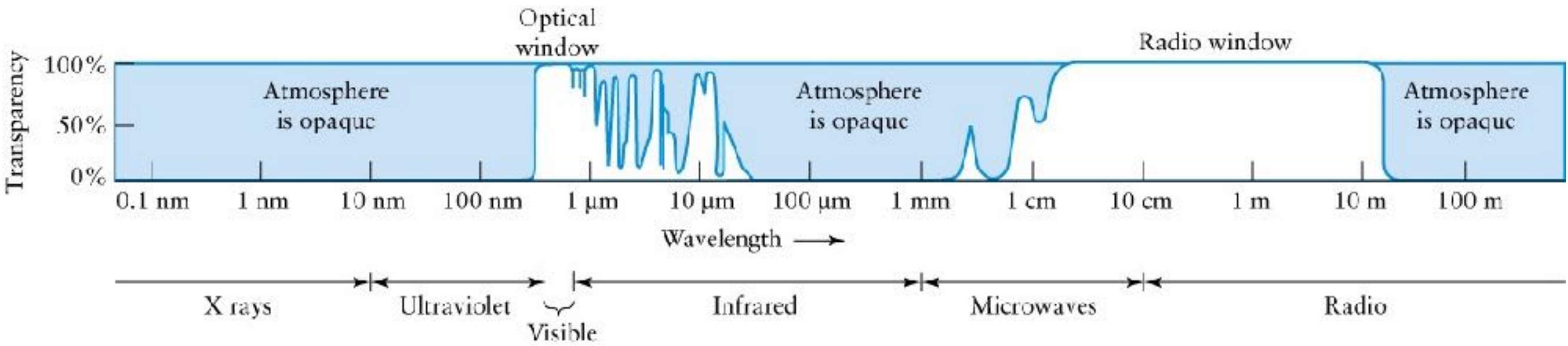
- More bad photons come through the telescope
- Sky is very bright in IR, compared to visible
 - Moonlight not an issue $> 1 \mu\text{m}$
 - OH emission lines $0.8 - 2.3 \mu\text{m}$
 - Thermal emission from telescope and atmosphere
- Even in K band, one wants to detect sources at 10^{-3} of sky ($13 \text{ mag-arcsec}^{-2}$)
- In mid-IR, sky is brighter than $0 \text{ mag-arcsec}^{-2}$

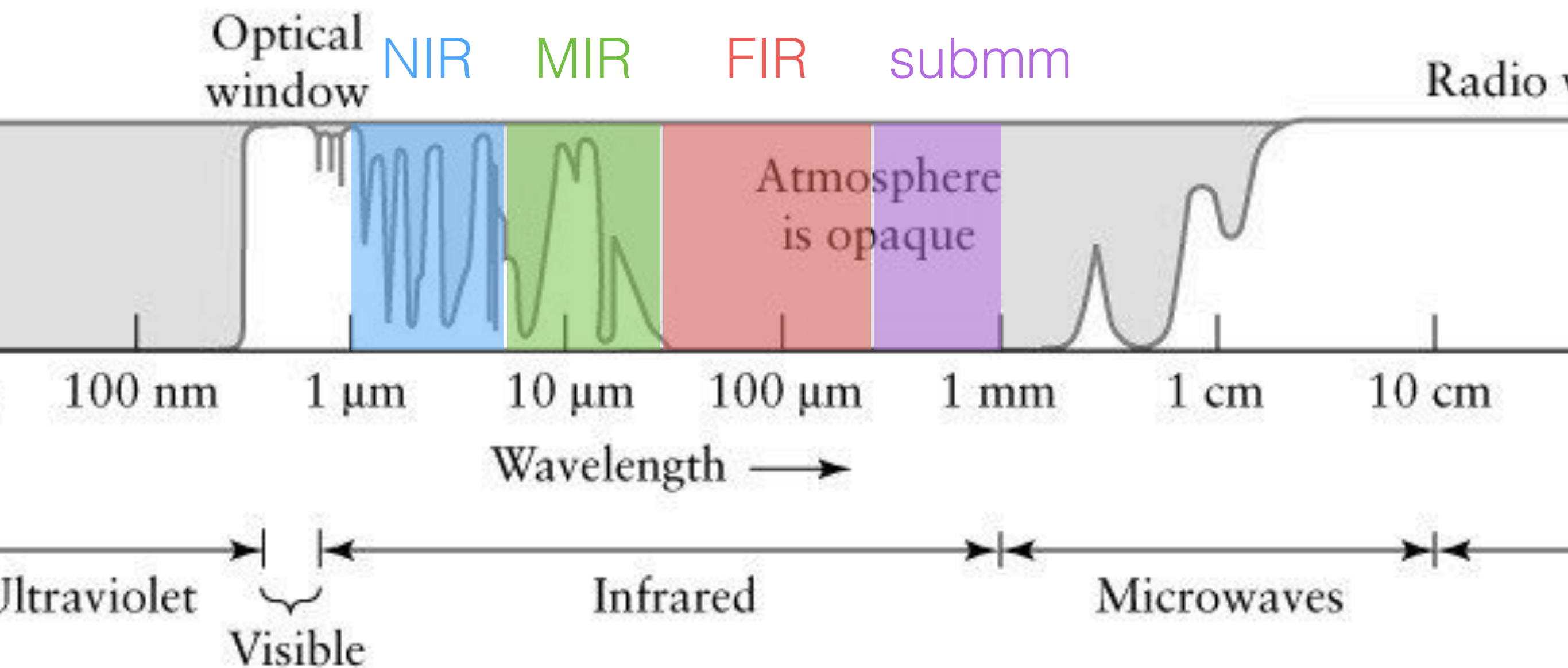
IRTF Secondary

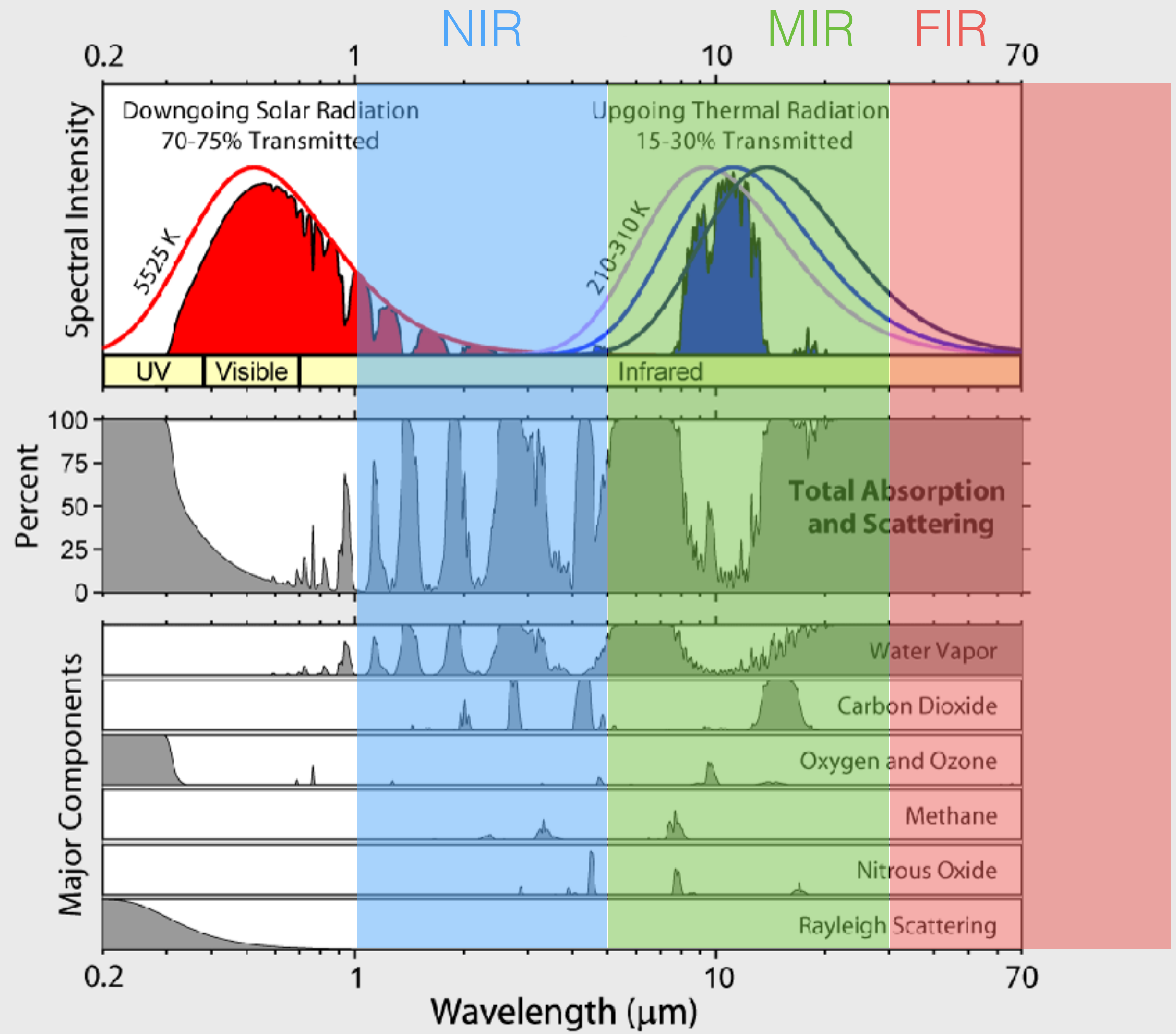


Infrared band sub-divisions

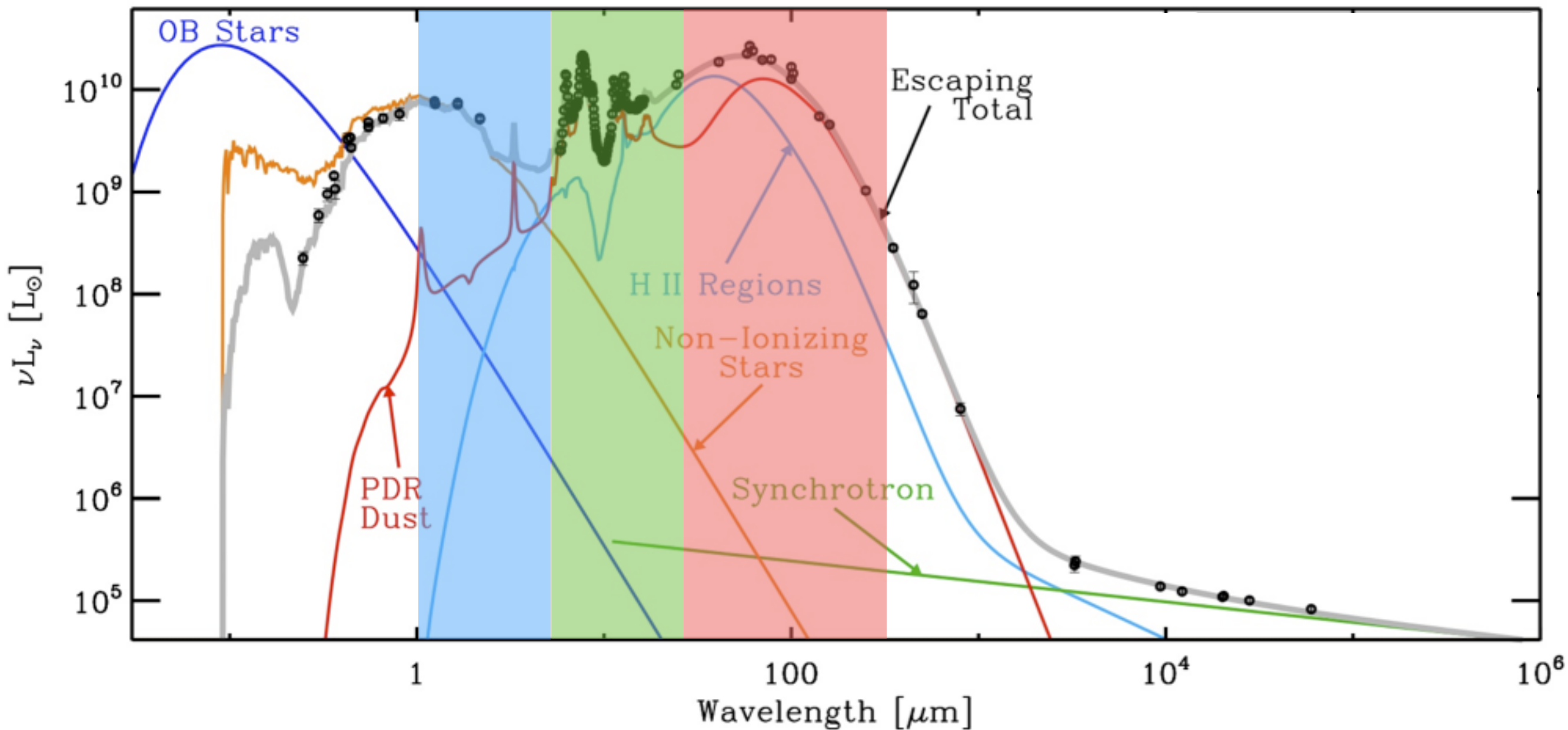
- **Near-infrared (NIR)** is the interval from 0.9-5.5 μm .
 - Short Wave Infra-Red (SWIR) is used specifically for 0.9-2.5 μm
 - *thermal* near-infrared refers to the part from 2.5-5.5 μm .
 - NIR detectors overlap with CCDs for wavelengths less than 1.1 μm and some of the newest IR devices will perform down to $\sim 0.5 \mu\text{m}$.
 - Because large format IR arrays are readily available, the NIR regime merges smoothly with the classical optical regime.
- **Mid-infrared (MIR)** extends from ~ 5 -30 μm
- **Far-infrared (FIR)** stretches from ~ 30 to $\sim 200 \mu\text{m}$.
 - Observations at these longer wavelengths are more challenging from the ground hence the interest in observations from the stratosphere.
- **Wavelengths longer than about 200 μm (or 0.2 mm) are now referred to as the sub-millimeter**, and although sub-millimeter astronomy is closely allied with infrared wavelengths in terms of the objects and regions of space which are studied, its techniques are more akin to those of radio astronomy.

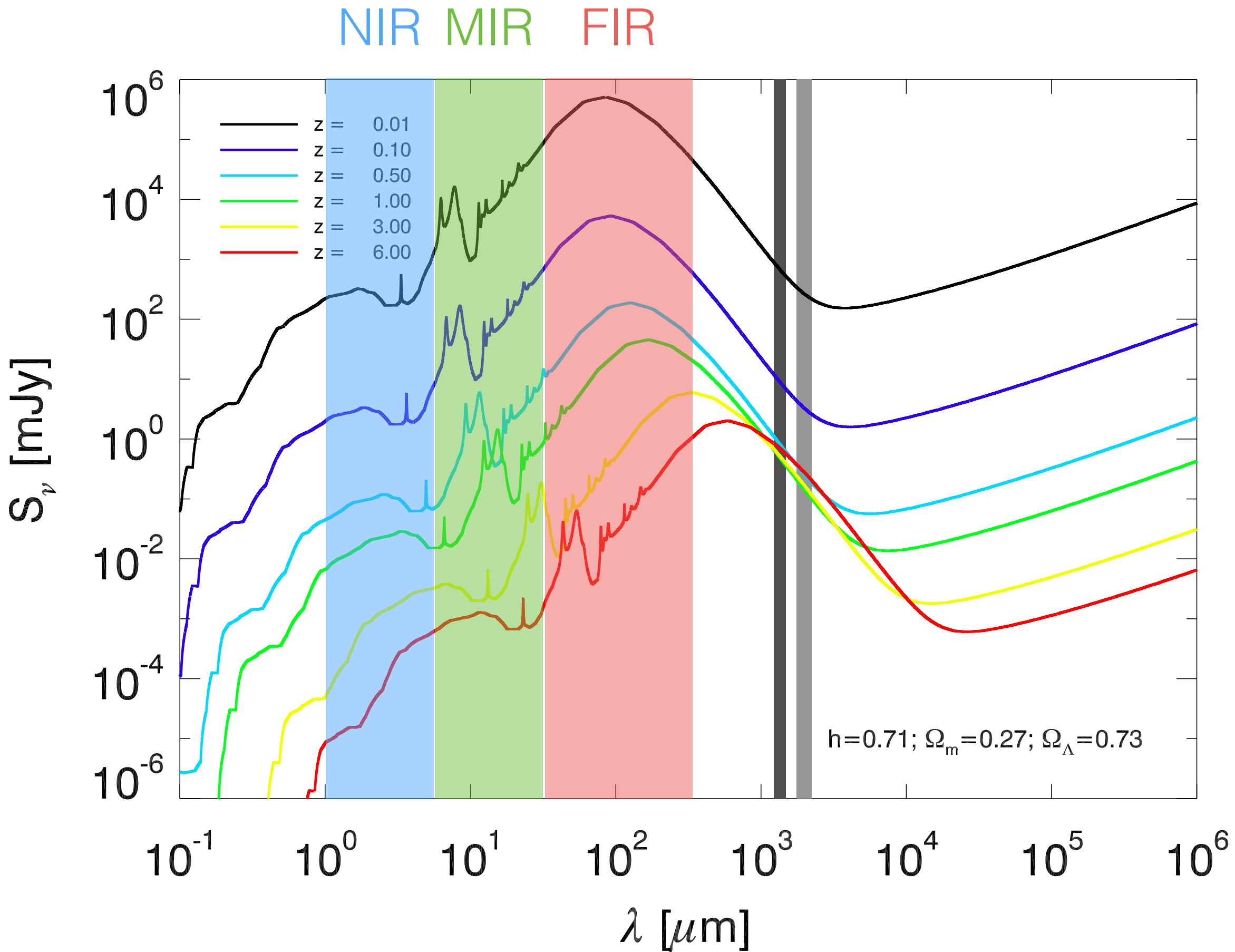






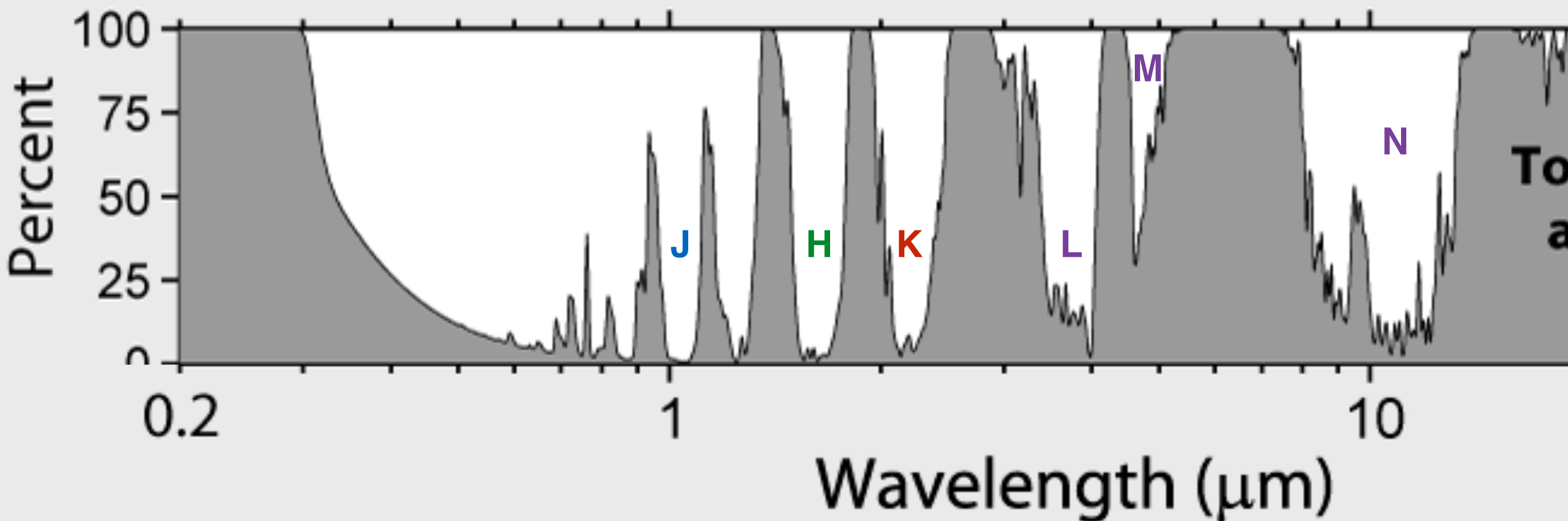
NIR MIR FIR M 82





NIR Windows Bands

- Water vapor (H_2O) and carbon dioxide (CO_2) block lots of IR radiation from space.
- Water vapor absorption is sensitive to altitude and wavelength.
- These windows of transparency allow us to define photometric bands.
- The standard windows are listed by central wavelength.



Counting up the Electrons...

$$V_{\text{total}} = V_{\text{bias}} + g * N_{\text{dark}} + g * \eta * N_{\text{sky}} + g * \eta * N_{\text{source}}$$

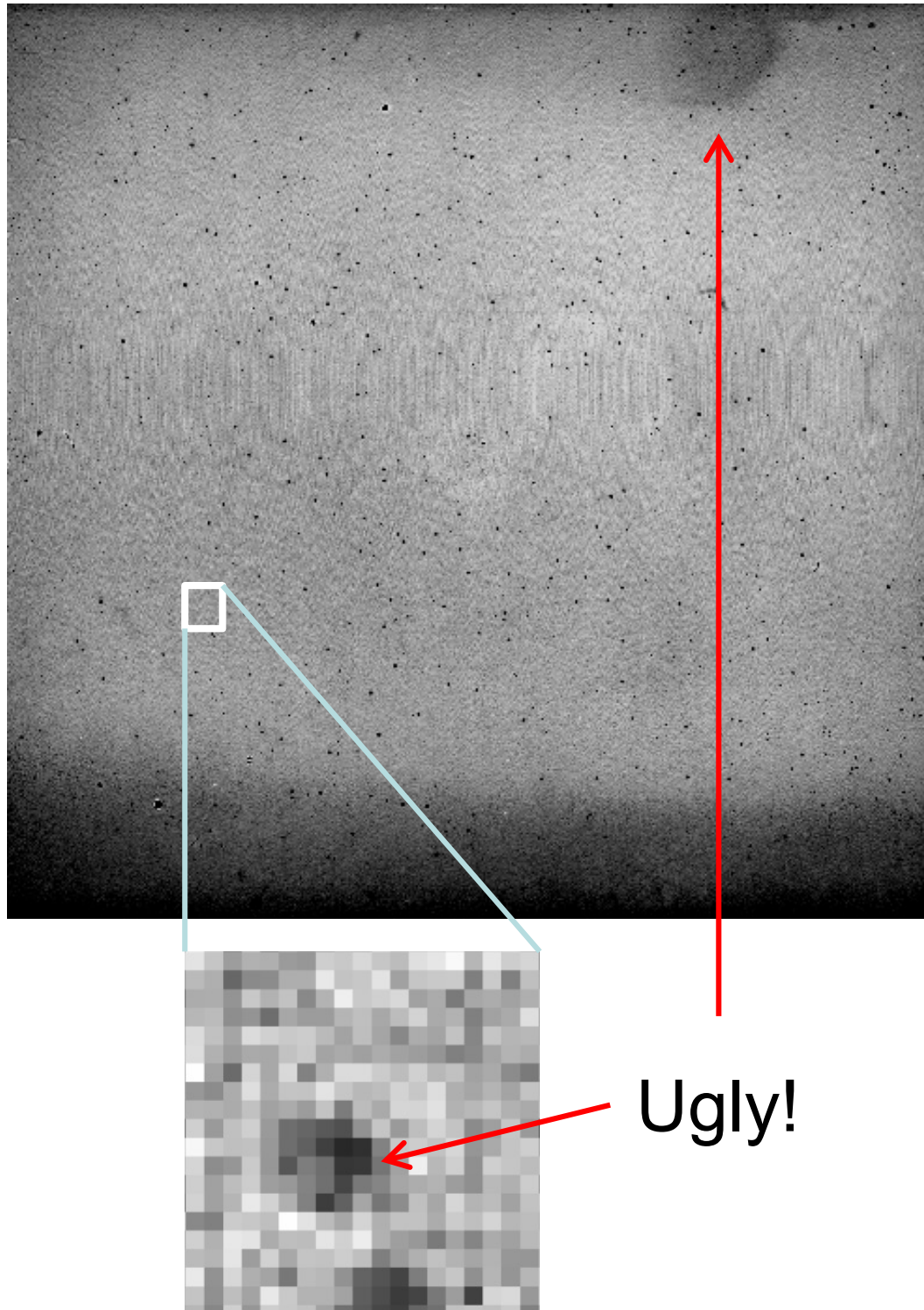
- V_{bias} is removed by double correlated sampling
- Take (multiple) dark images at same integration time as science observations, average, and subtract
- Divide by $g * \eta$
- Subtract constant N_{sky}

That's all there is to it!

All we need is to figure out $g * \eta$

Flatfielding

- Each pixel is independent, so $g^*\eta$ varies pixel-by-pixel
- “The only uniform CCD is a dead CCD” – Craig Mackay

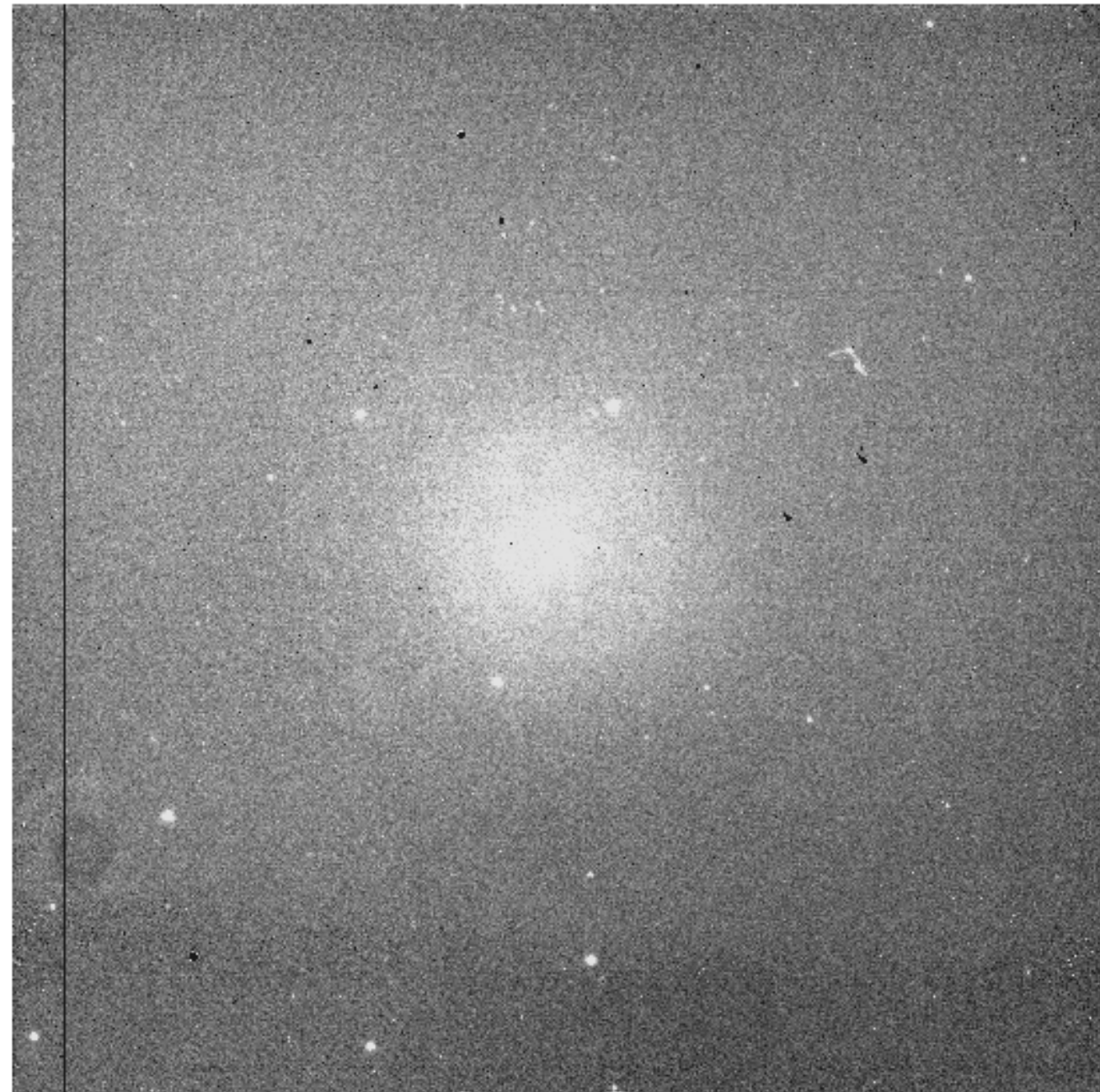


Generate a “flatfield” image

- Observe a uniformly illuminated target (dome screen, calibration screen)
 - Multiple images to improve statistics
 - Equal number with illumination off
 - Subtract (take out dark current, background)
 - Normalize to 1.0
- Can also use sky (more on that later)
 - Generate sky frame from multiple observations
 - Observe dark frames at same integration time
 - Subtract to remove dark current
 - Normalize to 1.0
- Wavelength dependent! Must do for each filter.

So let's give it a try.....

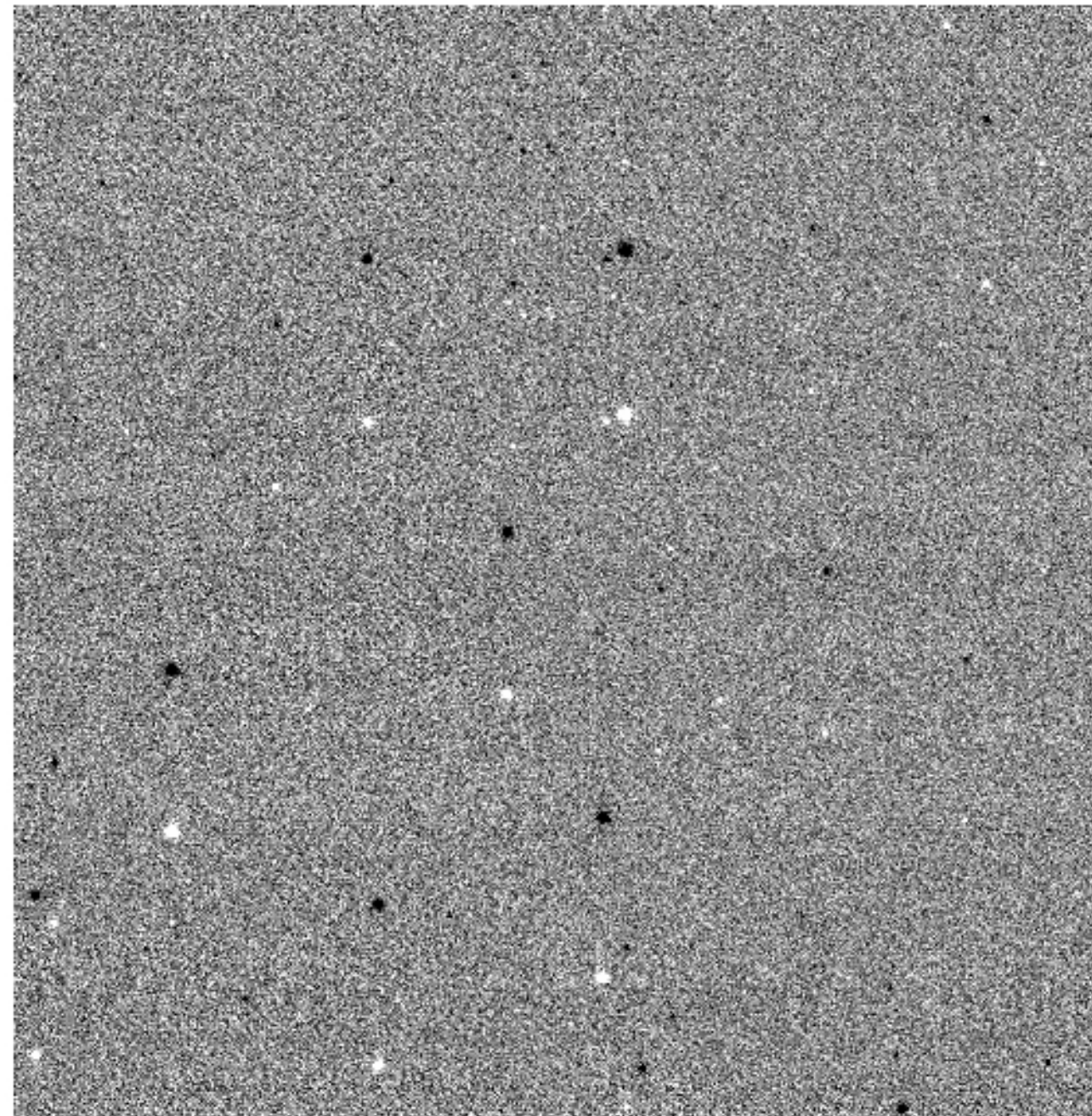
- Obtain science images
- Obtain calibration images
 - Dark frames at same integration time
 - Flatfield images of uniform target
- Subtract dark frame from science images
- Divide dark-subtracted images by flatfield
- → Image of science field with uniform sky level
- Subtract (constant) sky level from image
- But, here is what we get....
 - Still pretty ugly!



Small flatfield errors on sky still larger than faint science targets

Since the sky is the problem...

- Subtract out the sky (or as much as possible) *before* the flatfield correction
- Obtain two images of field, move telescope between
- Subtract two images
 - Eliminate almost all sky signal
 - Subtracts out dark current, maverick pixels
- Divide by flatfield image
- Result has almost no sky structure

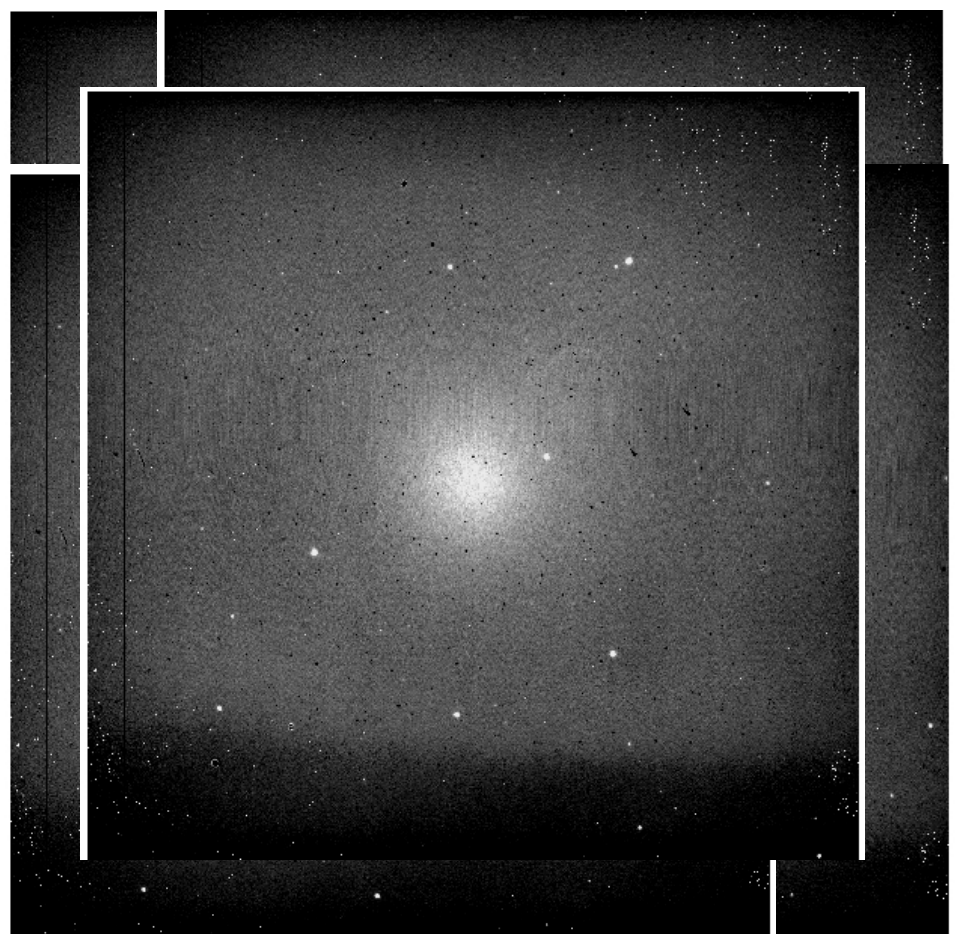


Subtracting sky minimizes effects of flatfield errors
(but noise increased by 1.4)

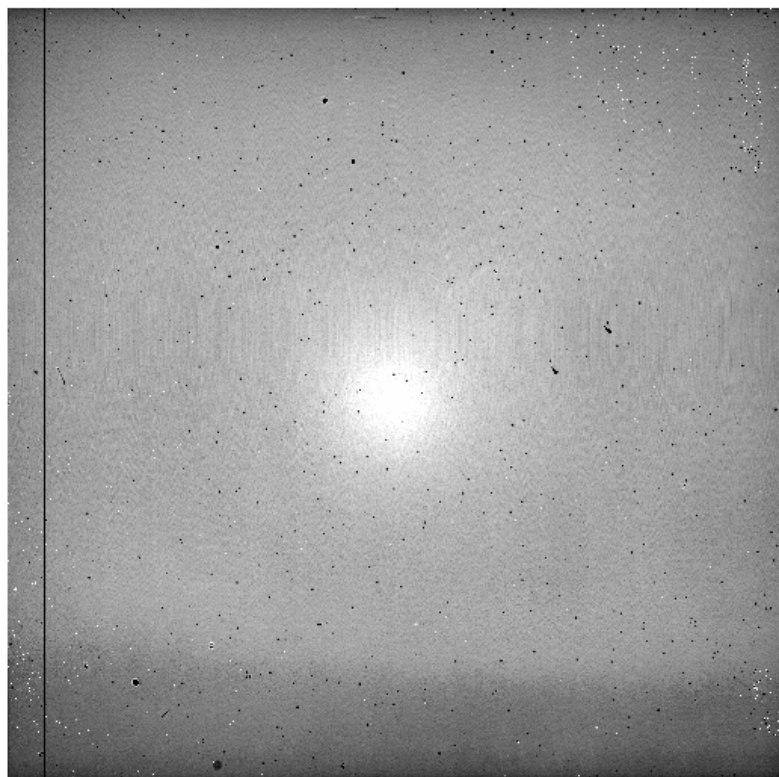
Typical sequence for IR imaging

- Multiple observations of science field with small telescope motions in between (dithering)
 - Sky background limits integration time, so multiple images necessary anyway
 - Moving sources on detector samples sky on all pixels
 - Moving sources on detector avoids effects of bad/noisy pixels
- Combine observations using median filtering algorithm
 - Effectively removes stars from result → **sky image**
 - Averaging reduces noise in sky image
- Subtract sky frame from each science frame → **sky subtracted images**
- Divide sky subtracted images by **flatfield** image
 - Dome flat using [lights on] – [lights off] to subtract background
 - Sky flat using [sky image] – [dark image] using same integration time
 - Twilight flats – need to be quick, since twilight is short at IR wavelengths
- Shift and combine flatfielded images
 - Use reference star common to all images to determine relative shifts
 - Rejection algorithm, bad pixel mask, or median can be used to eliminate bad pixels from final image

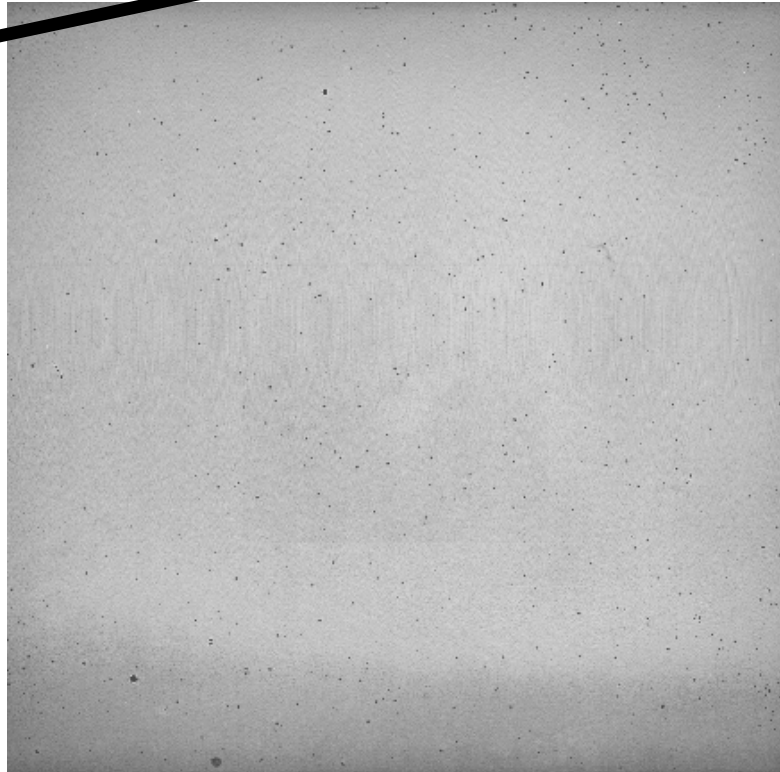
Here's what it looks like....



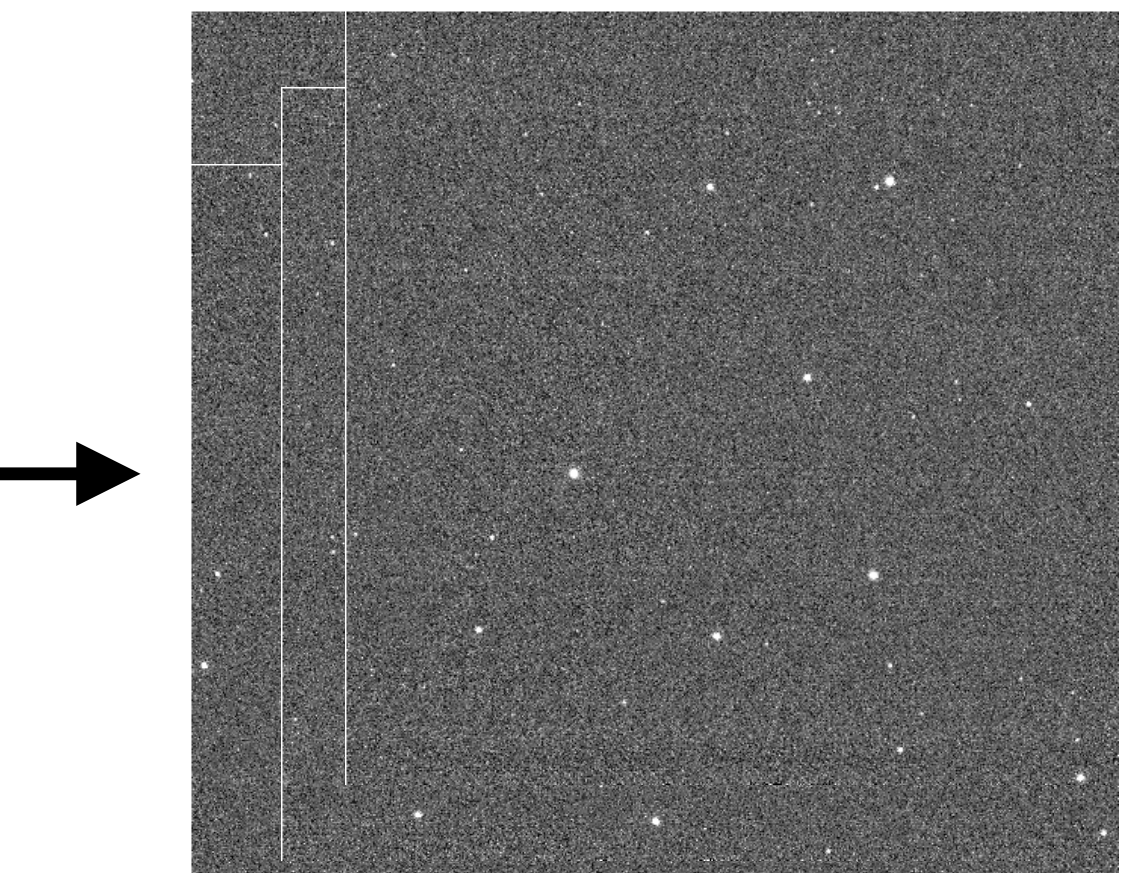
Median



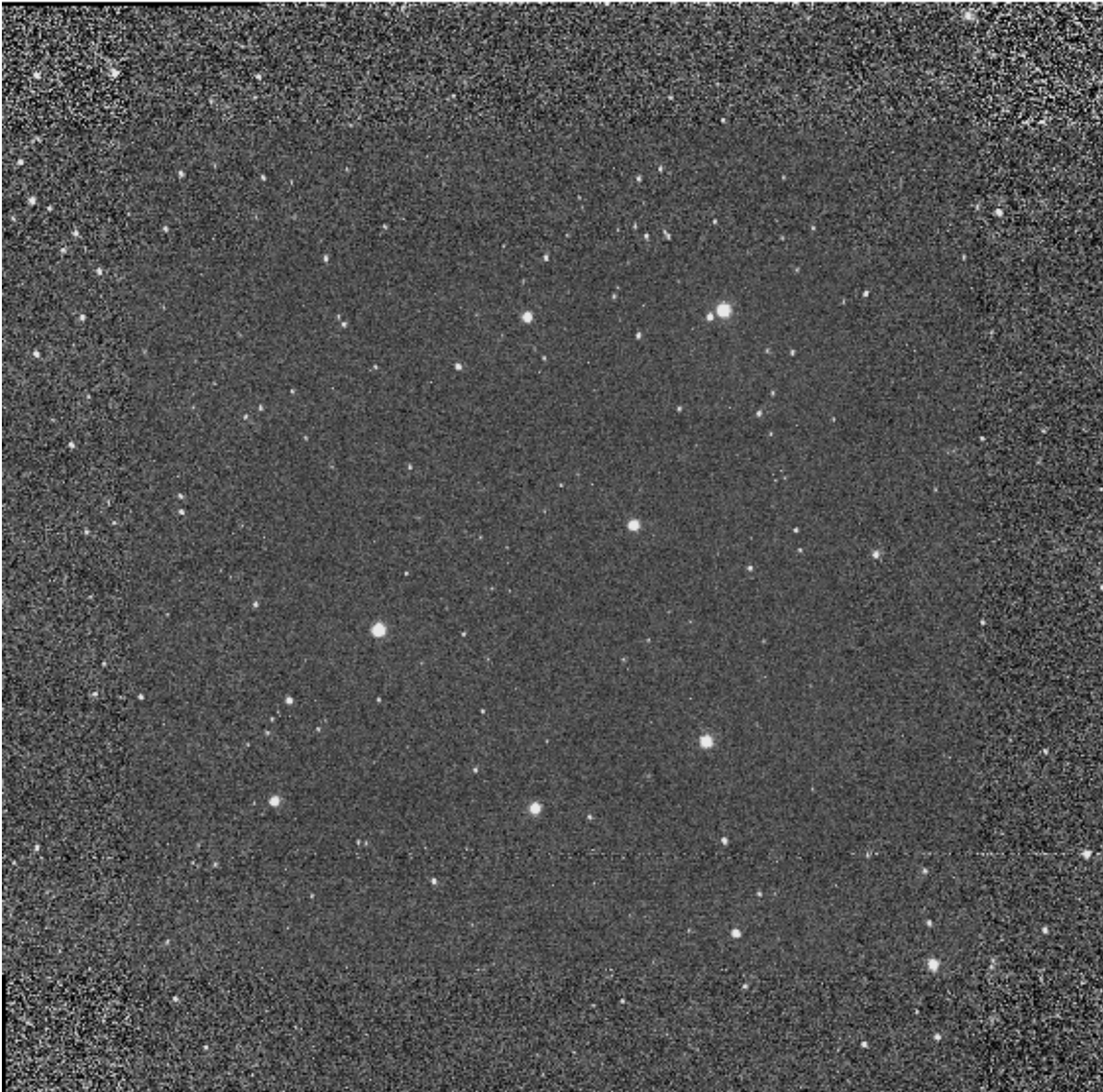
Subtract sky,
divide each by



Flatfield



Shift and combine images



- NGC 7790, Ks filter
- 3 x 3 grid
- 50 arcsec dither offset

Bad pixels eliminated
From combined image

Higher noise in corners
than in center (fewer
combined images)

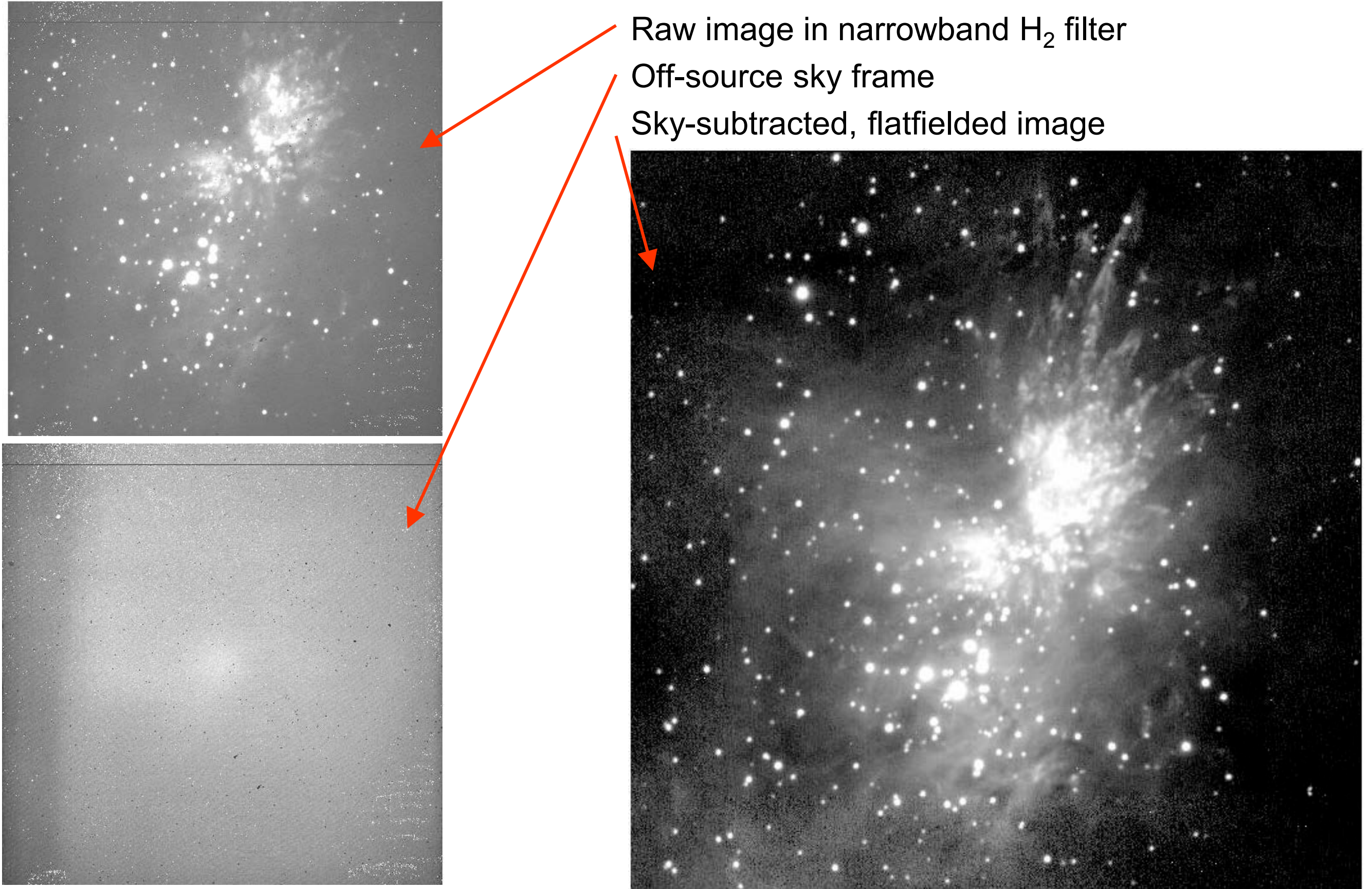
This works fine in sparse fields, but what about crowded fields, extended targets?

- In addition to dithered observations of science field (still necessary for sampling good pixels), it is necessary to obtain dithered observations of a nearby sparse field to generate a sky image.
- Requires additional observing overhead, but this is the only way to obtain proper sky subtraction

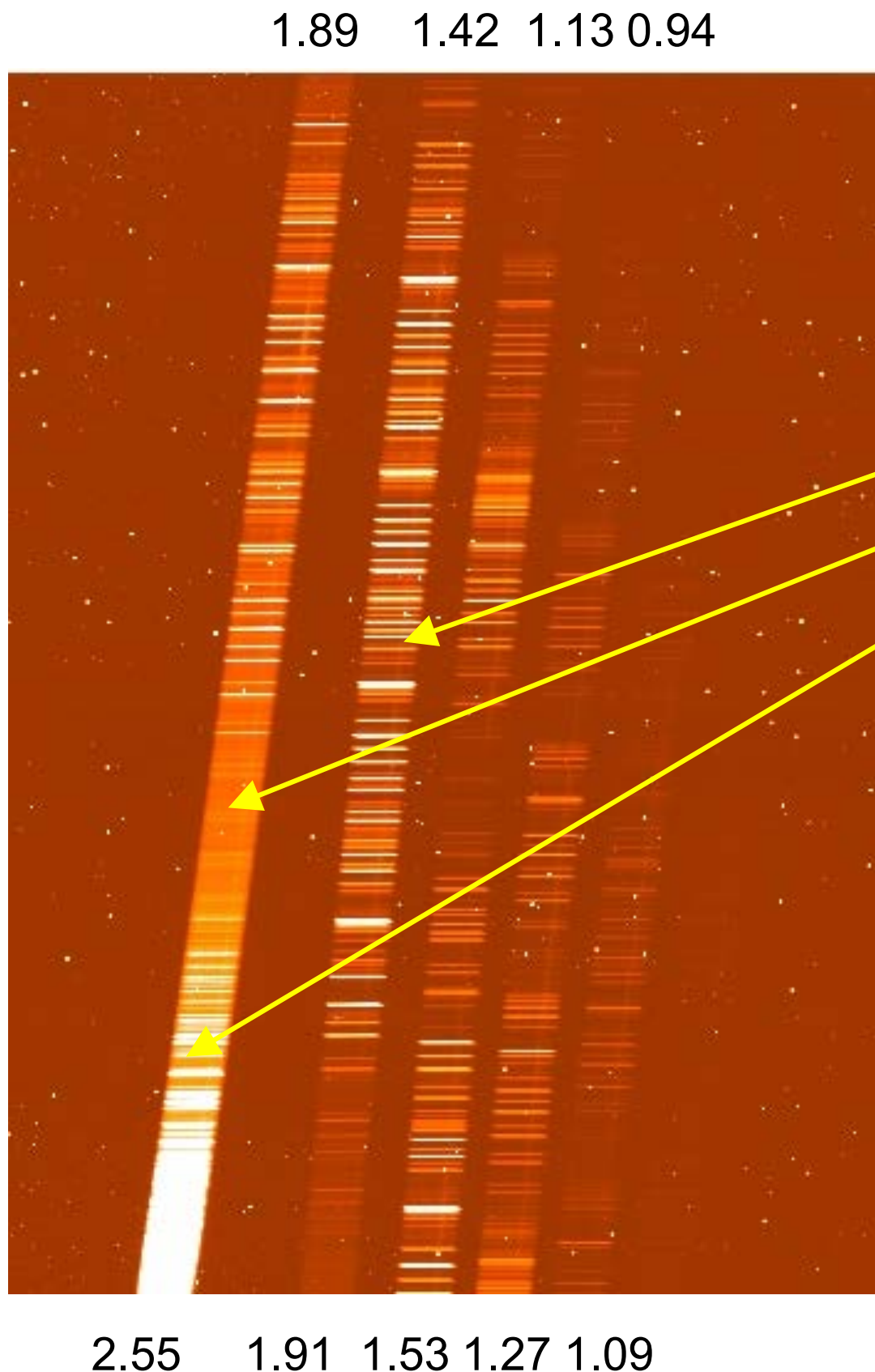
“And if you try to cheat, and don’t take the proper number of sky frames, then you get what you deserve”

--Marcia Rieke

An example: M42

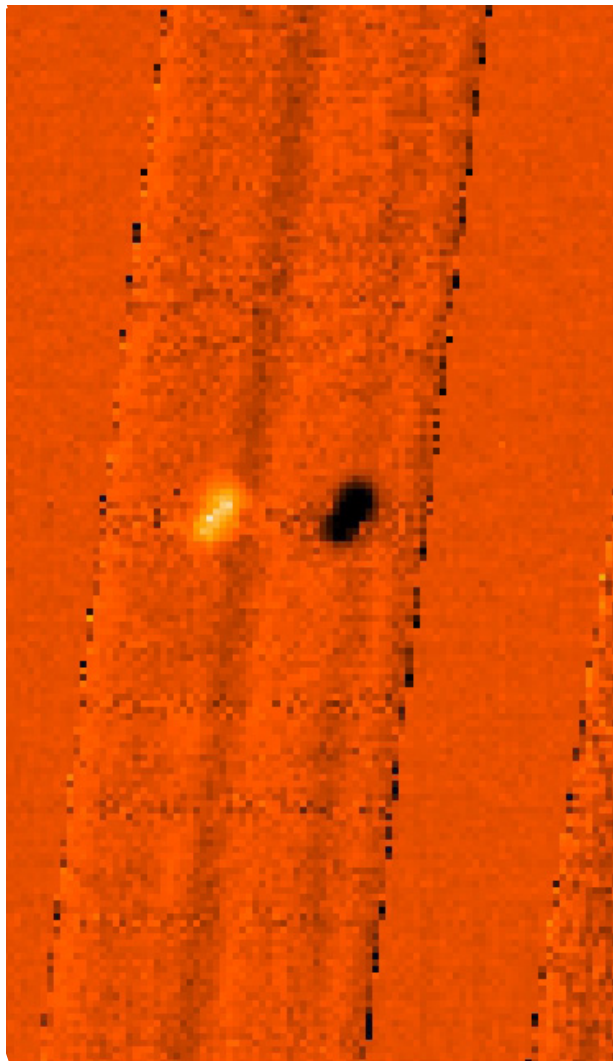
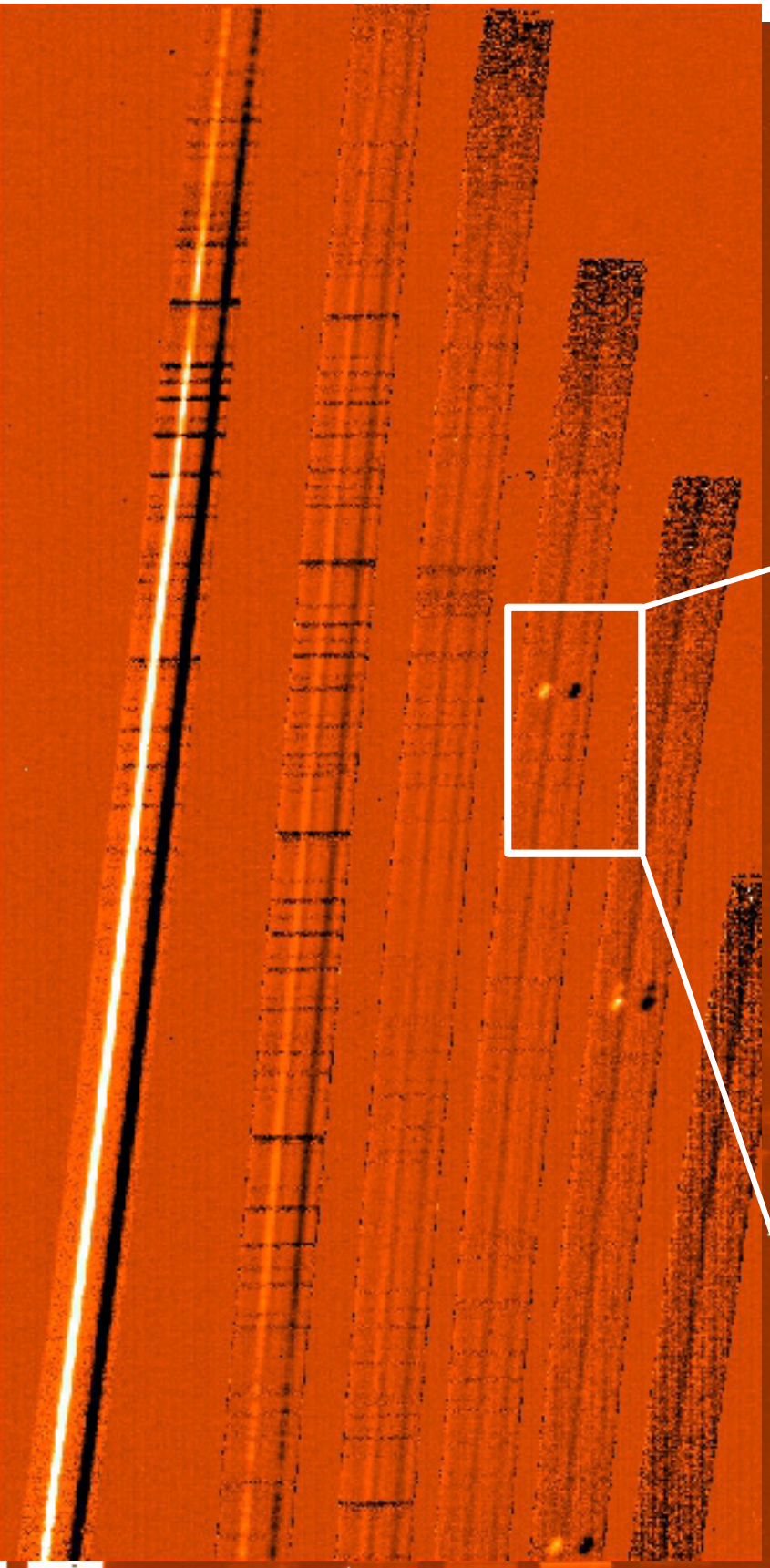


Spectroscopy uses similar strategy



- Example: GNIRS spectrum
 - $R \sim 2000$, cross-dispersed
 - 0.7 – 2.5 μm in six orders
- Strong, wavelength-dependent sky
 - OH emission lines 0.8 – 2.3 μm
 - Thermal continuum 2.0 + μm
 - Atmospheric absorption > 2.3 μm shows up as emission in thermal
- Need to subtract out sky

Subtract sky by dithering along slit



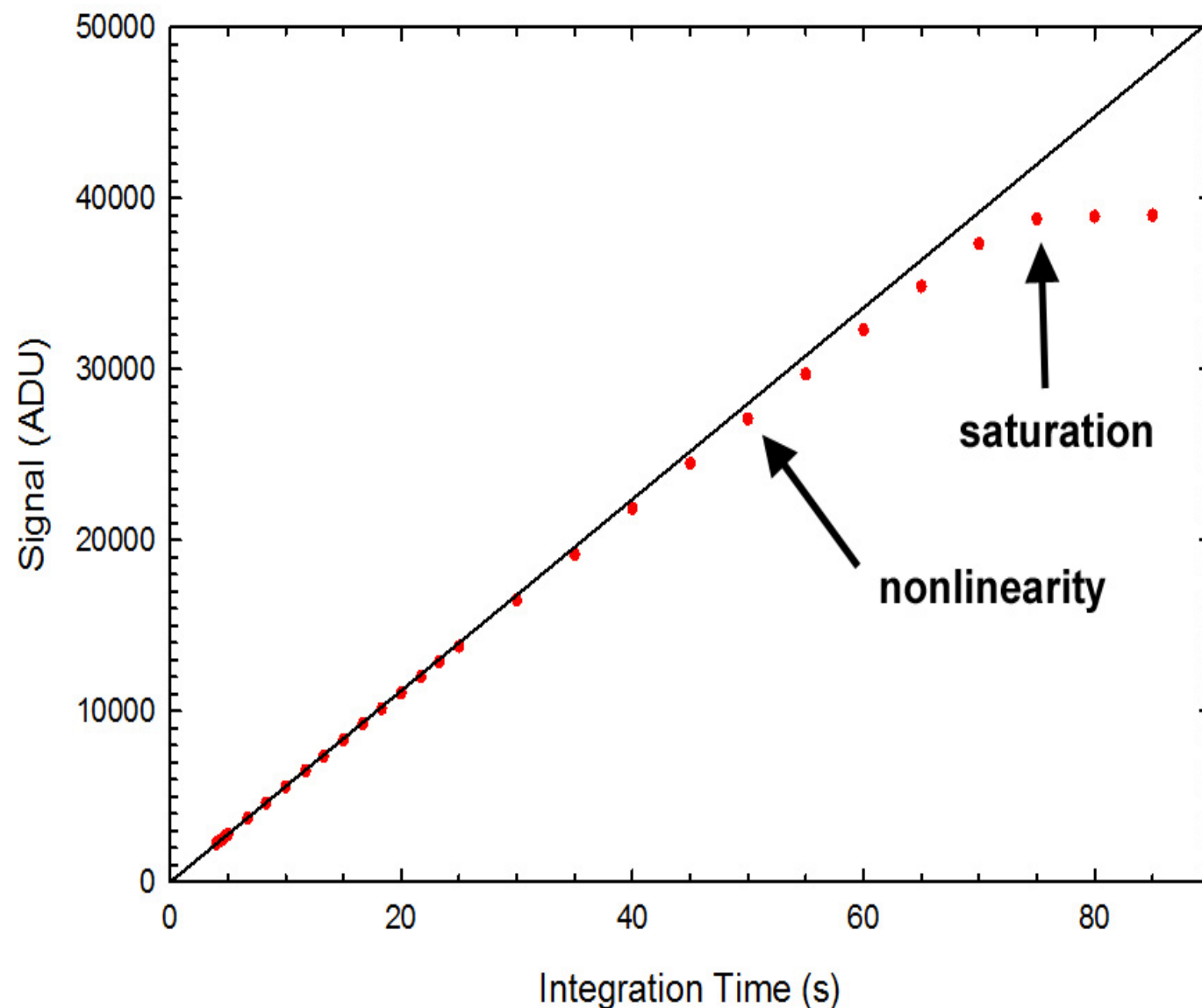
- Initial 600s exposure
- Move target 4 arcsec along slit, expose
- Subtract
- Eliminates most of sky lines
 - OH emission time variable
 - Remove residual sky using software
 - Additional noise in OH lines

Additional “Features” to Consider

- Issues pretty much common to all IR arrays:
 - Nonlinear response
 - Bad pixels
 - Geometric field distortion
 - Pupil Ghosts
 - Fringing
 - Image Persistence
 - “Phobos” or “tachyon” events
- Some of these can often treated silently as part of any scripted data reduction process.
- Some are unavoidable, but can be alleviated by observing strategy.

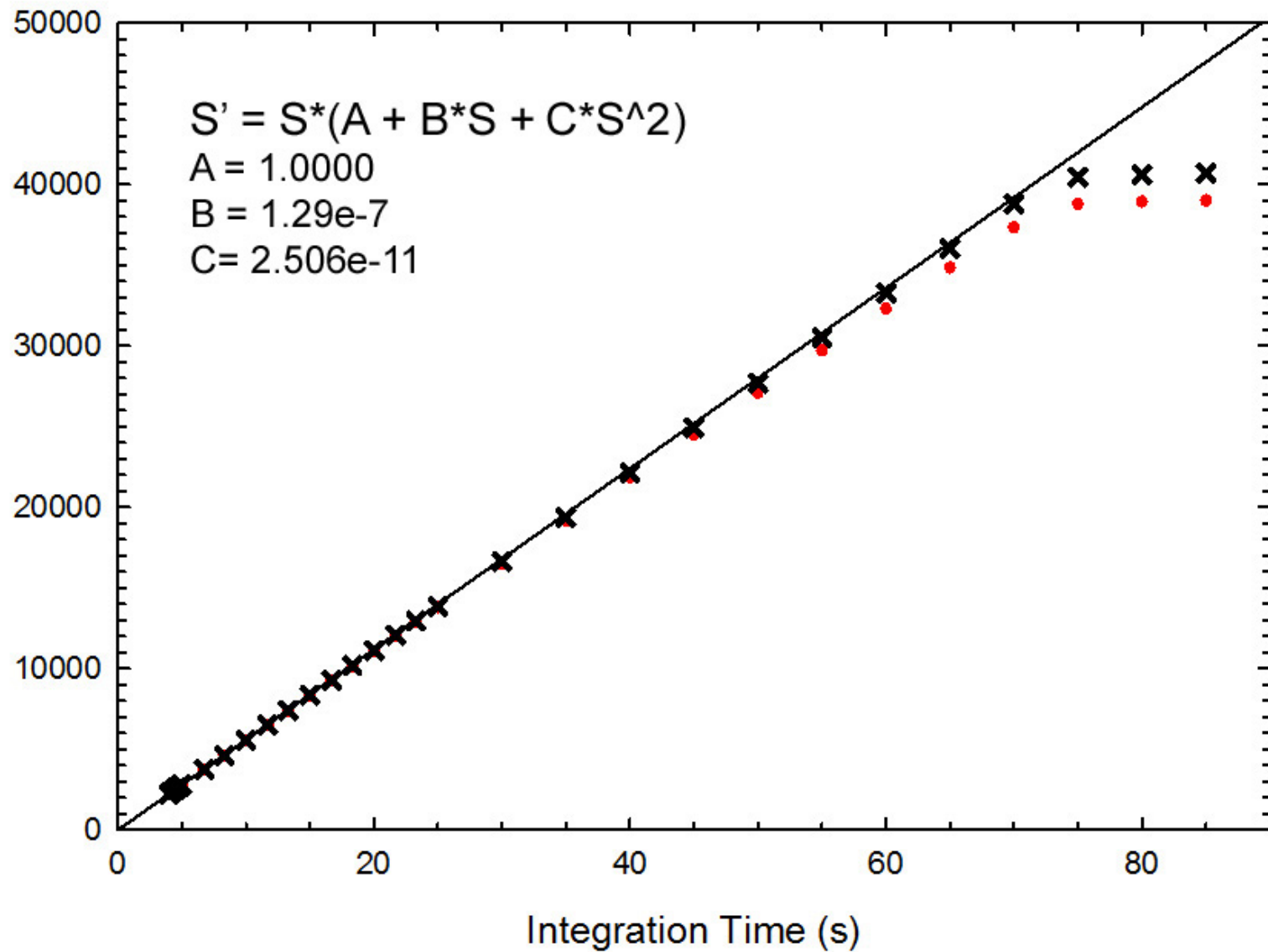
Detector Nonlinearity

- Biasing a detector pixel creates a potential well, essentially a capacitor, on which charge is collected
- As potential well fills up, capacitance increases, so measured voltage/charge relation on unit-cell readout changes [$V = q/C(V)$]
- More charge required for $\Delta V \rightarrow$ sublinear response



Nonlinearity typically $\sim 1\%$ at 50% full well, $\sim 3\%$ at 85% full well, but will depend on the array and bias voltage

Detector Nonlinearity (2)

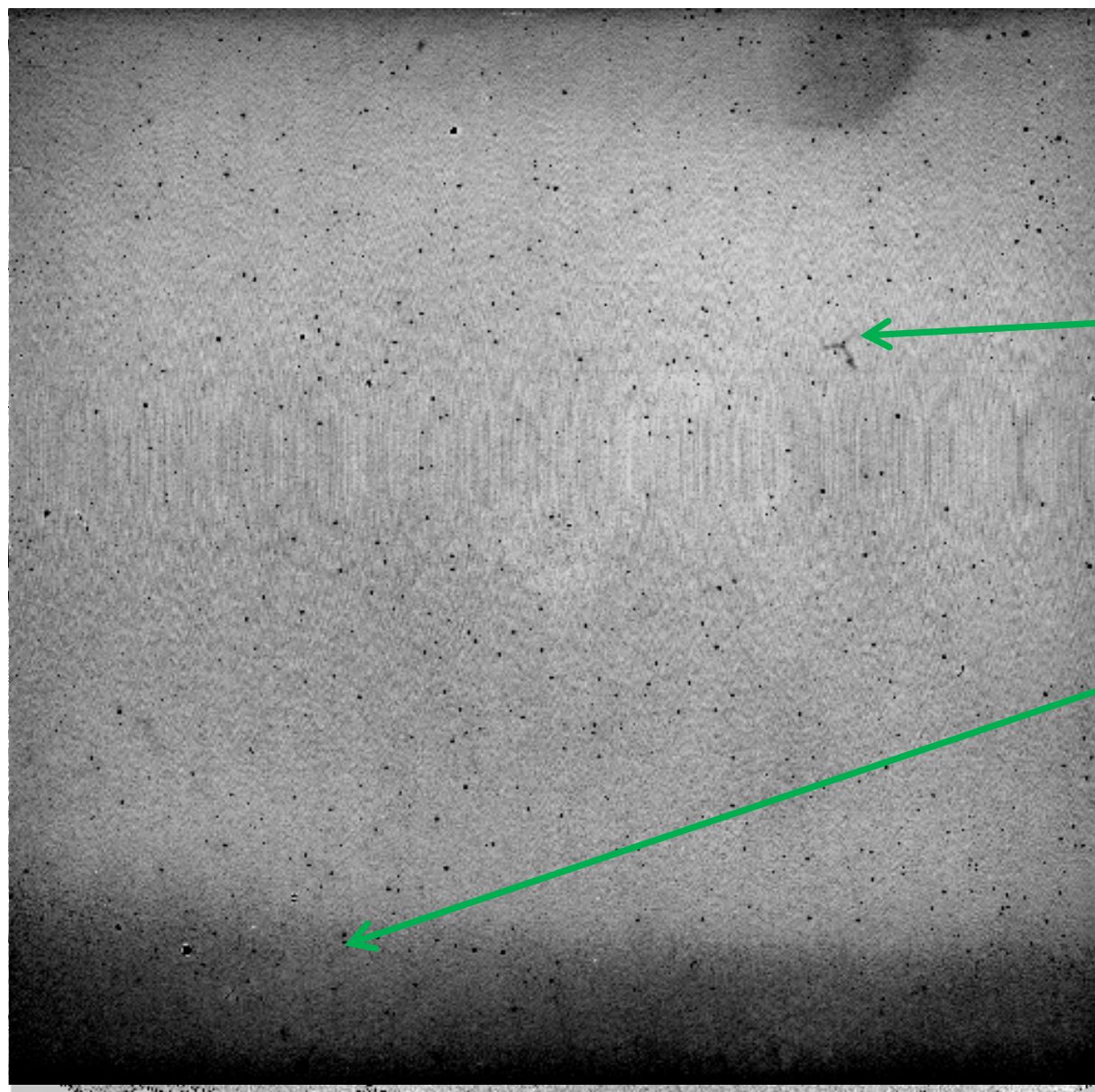


- Nonlinearity can be fit fairly well by quadratic function
- Generally can correct linearity to better than 1% to 85% of full well
- Must correct raw data!

If possible, strategy is to avoid linearity issues by staying below 50% full well while observing

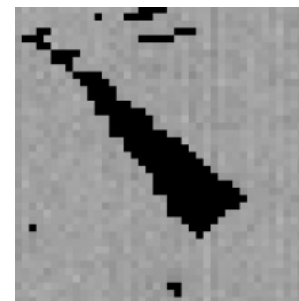
Array Defects

- In addition to sensitivity variations (cf. flatfielding), arrays are generally far from pristine.
- Hybridizing, thinning, A/R coating, thermal stress.....

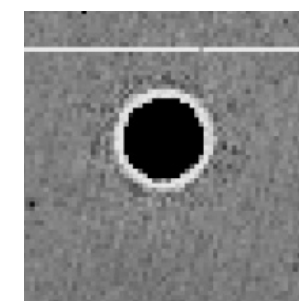


Cracks!

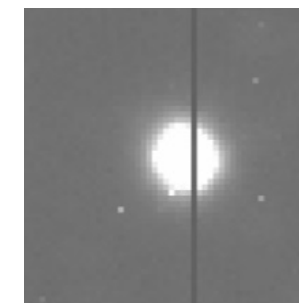
No contact (during hybridizing)



Arrowhead (dig)

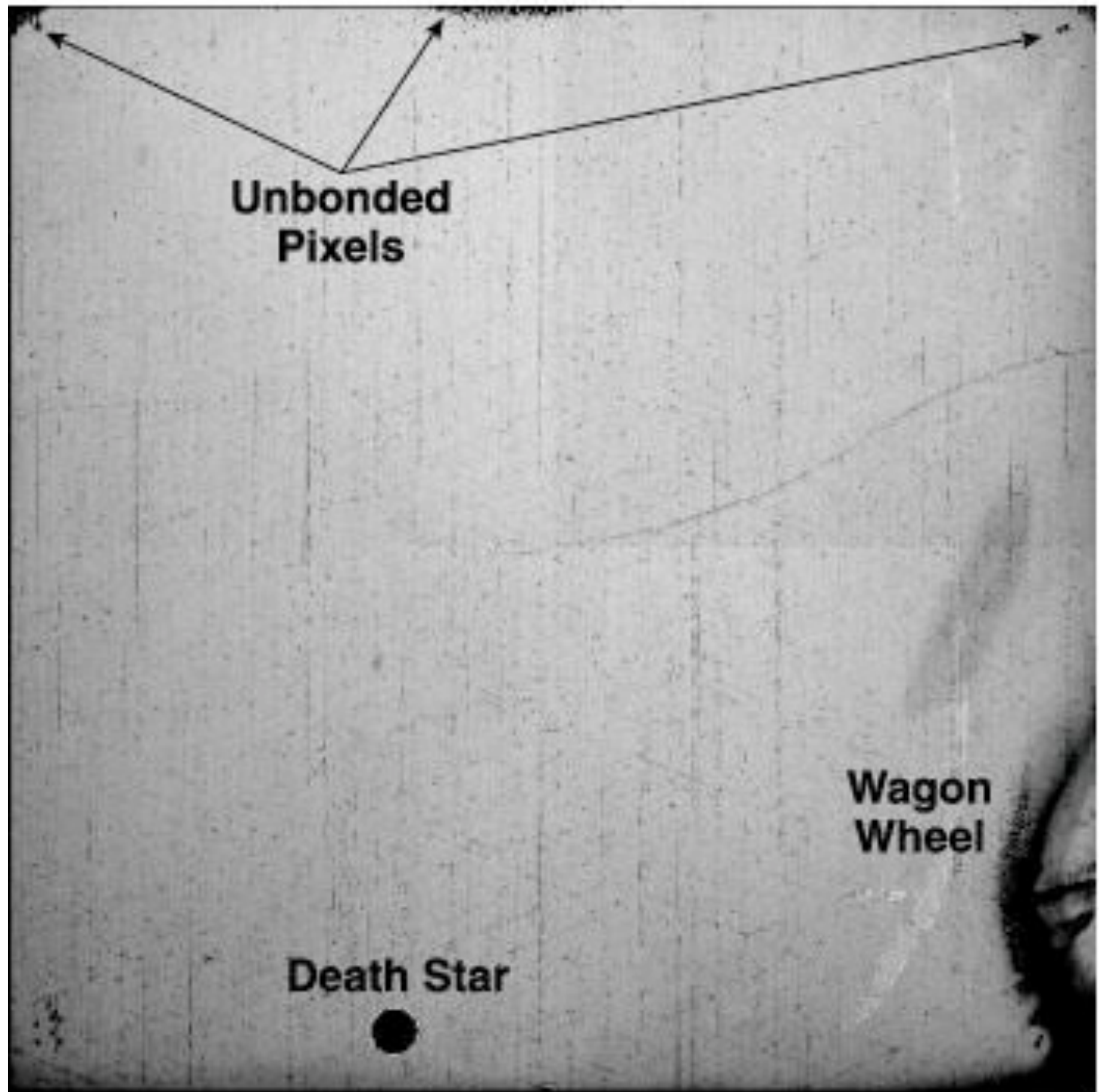


Dead Row
Photoemitting Defect

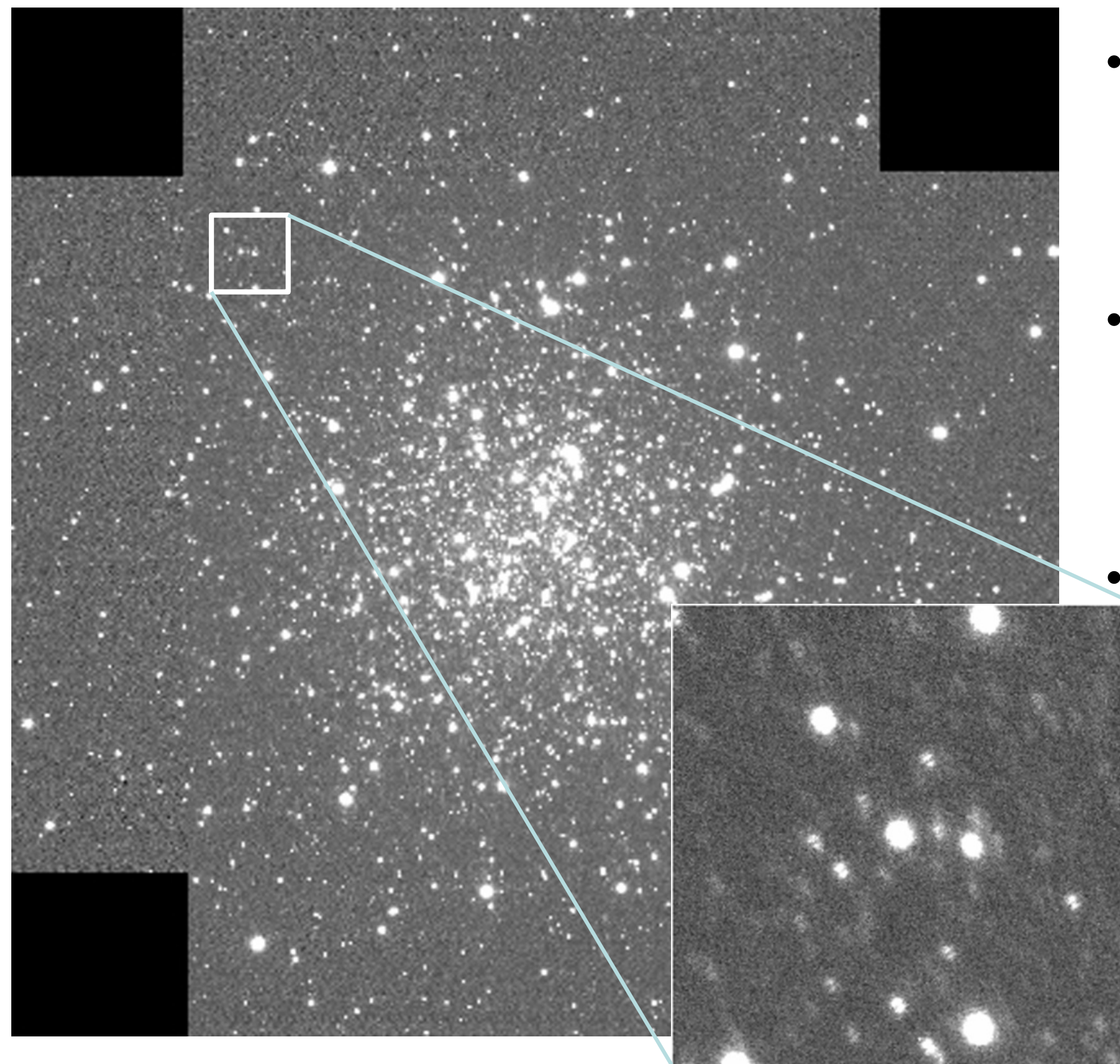


Dead Column
through star
Help!

From WFC3/IR

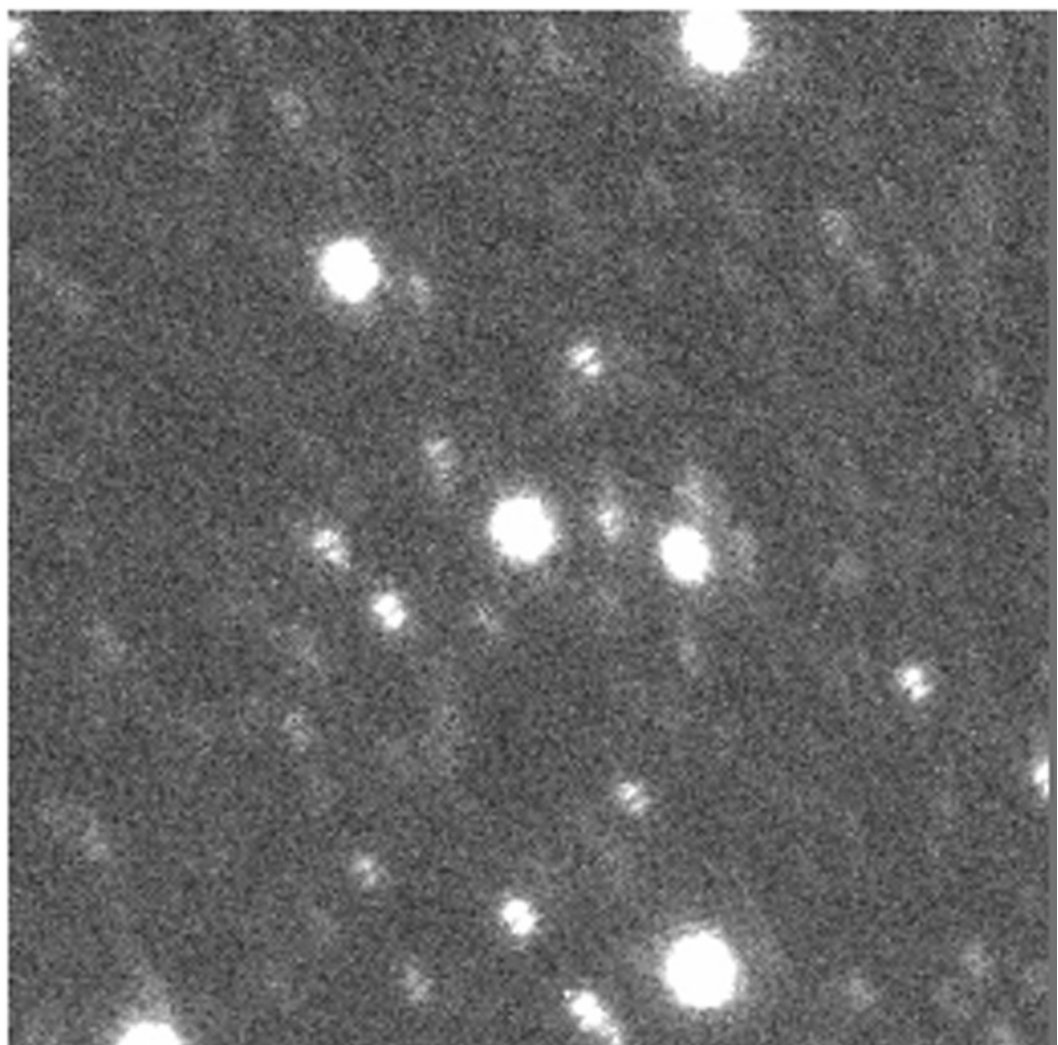


Field Distortion

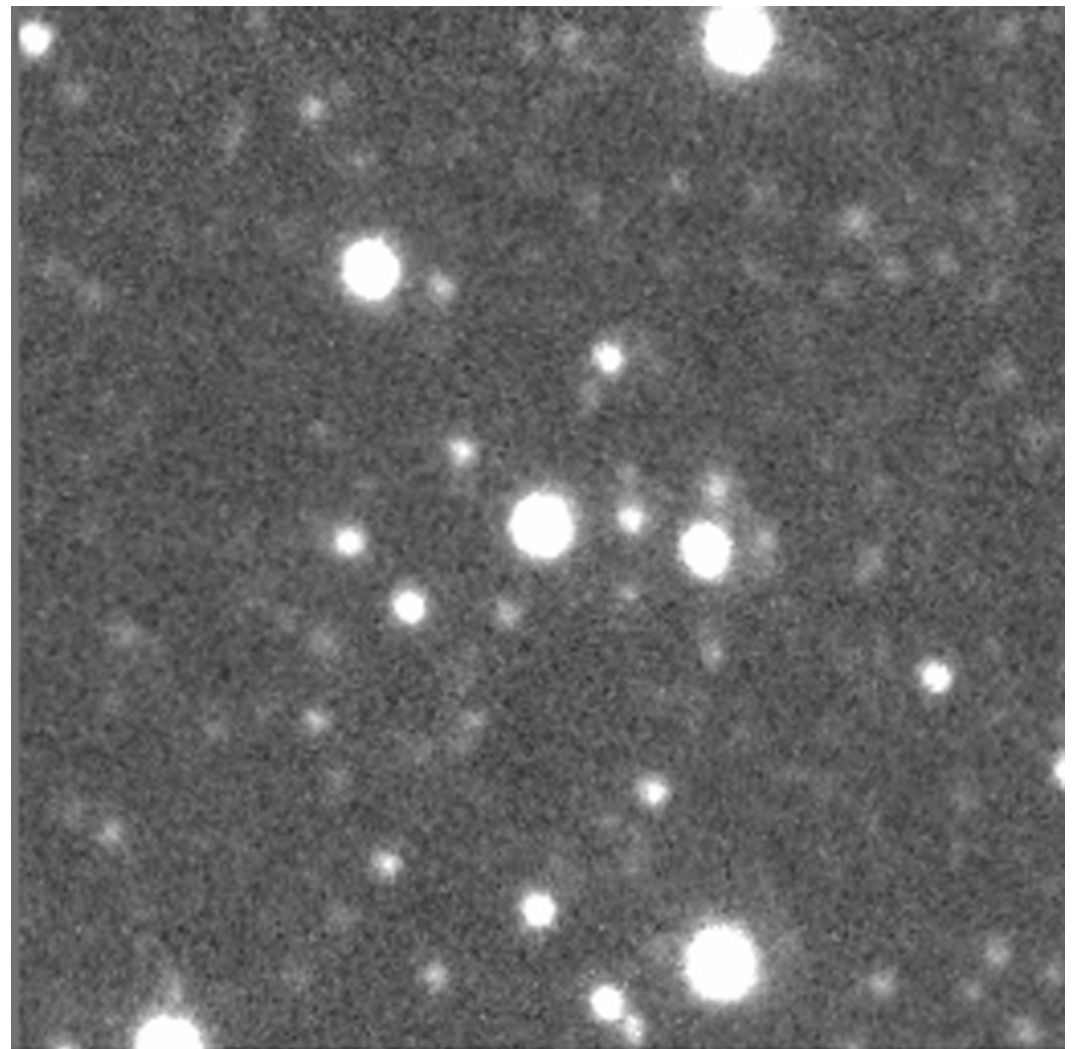
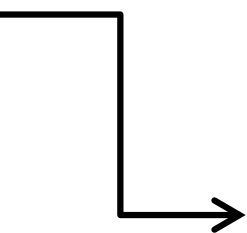


- Telescope focal surfaces are generally not flat, whereas detectors are
- Field reduction and flattening optics generally result in some field distortion
- This leads to poor registration of images when generating maps or combining many dithered images

Field Distortion



- Tasks such as IRAF ‘geomap’ can be used to map distortion from astrometric field
- ZEMAX analysis of optical system can be used as input to ‘geomap’.
- Task ‘geotran’ will correct distortion

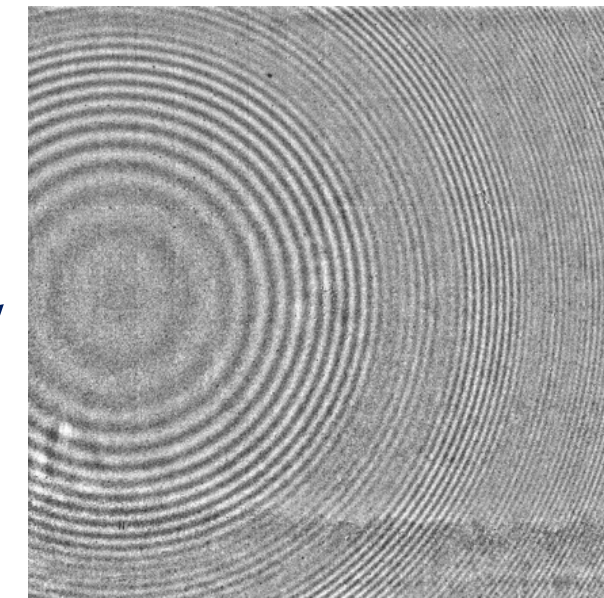


Fringing

- In both CCDs and IR arrays, the detector becomes transparent near its long wavelength response limit
- Sky emission lines can produce Fabry-Perot like interference fringes in the image
- Interference fringes can also be produced between parallel surfaces within the instrument optics.
- As with pupil ghosting, solution is to create a template which can be fit to the fringe pattern for subtraction (IRAF task ‘rmfringe’)

OH H-band Fringe Removal

Template



'rmfringe'
+ 'rmpupil'

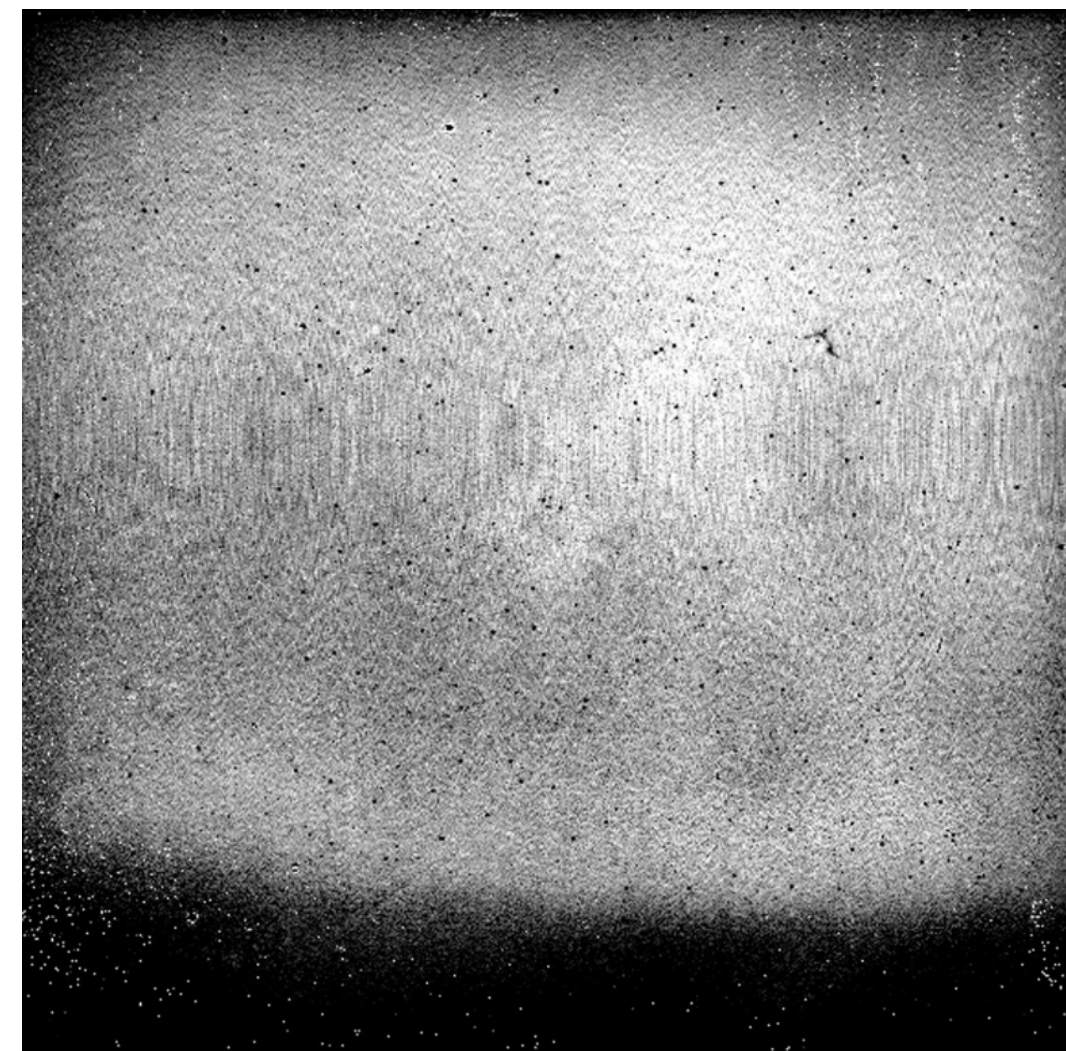
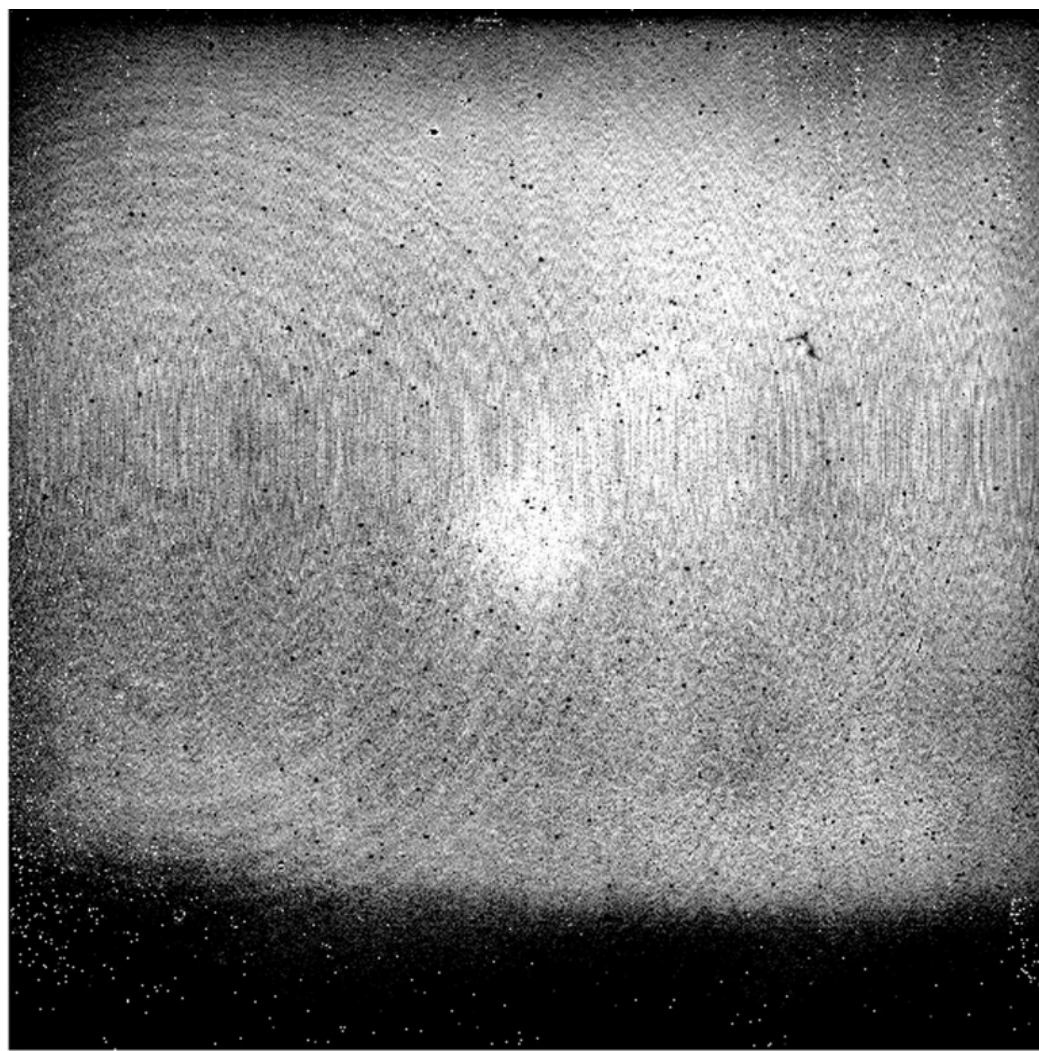


Image Persistence

- Long-exposures under low background following an exposure at a high flux level can show an “afterimage” of the previous exposure.
 - Afterimage can persist for multiple images, with long decay time
- Physical cause seems to be ‘traps’ generated by high flux levels, which decay slowly, creating elevated dark current.
 - Generally, but not always, a feature of older detector arrays, particularly InSb
 - Effect appears to be significantly reduced in recent generation HgCdTe arrays
 - Anecdotal evidence that persistence is less evident when detector is maintained in high vacuum for long periods (mythology?)

Image Persistence (2)

- Effect can be annoying and make data reduction difficult
- Example: GNIRS spectrum following acquisition of target shows afterimage of acquisition field.

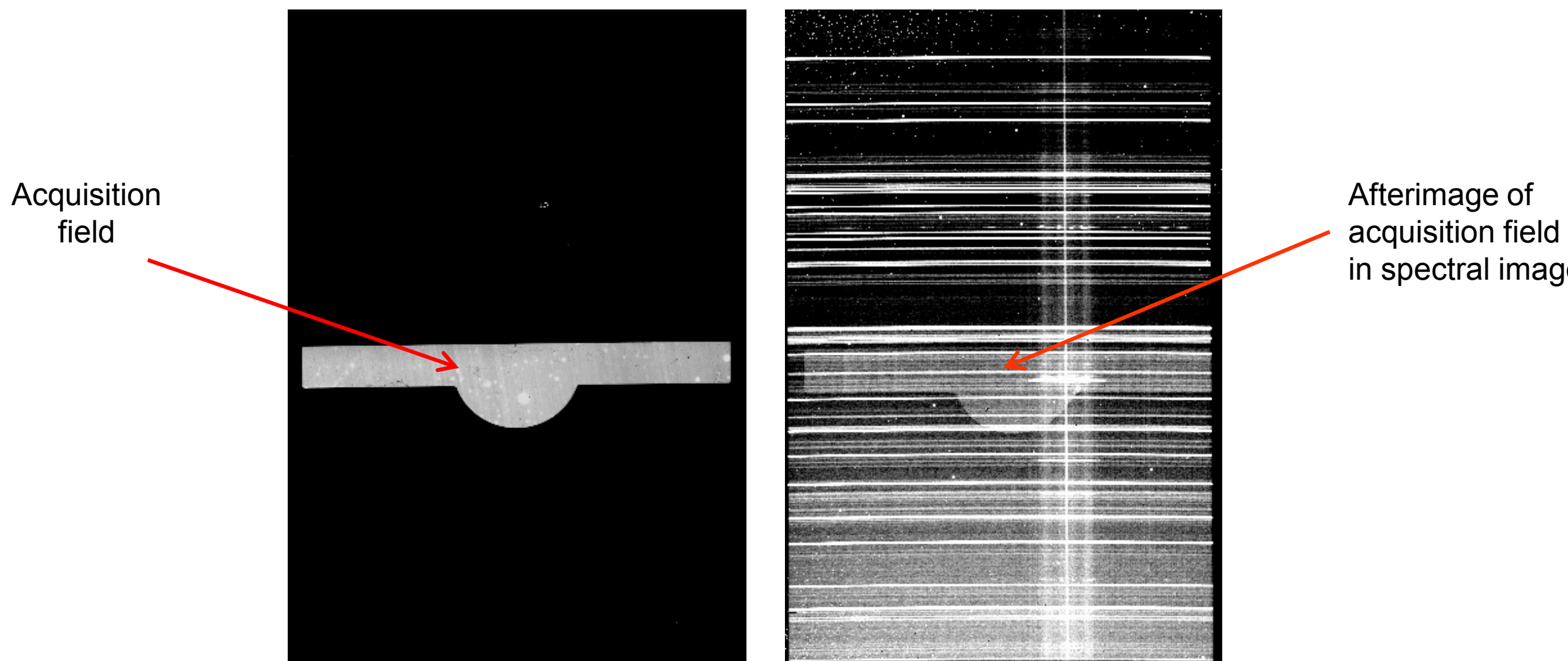


Image Persistence (3)

- Much mythology associated with minimizing this effect
 - Frequent readout during ‘idle’ time between exposures
 - Taking short ‘junk frames’ between acquisition and science images
 - These seem to be of limited utility
- Best approach is to minimize or avoid the effect through observing strategy
 - In instruments which use the same array for acquisition and science images, utilize narrowband filters for acquisition and keep signal levels well below full well
 - For spectroscopy, use different dither offsets from the nominal target position for bright telluric standard and faint science exposures to avoid persistence from the telluric spectra.

You can't avoid persistence issues for bright sources

- impacts repeatability - higher scatter than Poisson errors
- dither so that source is on different pixels

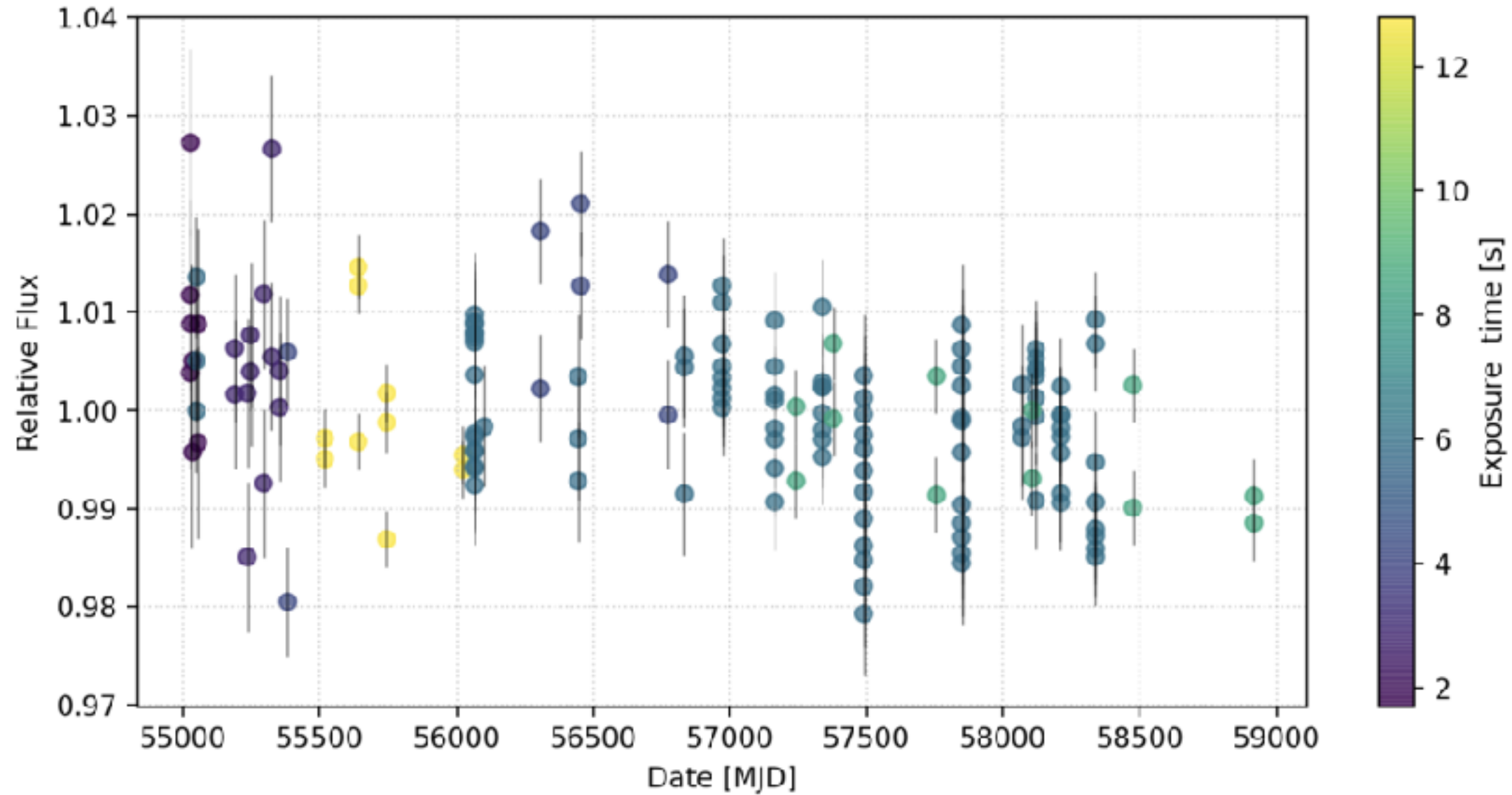
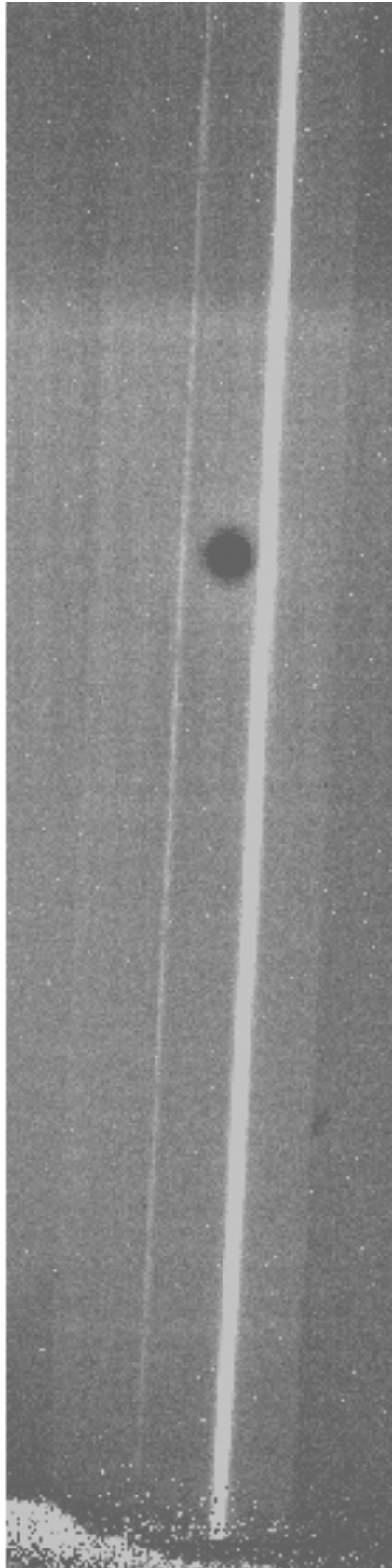


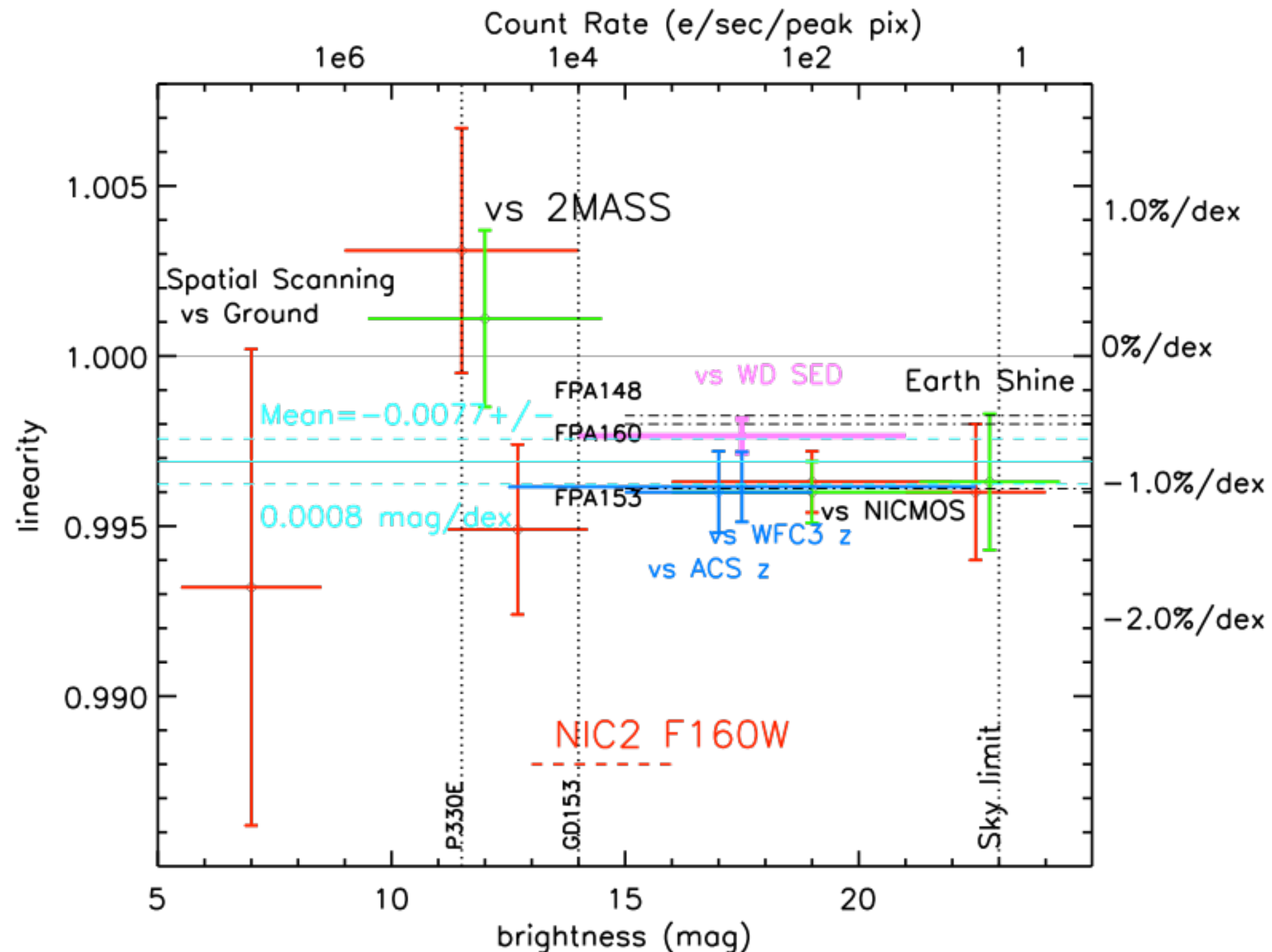
Figure 1: Aperture photometry measurements of the spectrophotometric standard star GD153 measured over several years by WFC3/IR in the F160W filter. The 1.00 line on the y axis corresponds to the median value FLT measurements. Each point represents a single exposure of the star, and the various colors/colorbar represent the exposure time of the observation. The error bars are the computed Poisson and background error of the photometry (and does not include other noise terms such as calibration uncertainty). Note that a large majority of this data did not use the dithering strategy discussed above. Plot from [ISR 2020-10](#).

‘Phobos’ Events



- ‘Phobos’ or ‘tachyon’ events are crater-like features which can appear almost anywhere on the array
- Generally appear as a ‘hole’ with negative signal often with a surrounding annulus of positive signal
- May be result from internal stresses within the detector causing an electrical discharge
 - Anecdotal evidence that they occur more often shortly after the array has been cooled from ambient
 - But they are also seen after the instrument has been cold for a long time
- Not much can be done except to hope that they don’t occur on an important part of the detector

IR detectors exhibit another kind of non-linearity - not just with total counts (i.e. charge) but with **count-rate (i.e. source magnitude)**



Originates from the physical phenomenon where the detector's response to incoming light becomes non-linear at high photon flux rates, **meaning the signal produced doesn't scale proportionally with the incident light intensity**

- primarily due to limitations in charge carrier lifetime and recombination dynamics within the semiconductor material itself - at high production rate, charge carriers interact with each other
- recombine faster i.e. the detector becomes less efficient at converting photons to electrical signals as the photon arrival rate increases.

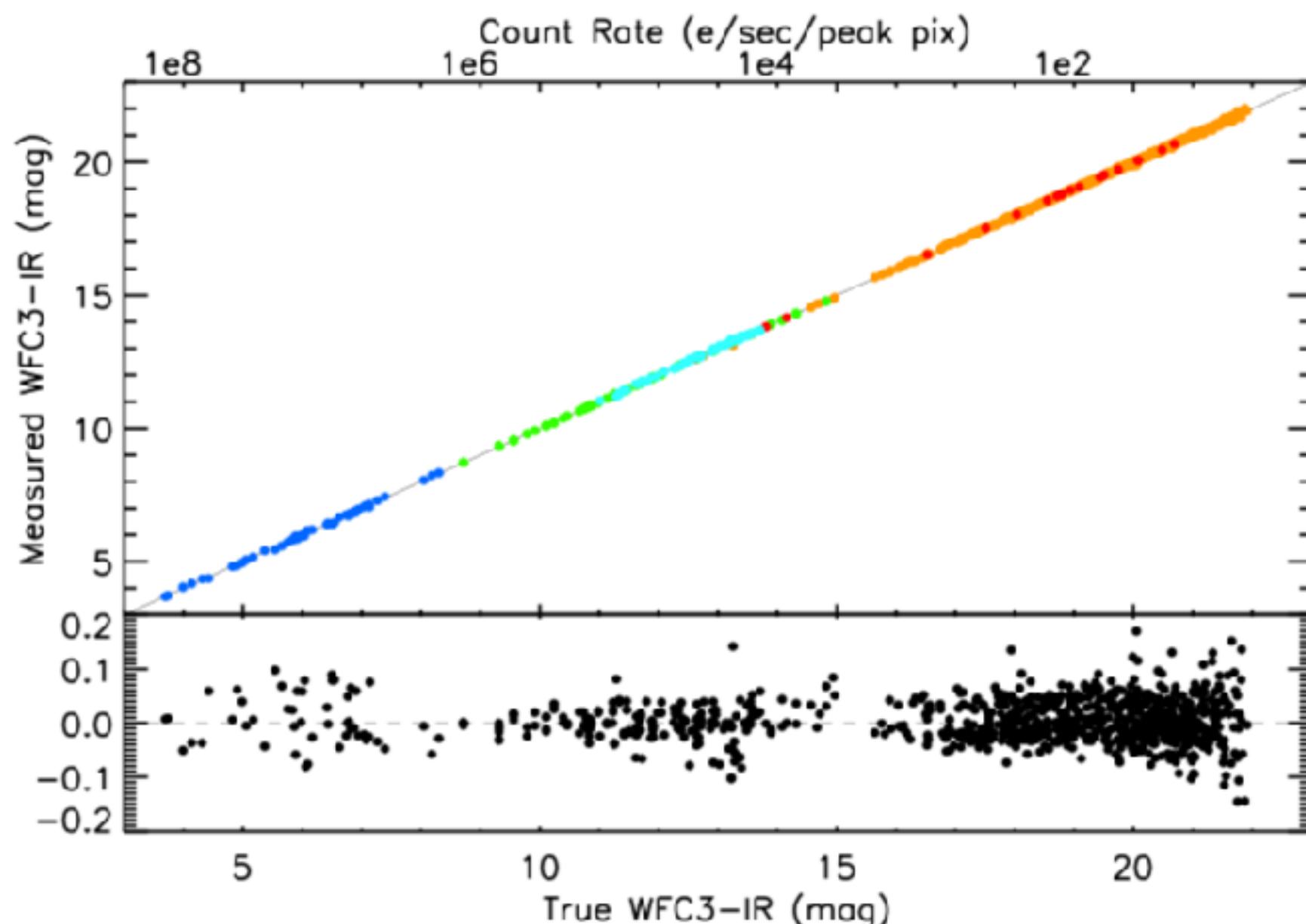


Figure 3: Magnitude ladder used to measure the CRNL for WFC3 over 16 astronomical magnitudes. Bottom plot shows residuals from the best fit 0.0077 ± 0.0008 mag/dex result presented in Riess et al. (2019).

And after all of that, IR detectors degrade over time, and their sensitivity changes (CCDs also do this in-orbit).

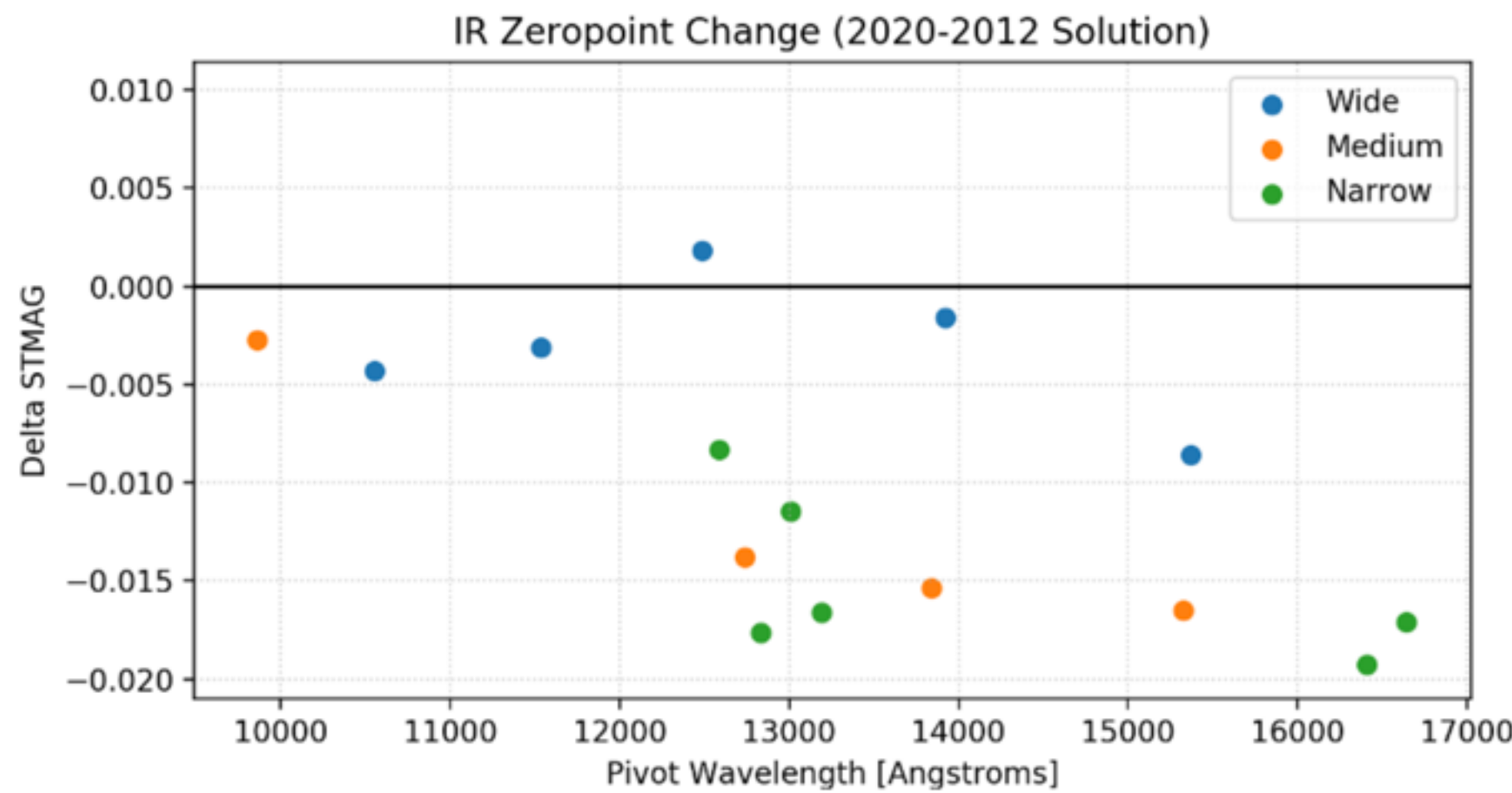
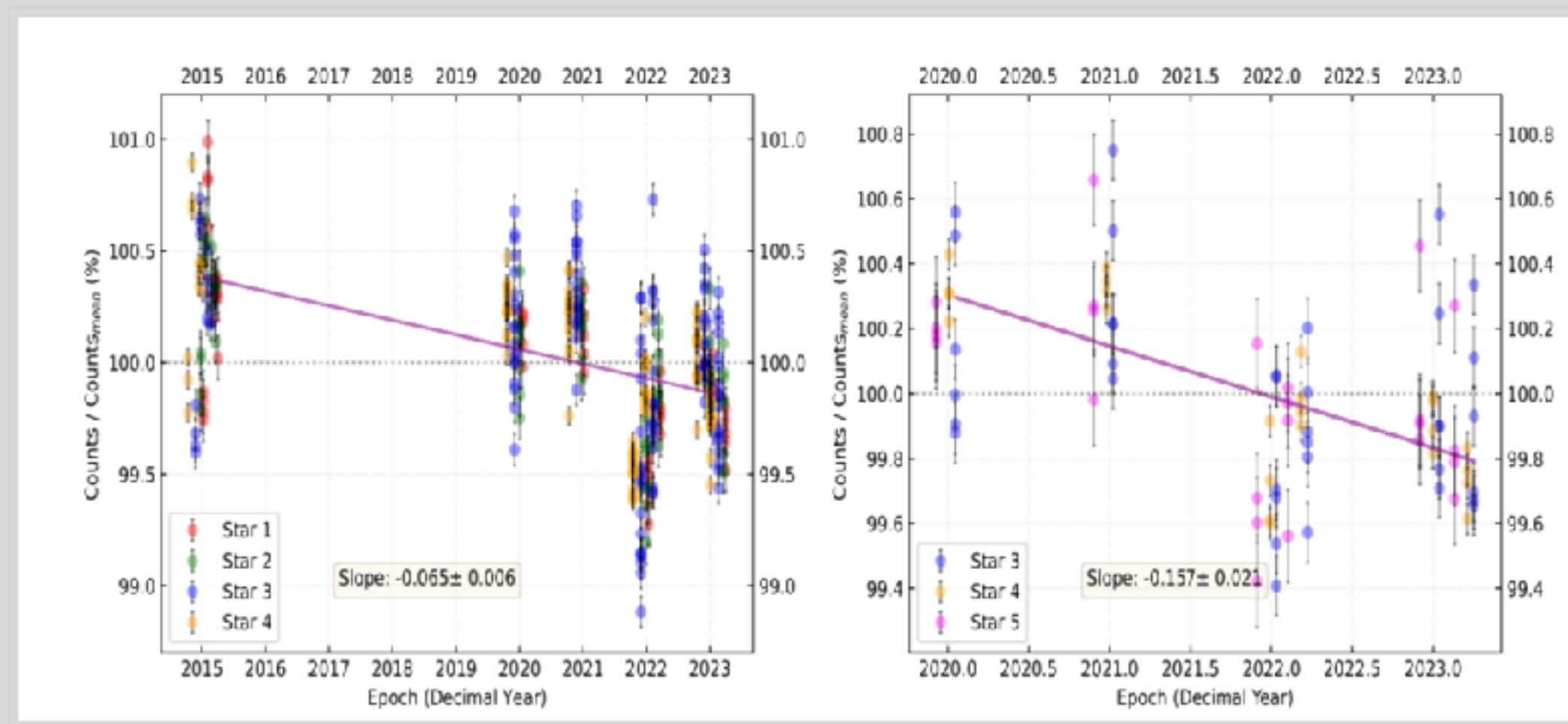


Figure 4: : Change in the STMAG zeropoints for WFC3/IR. The systematically larger change in the redder wavelengths is primarily due to the new synthetic models.

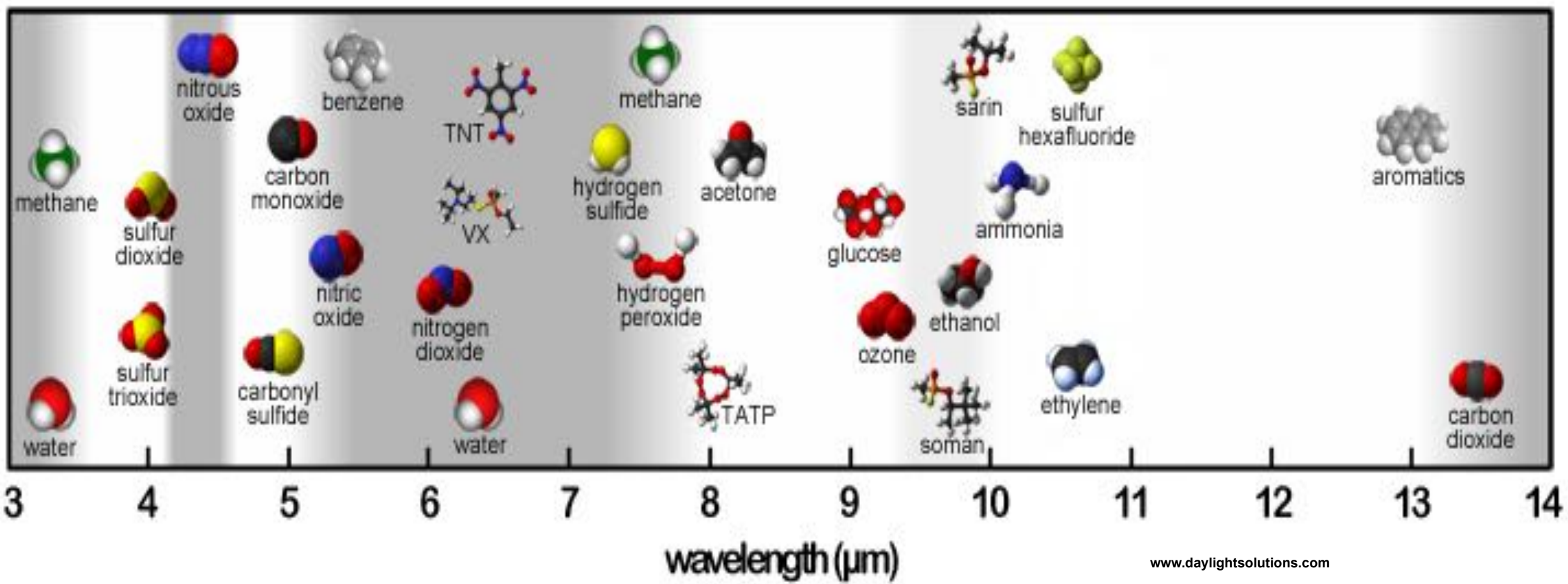
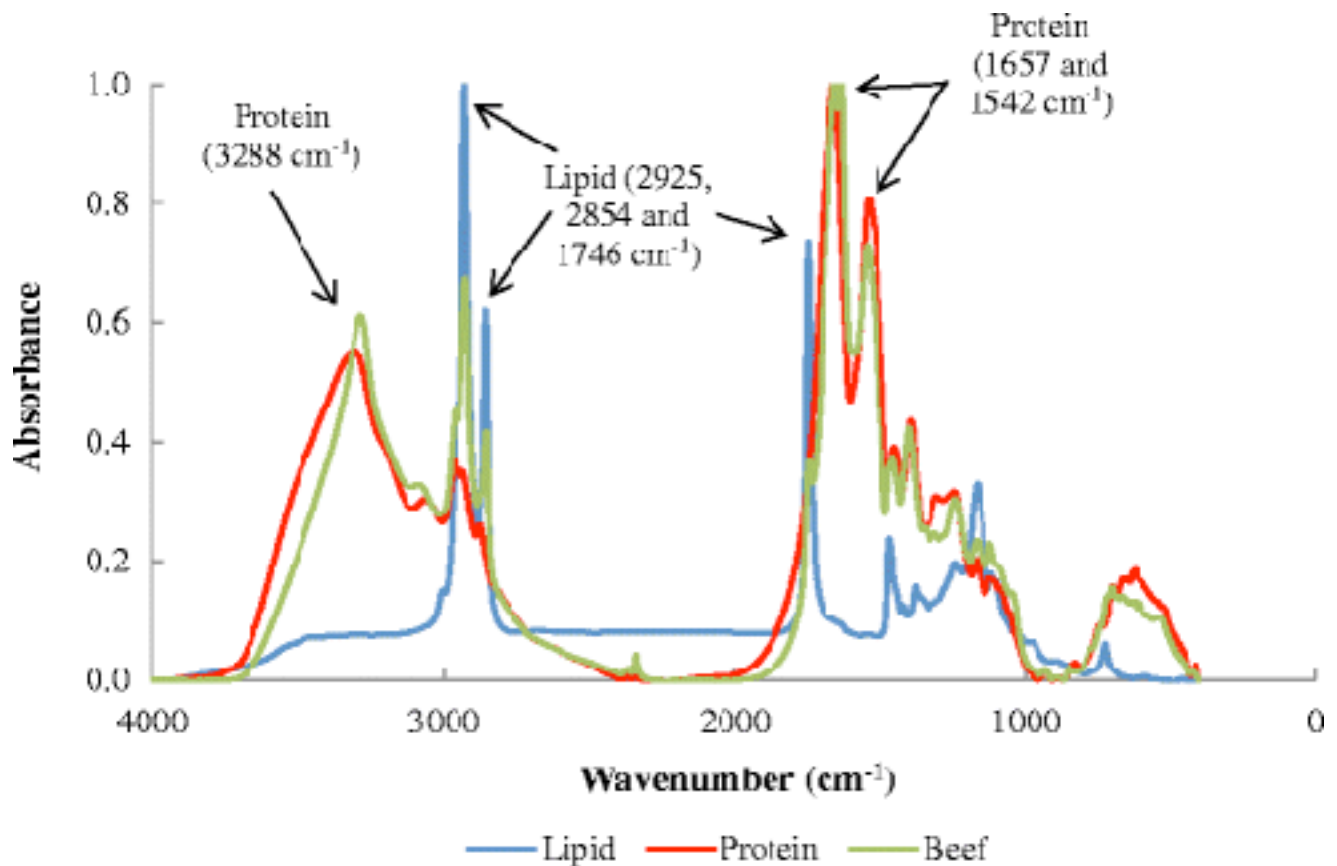
And after all of that, IR detectors degrade over time, and their sensitivity changes (CCDs also do this in-orbit).

Figure 7.14: (left) Photometric repeatability in the IR measured from spatially-scanned F140W observations over 10 epochs between 2015 and 2024. Measurements from each star, plotted relative to their mean over all ten epochs, are plotted against time. Data for the different stars from a given epoch are plotted with small artificial time offsets between them for display purposes only. The mean photometry is represented by the black dotted line at 100%. The solid purple line represents a linear fit to the data. The corresponding slope, quantifying the rate of sensitivity evolution is also shown. Figure reproduced from [WFC3 ISR 2024-01](#); (right) Same as left side, but with F098M data distributed over six epochs



Mid-IR

- The mid-IR is home to fundamental vibrational resonances of a wide range of molecules
 - Breath Analysis
 - Industrial Process Monitoring
 - Environmental Monitoring
- Absorption/Transmission Spectroscopy
 - Broadband spectroscopic data on liquids/powders/solids
 - Biomedical Imaging
 - In-vivo imaging
 - Micro-biology
 - Pharmaceutical Industry
 - Drug Development
 - Process/Quality Control
 - Counterfeit Analysis
 - Food Industry
 - Meat processing
 - Beverage quality screening
 - Material Science

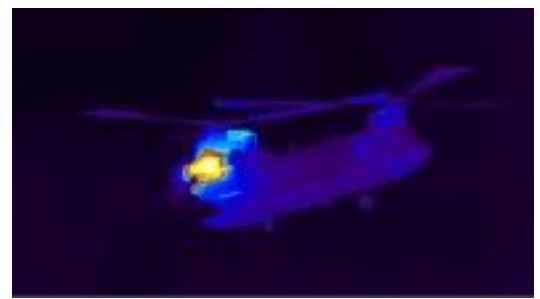


Mid-IR

- Everything emits in the mid-IR.....
- Important frequency range for defense applications
 - Thermal imaging
 - Countermeasures



- www.imaging1.com
(Sierra Pacific Innovations)



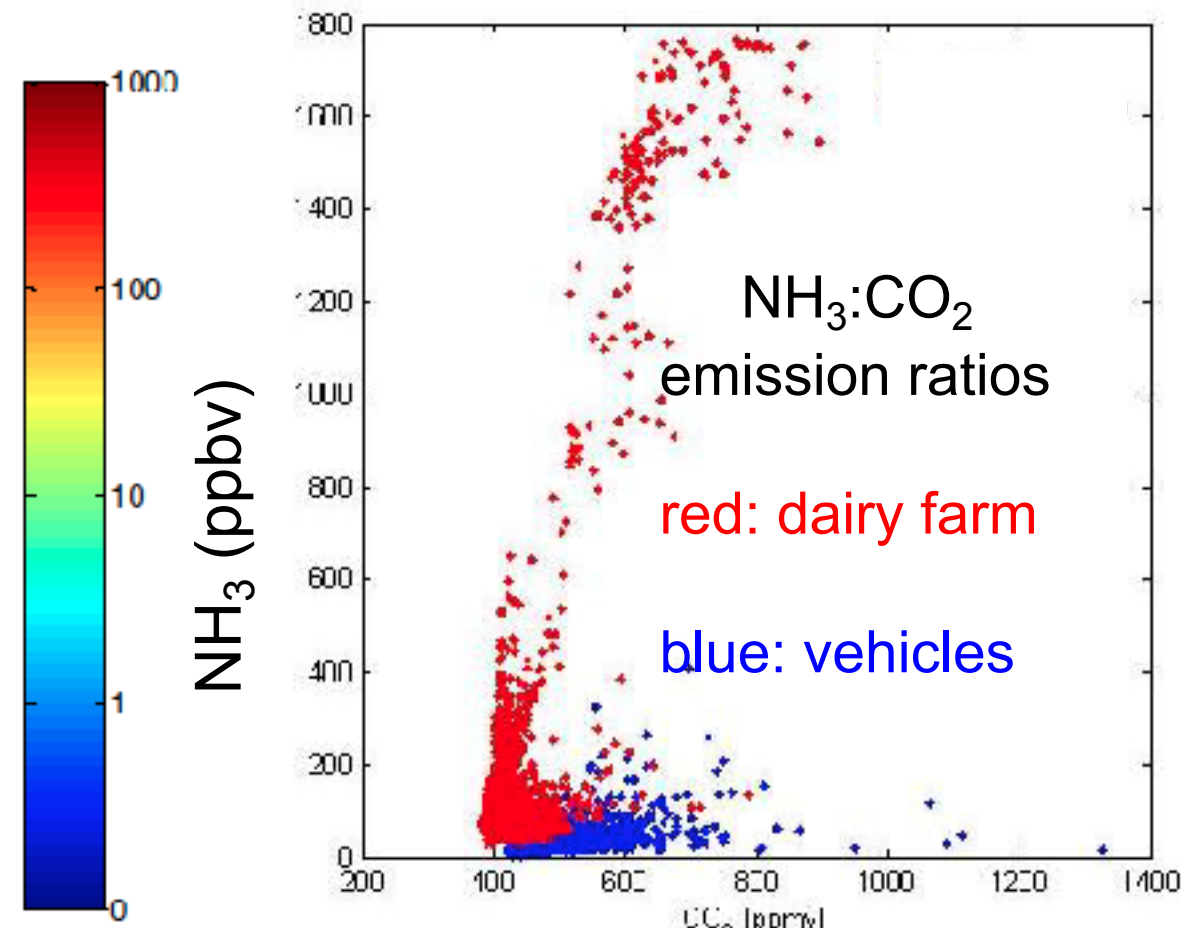
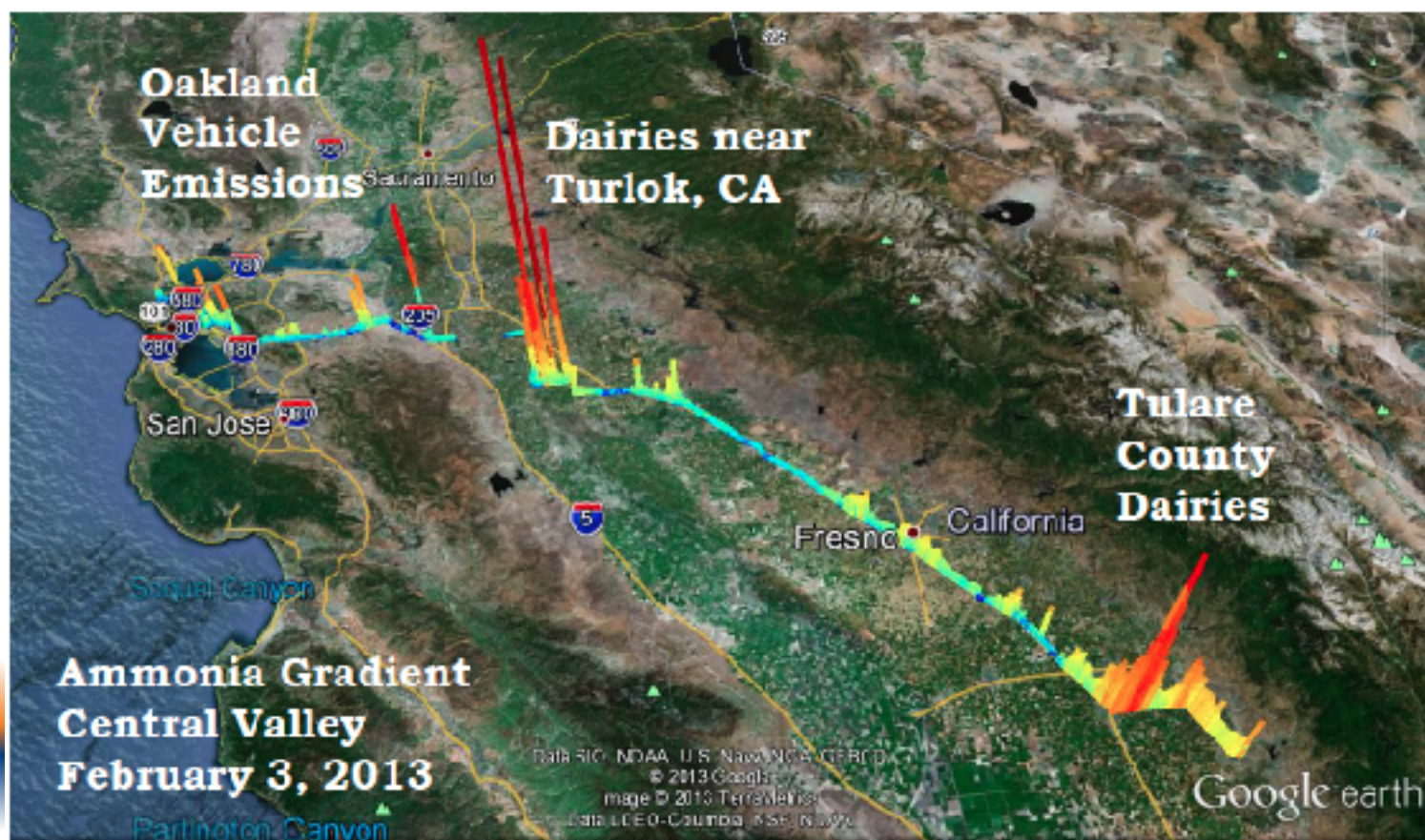


Ultrasensitive NH_3 sensor for urban air quality

(Tao et al., Opt. Lett., 2012; Sun et al., Appl. Phys. B, 2012; Miller et al., AMTD, 2013)



- Mobile mapping, > 4500 km in CA/NJ
- Quantify emissions by tracer-tracer plots where one tracer's emissions known
 - dairies: 0.8% NH_3 per CH_4 emitted
 - vehicles: 2% NH_3 per CO emitted
- NASA TES NH_3 satellite validation
- fast response: >10X change in conc. in 1 s



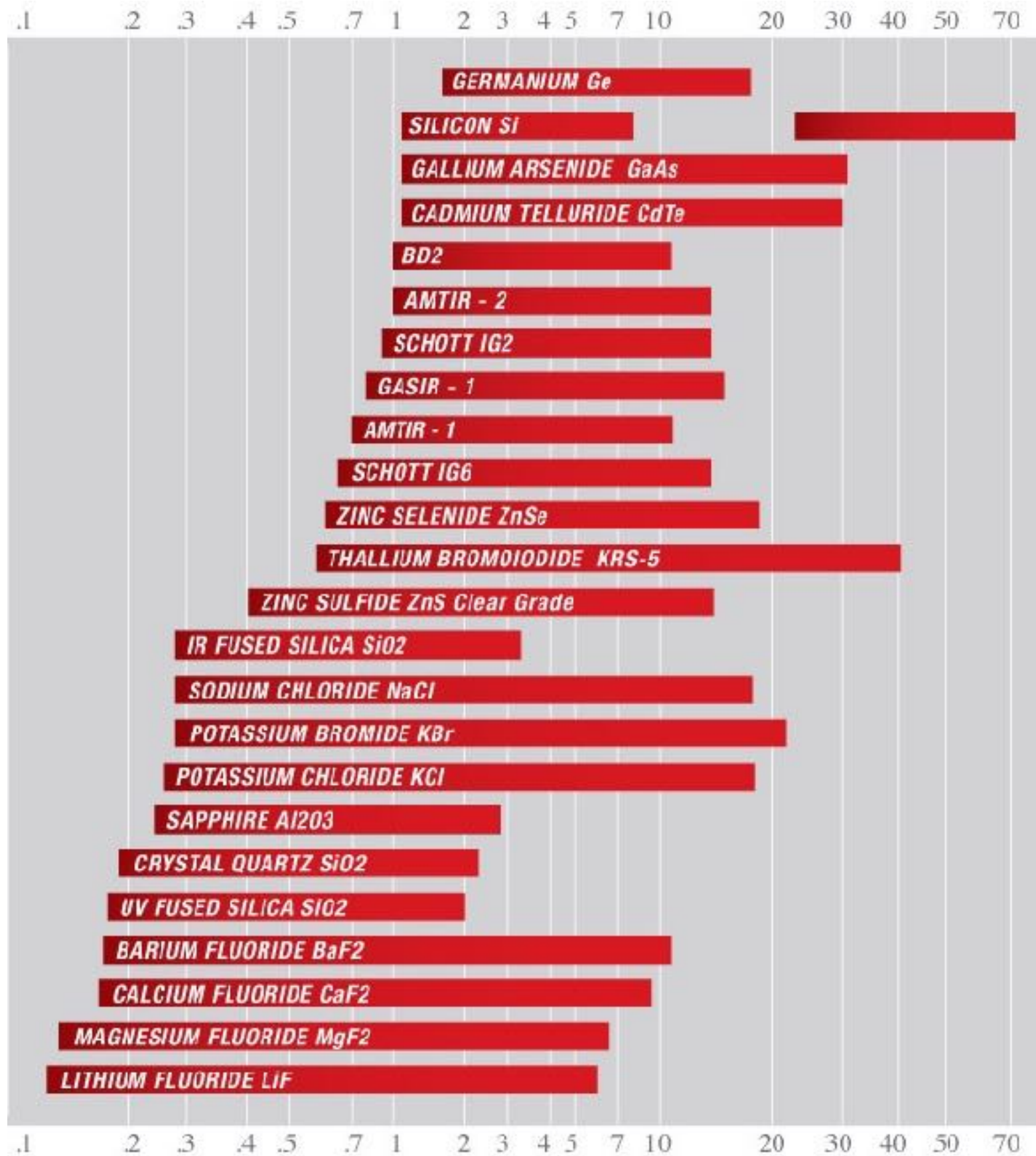
Infrared instruments

□ Challenges of IR instrument design and construction:

- Everything, not just the chip, must be at cryogenic temperatures.
- Many of the more robust IR optical materials (e.g. zinc sulfide, zinc selenide) don't transmit well in the visible, which hampers alignment and set up.
- On the other hand, crystalline materials like calcium fluoride and barium fluoride which do transmit both optical and IR light are fragile and harder to work optically.
- Cryogenic refractive indexes are also needed.
- Elimination of diffusely scattered light using blackened baffles requires care because anything truly black has almost 100% emissivity and will therefore be a strong infrared emitter unless very cold.
- All dimensions will change during cool-down of the instrument and worse, parts not made from the same materials will shrink by different amounts due to dissimilar coefficients of expansion.
- Lens holders could crush their optical components, optical separations will change and materials may experience stress.
- All these things must be calculated beforehand and each component must be constructed in such a way as to achieve the correct dimensions after it is cold.

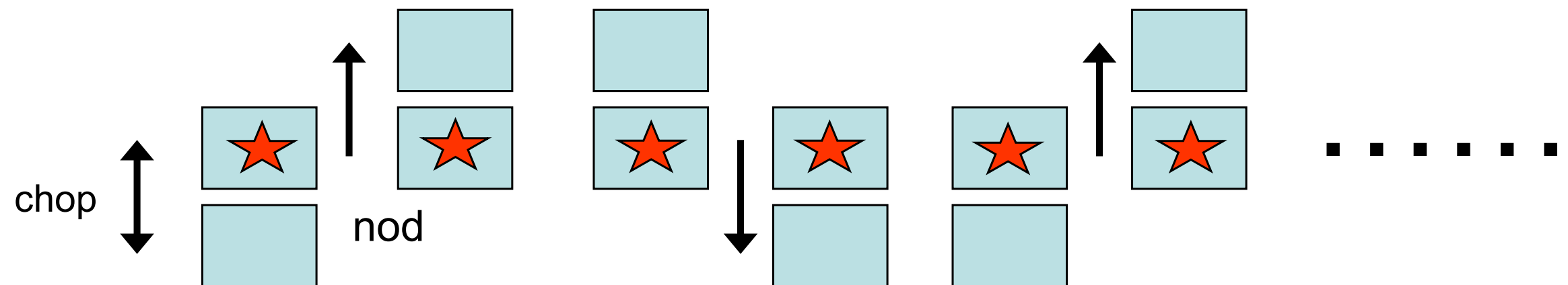
Materials

- Most optically transparent materials in the mid-IR are semiconductors
- High index of refraction (high Ref.)
- Phonon resonances in 20-60um range



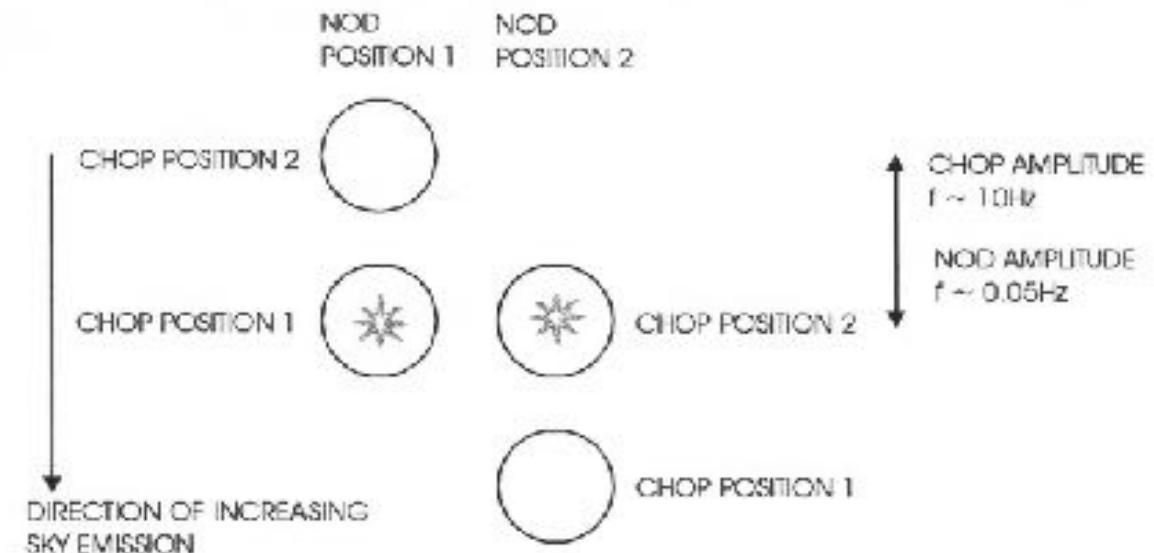
Mid-infrared strategy

- Sky background at 10 μm is 10^3 – 10^4 greater than in K band
 - Detector wells saturate in very short time (< 50 ms)
 - Very small temporal variations in sky >> astronomical source intensities
 - Read array out very *rapidly* (20 ms), coadd images
 - Sample sky at high rate (~ 3 Hz) by *chopping* secondary mirror (15 arcsec)
 - Synchronize with detector readout, build up “target” and “sky” images
 - But tilting of secondary mirror introduces its own *offset* signal
 - Remove offset by *nodding* telescope (30 s) by amplitude of chop motion
 - Relative phase of target changed by 180° with respect to chop cycle
 - Relative phase of offset signal unchanged
 - Subtraction adds signal from target, subtracts offset
 - <http://www.gemini.edu/sciops/instruments/t-recs/imaging>



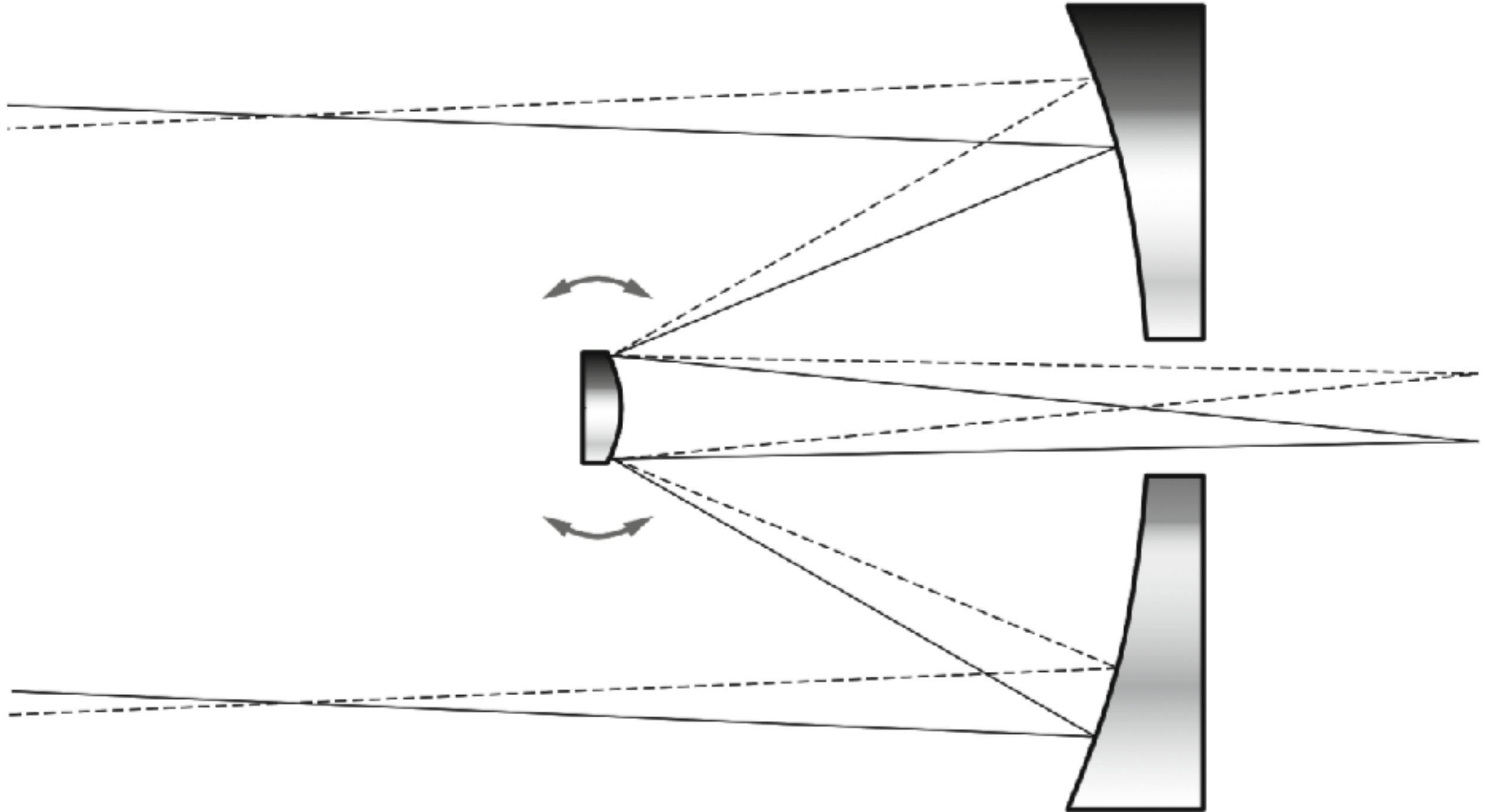
Chopping

- The beam is switched rapidly from the source position and a nearby reference position, by an **oscillating or "wobbling" secondary mirror in the telescope itself.**
- **Chopping** takes place at a frequency of $\sim 10\text{-}20\text{ Hz}$.
- By forming the difference, the sky signal is eliminated provided it has remained constant.

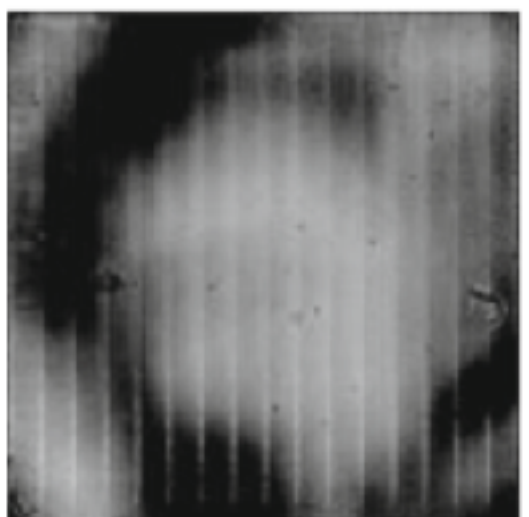


In addition, it is still usually necessary to move the entire telescope every minute or so to enable the sky on the "other side" of the object to be measured and thereby eliminate any systematic trend or gradient; this step is called "**nodding**" and the amount of the nod is usually the same as the "throw" of the chop for symmetry (Fig. 11.2).

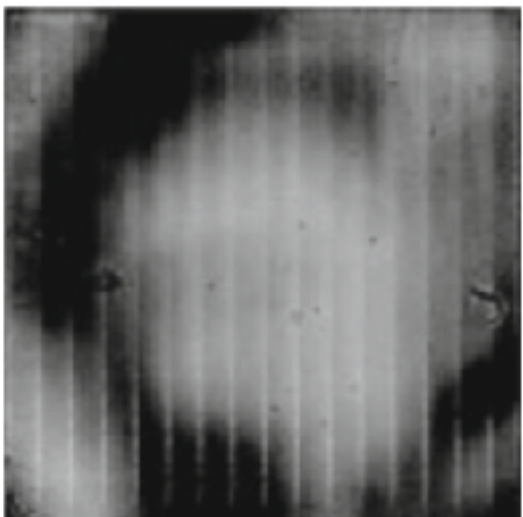
Chopping



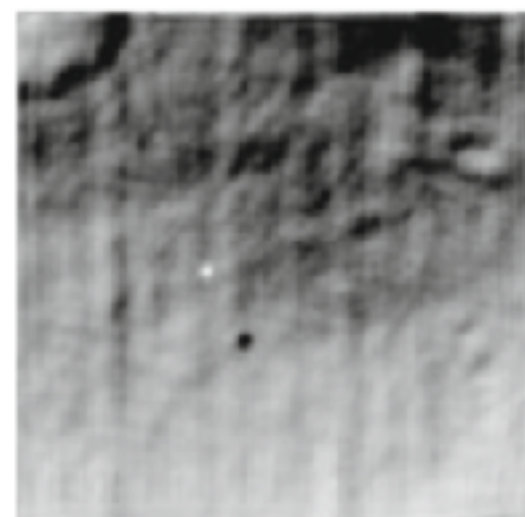
Chop 1



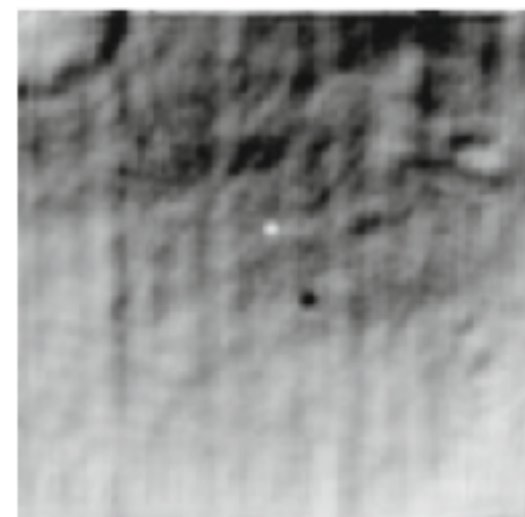
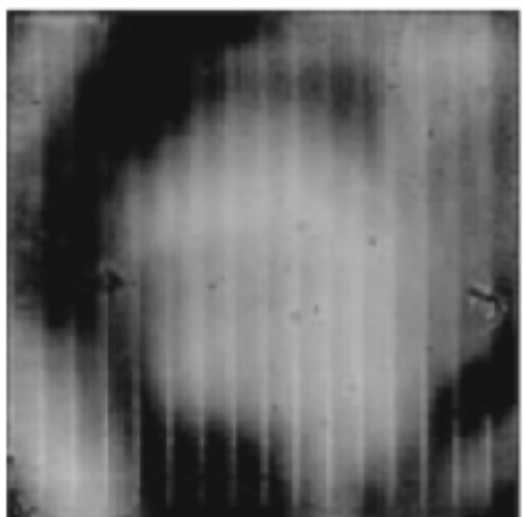
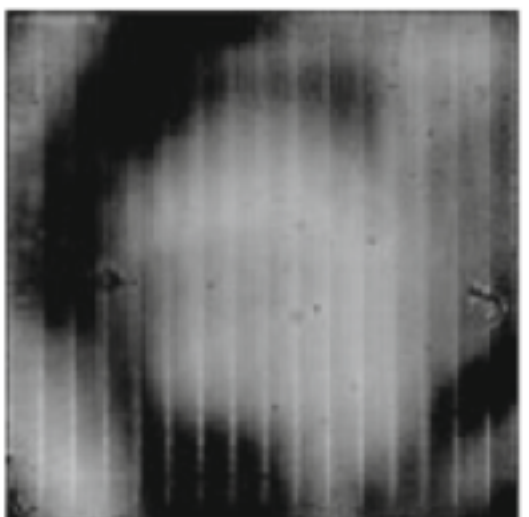
Chop 2



Chop 1 – Chop 2

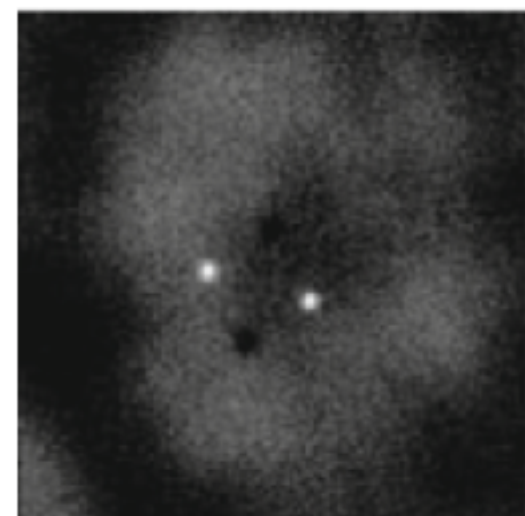


Nod A

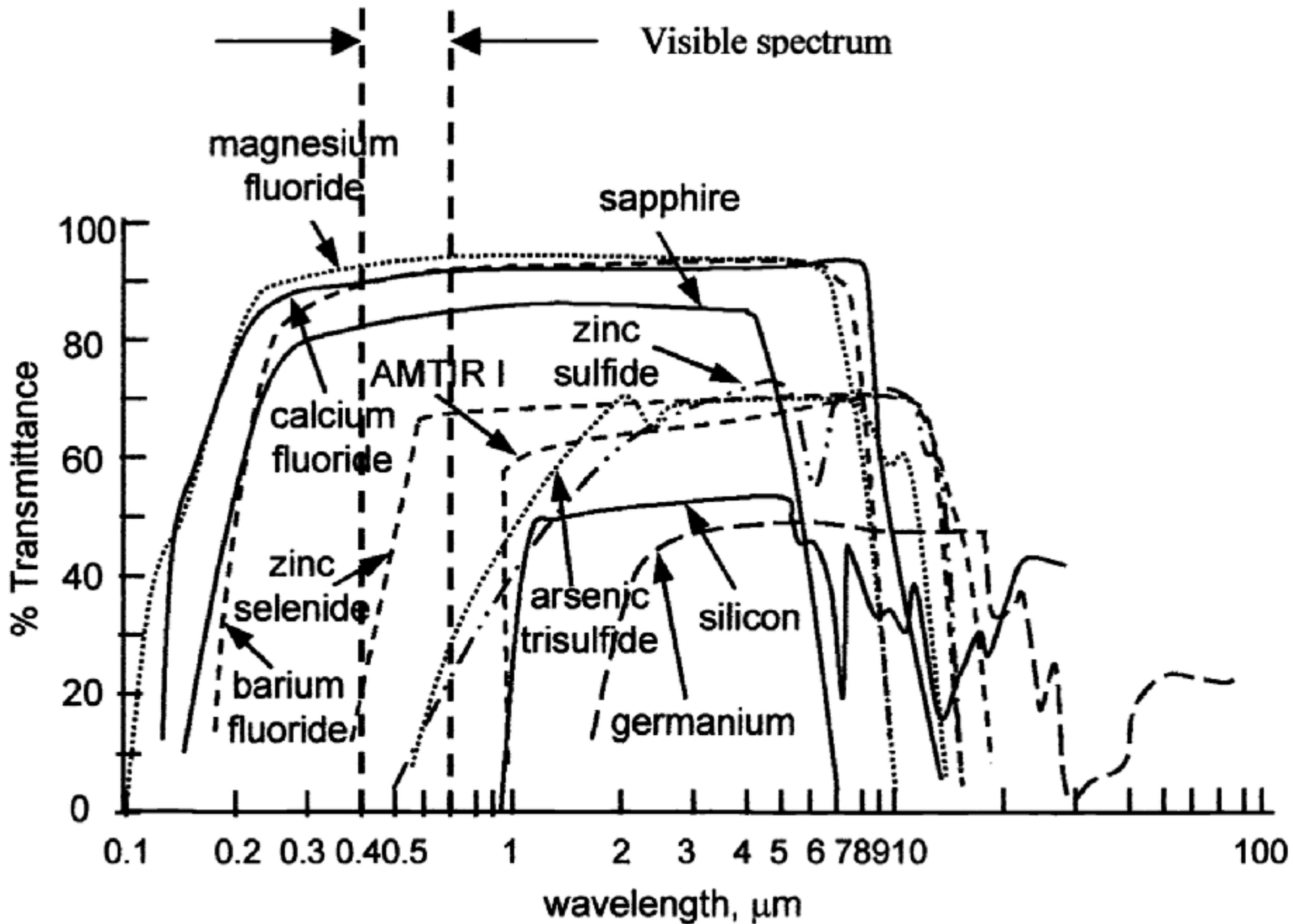


Nod B

Nod A (chop 1 – chop 2) – Nod B (chop 1 – chop 2) =



What if you want to go further into the IR, past the MIR



Far-infrared Ge arrays

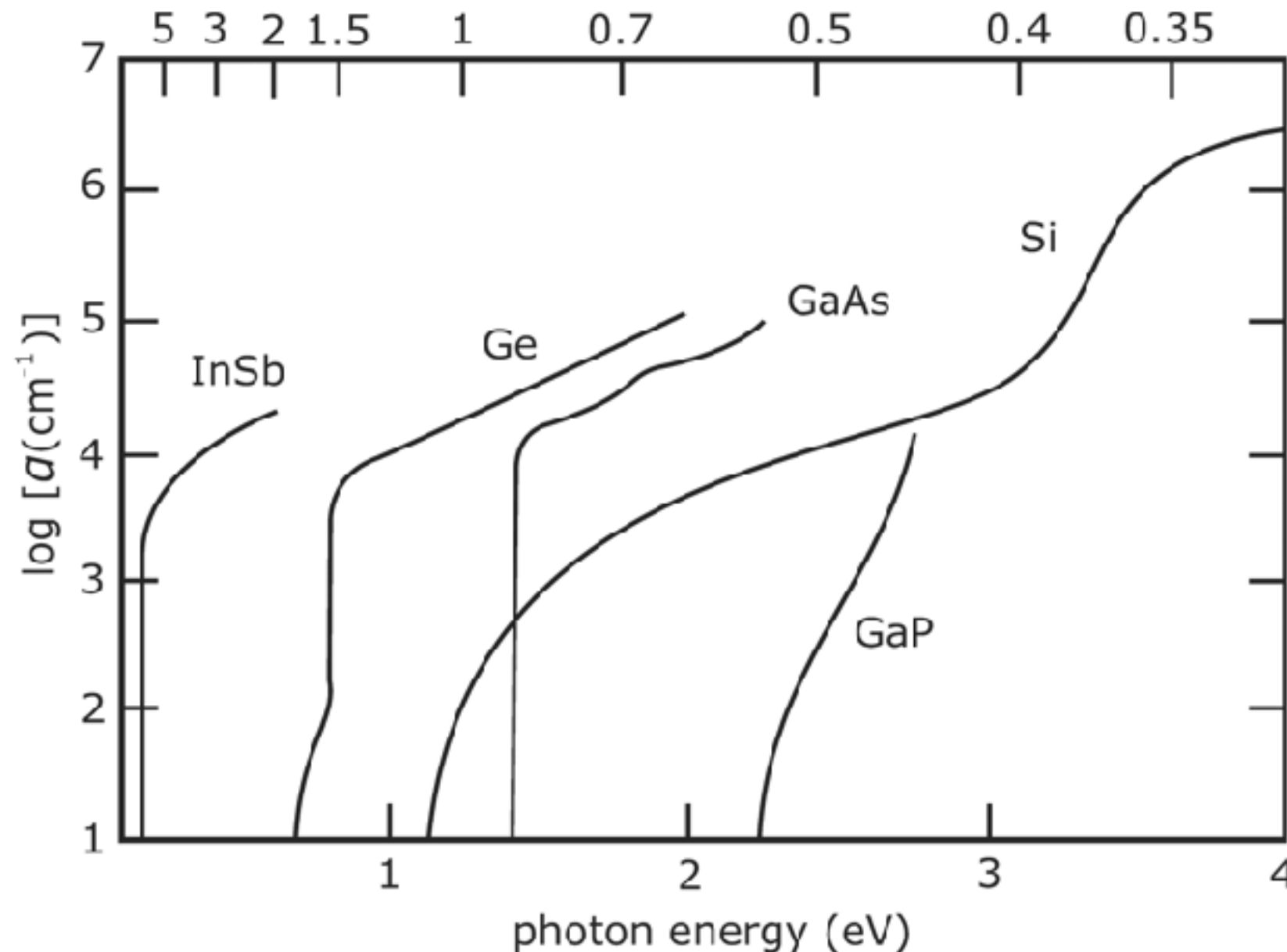
- Longer than 40 μm there are no appropriate shallow dopants for silicon and therefore extrinsic germanium (Ge) must be used.
- There are a number of problems with the use of germanium.
 - To control dark current, Ge must be relatively lightly doped; then absorption lengths are 3-5 mm.
 - Because diffusion lengths are also large (250-300 μm), pixel dimensions of 500-700 μm are required to minimize crosstalk.
 - Large pixels imply higher hit rates for cosmic rays, especially in space, and this in turn implies that the readout device must have very low noise so that the background limit is reached in the shortest possible exposure time.
 - But a large detector pixel means a large capacitance and more noise.
 - Also, the photoconductive gain is inversely proportional to the inter-electrode spacing resulting in poor QE unless side-illuminated detectors with transverse contacts are used.
 - Finally, because of the very small energy band gaps, these detectors must operate at liquid helium temperatures well below the silicon "freeze-out" range.

The net absorption is characterized by the absorption coefficient, a . Note the difference between direct and indirect absorption (e.g., silicon vs. GaAs). Quantum mechanical selection rules do not permit transfers at the band gap energy for indirect absorbers.

The quantum efficiency is:

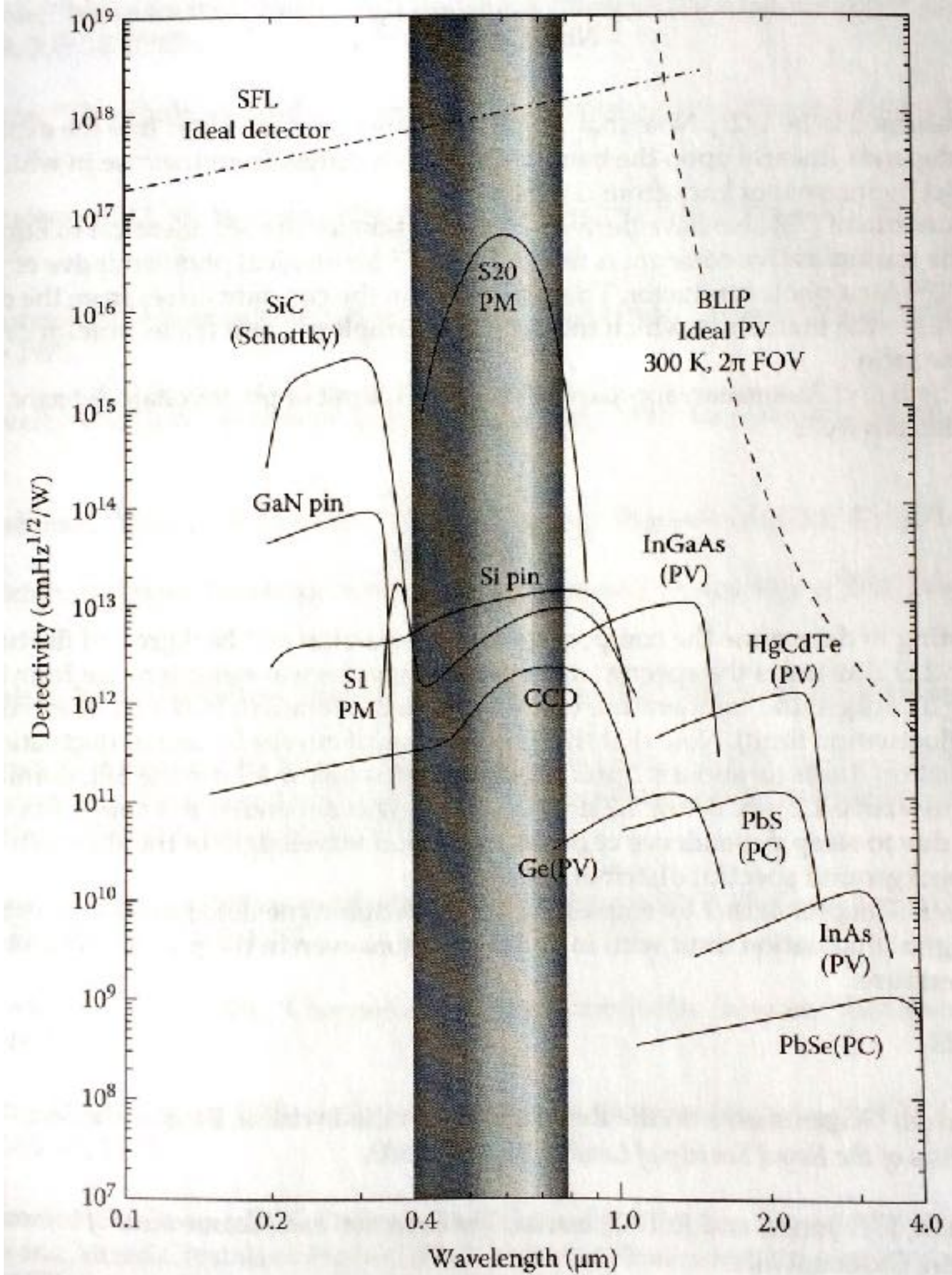
$$\eta_{ab} = \frac{S_0 - S_0 e^{-a(\lambda) d_1}}{S_0} = 1 - e^{-a(\lambda) d_1}, \quad (3)$$

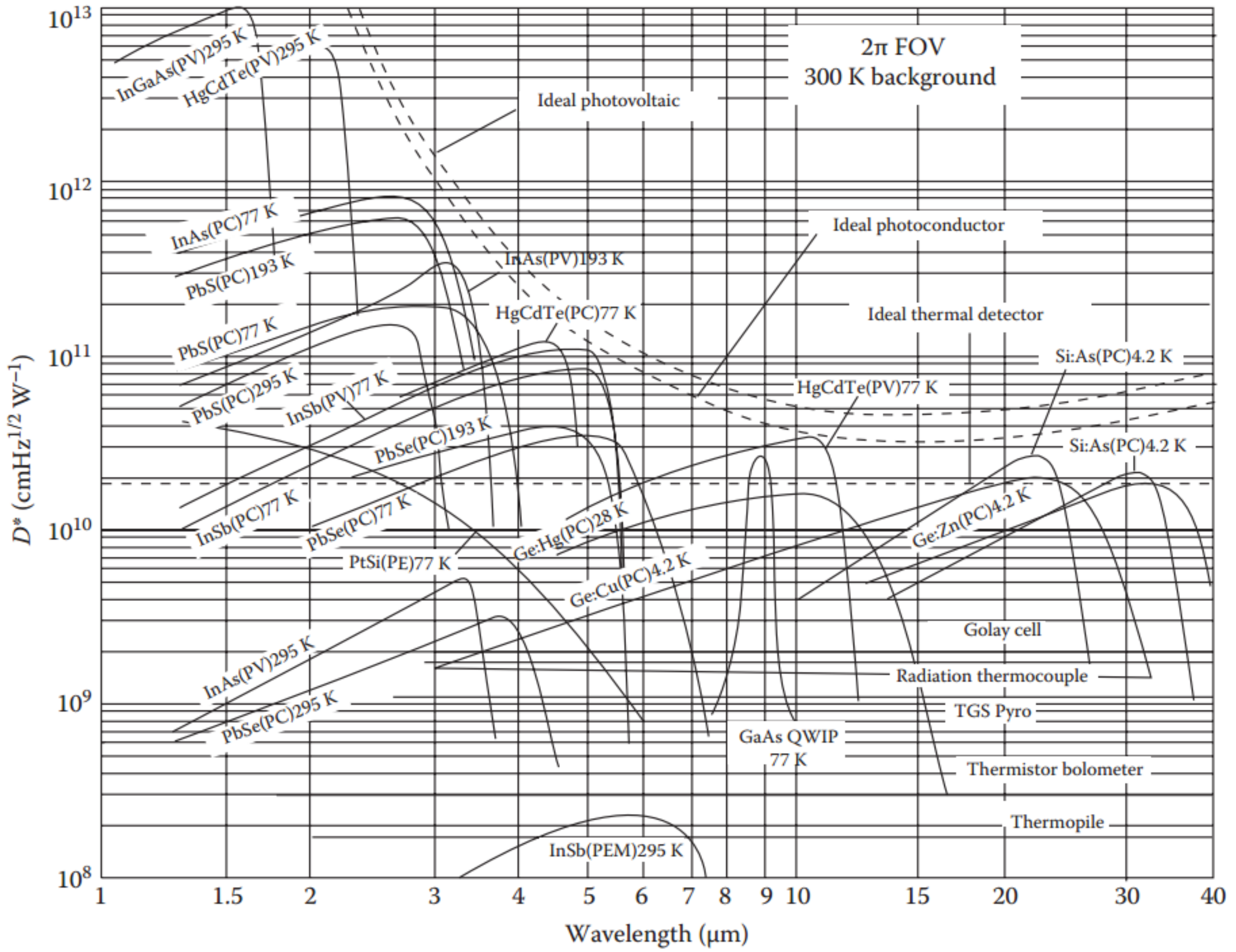
wavelength (μm)

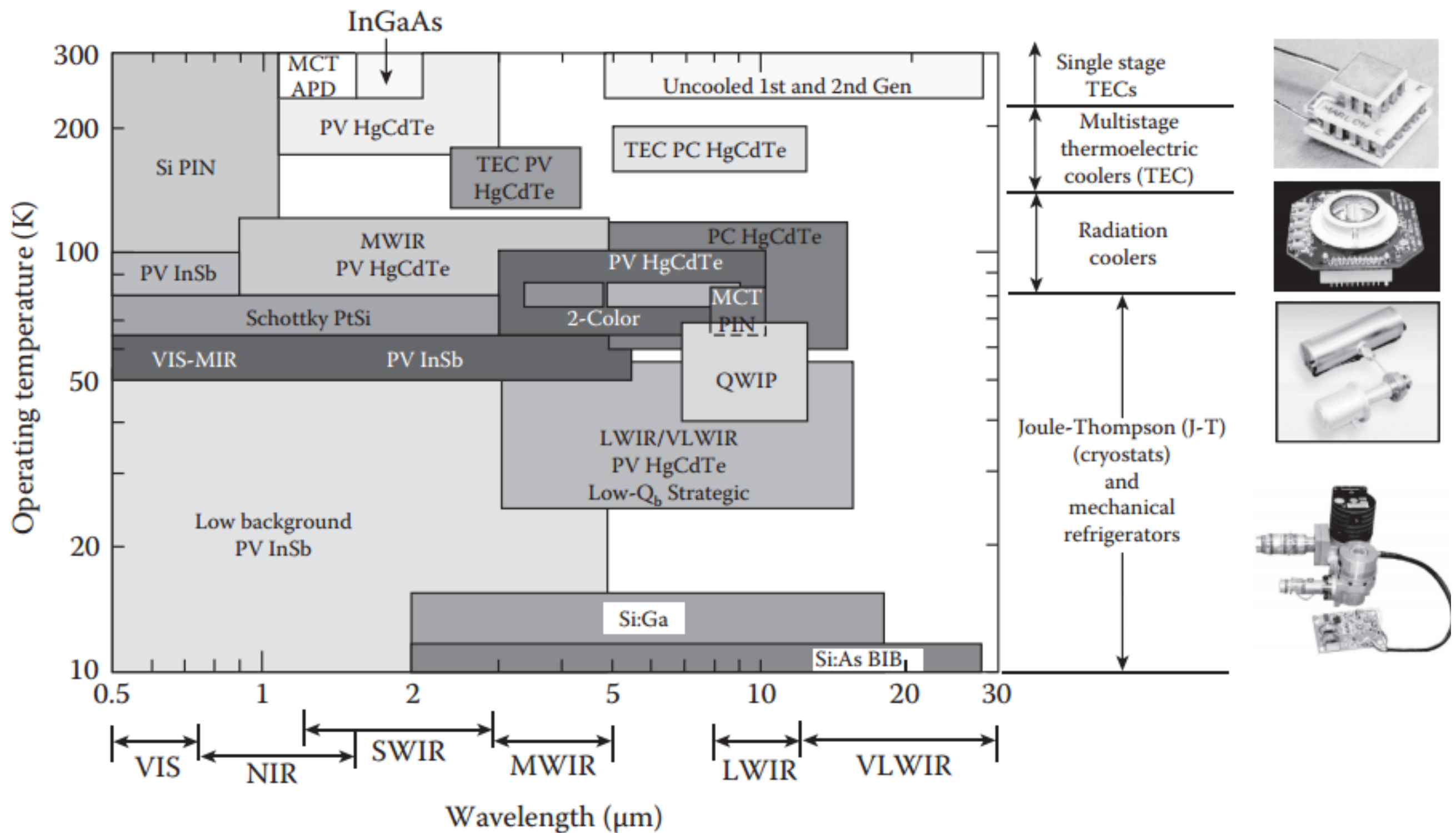


- Here are some photodiode materials and their cutoff wavelengths.
HgCdTe has a variable bandgap set by the relative amounts of Hg and Te in the crystal. AlGaAsSb behaves similarly.
- Indirect absorbers will have poor QE just short of the cutoff

Material	Cutoff wavelength (μm)
Si	1.1 (indirect)
Ge	1.8 (indirect)
InAs	3.4 (direct)
InSb	6.8 (direct)
HgCdTe	$\sim 1.2 - \sim 15$ (direct)
GaInAs	1.65 (direct)
AlGaAsSb	0.75 – 1.7 (direct)







Detector Type		Advantages	Disadvantages
Photon	Thermal (thermopile, bolometers, pyroelectric)	Light, rugged, reliable, & low cost Room temperature operation	Low detectivity at high frequency Slow response (ms order)
	IV-VI (PbS, PbSe, PbSnTe)	Easier to prepare More stable materials	Very high thermal expansion coefficient Large permittivity
	II-VI (HgCdTe)	Easy bandgap tailoring Well-developed theory & experience Multicolor detectors	Nonuniformity over large area High cost in growth and processing Surface instability
	Intrinsic		Heteroepitaxy with large lattice mismatch Long wavelength cutoff limited to 7 μm (at 77 K)
	III-V (InGaAs, InAs, InSb, InAsSb)	Good material & dopants Advanced technology Possible monolithic integration	High thermal generation Extremely low temperature operation
	Extrinsic (Si:Ga, Si:As, Ge:Cu, Ge:Hg)	Very long wavelength operation Relatively simple technology	Low quantum efficiency Low temperature operation
Free carriers (PtSi, Pt ₂ Si, IrSi)	Type I (GaAs/AlGaAs, InGaAs/AlGaAs)	Matured material growth Good uniformity over large area Multicolor detectors	High thermal generation Complicated design and growth
	Type II (InAs/InGaSb, InAs/InAsSb)	Low Auger recombination rate Easy wavelength control Multicolor detectors	Complicated design and growth Sensitive to the interfaces
	Quantum dots InAs/GaAs, InGaAs/InGaP, Ge/Si	Normal incidence of light Low thermal generation	Complicated design and growth

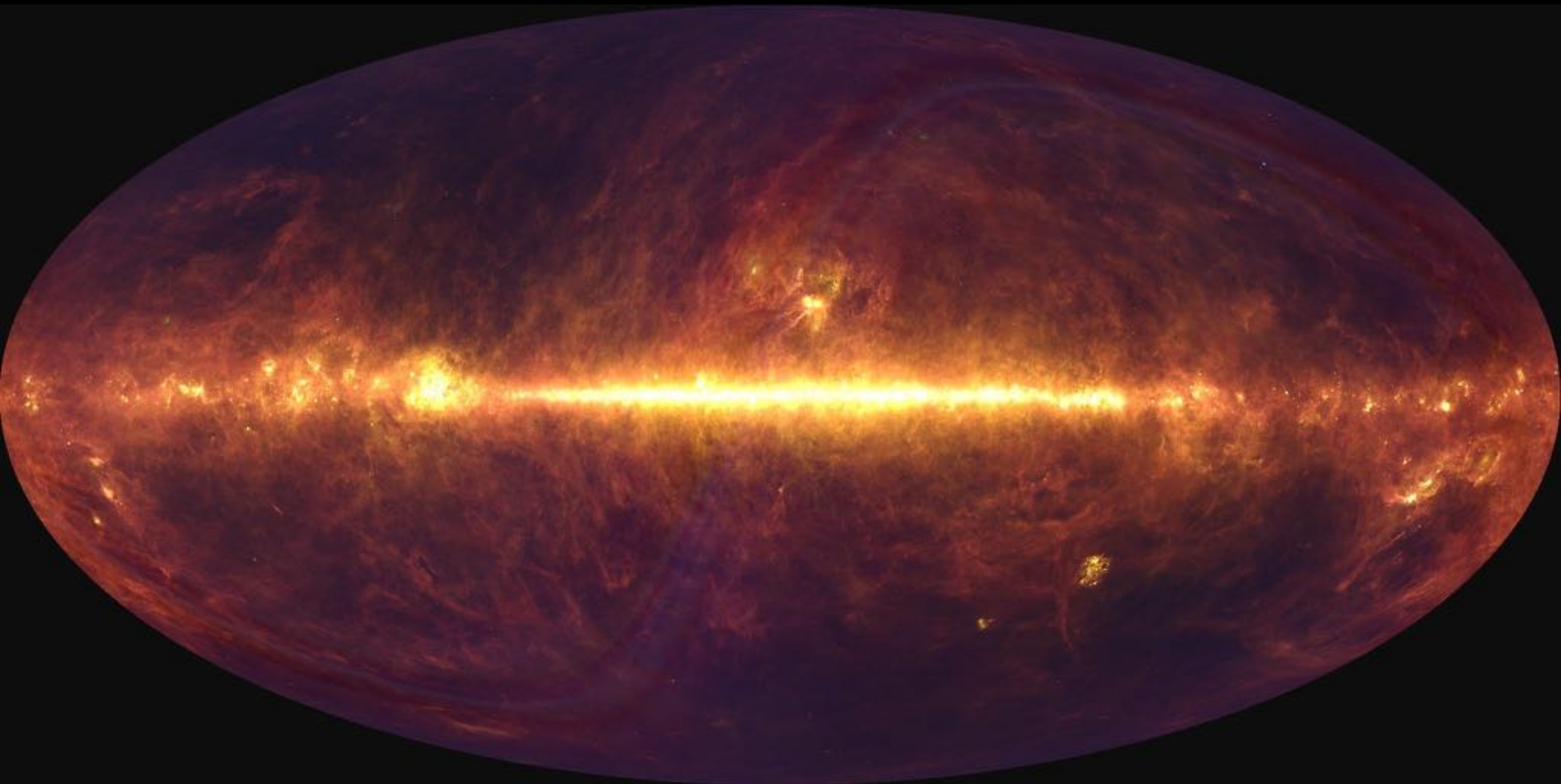
IR Experiments

Infrared Astronomical Satellite (IRAS)

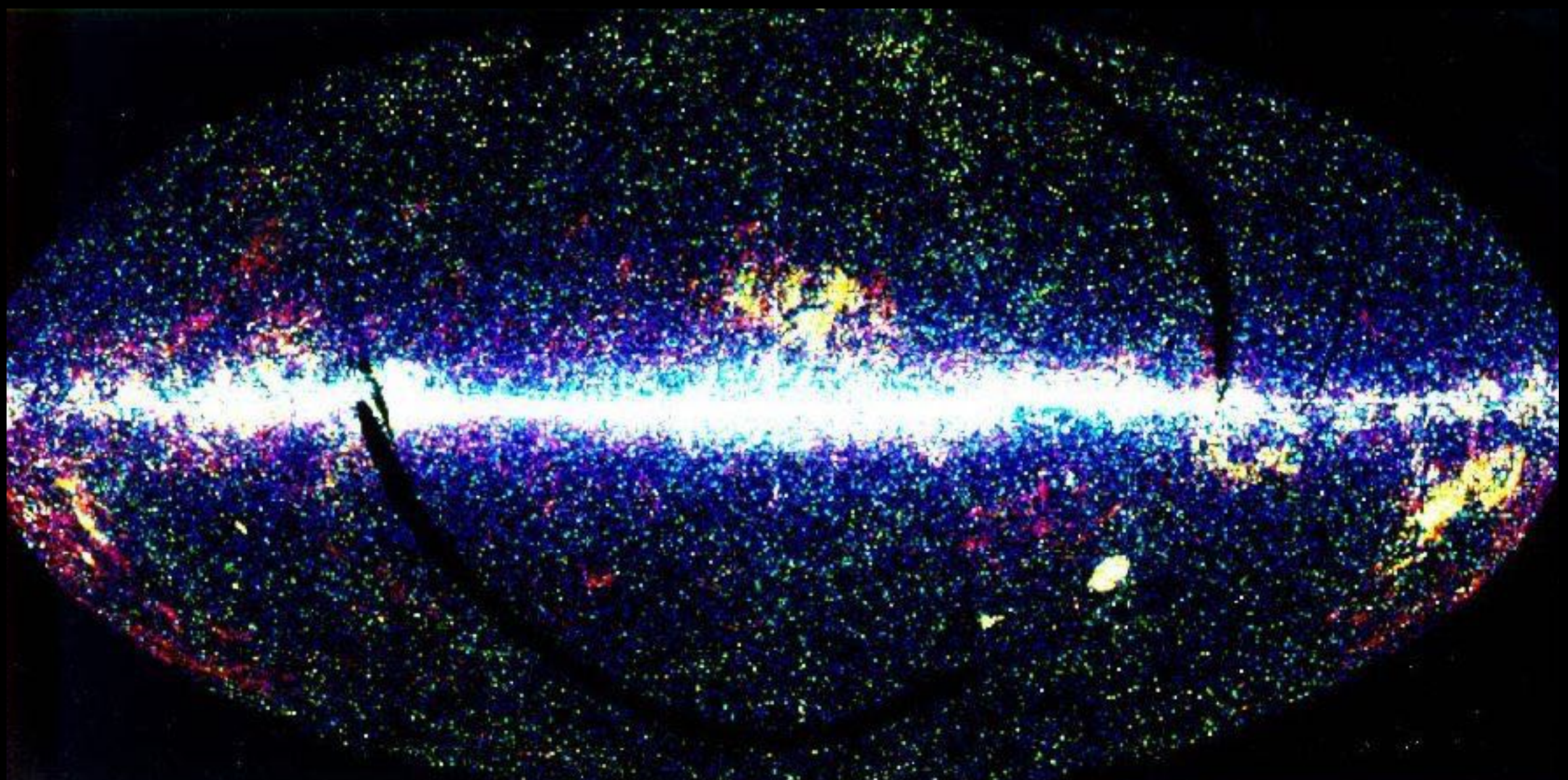
- First telescope to survey entire IR sky
- cooled to 2K with liquid Helium
- 1983 → 1983 (10 months)
- Mapped 96% of sky 4 times
- 12, 25, 60, 100 μm
- 30"-2' resolution
- discovered 350,000 sources
- 75,00 infrared starburst galaxies
- debris disks → planetary systems in formation
- Huge impact on astronomy
- People STILL writing PhD theses with data !



IRAS 25, 60, 100 um

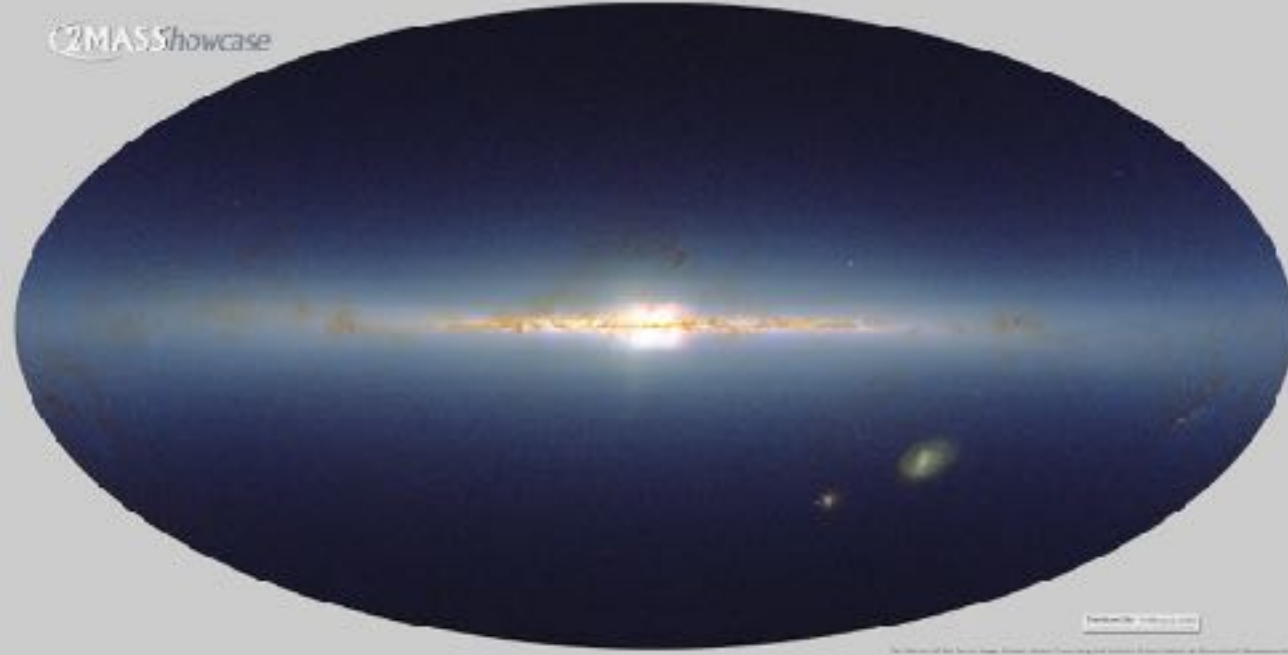


IRAS Point Source Catalog



2 Micron All Sky Survey (2MASS)

- 1997-2001
- U.Mass, Caltech, IPAC
- Two 1.3m telescopes in Mt Hopkins, AZ, and CTIO, Chile
- J (1.25 μm), H (1.65 μm), and K_s (2.17 μm) to limiting magnitude ~ 14
- 300 million point sources and 1 million extended sources cataloged
- found many brown dwarfs
- cataloged many new star clusters
- catalogued many nearby galaxies and stars
- Is the standard reference catalog for astrometry.

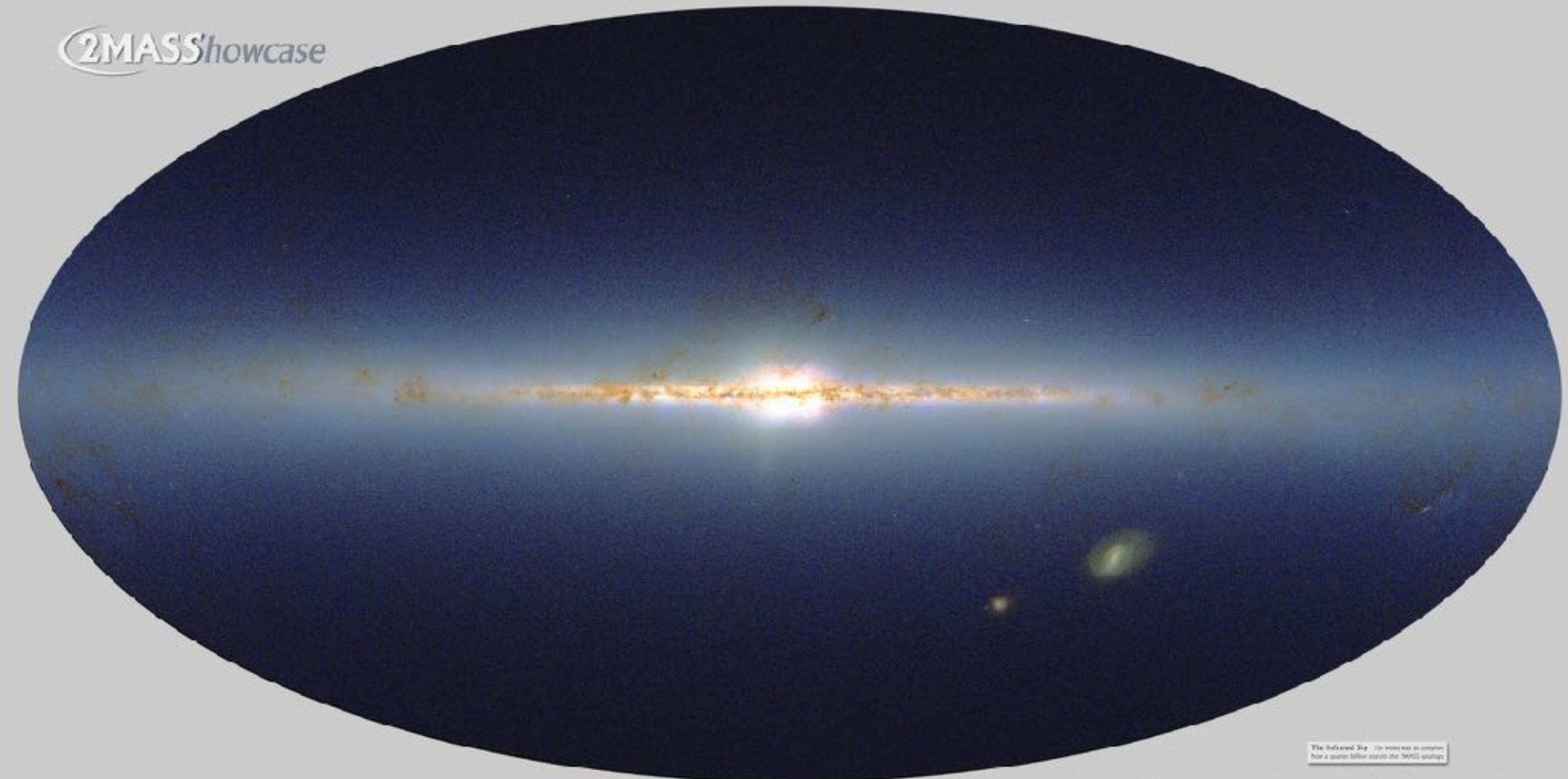


2MASS Showcase



The Infrared Universe Light from 1.6 million galaxies reveals the structure of the local universe

2MASShowcase



The Infrared Sky: An Interview with a Computer
from a Quasar Fellow student the 2MASS website

Two Micron All-Sky Survey Image: Xavieir Infrared Processing and Analysis Center, Caltech & University of Massachusetts

2MASS Showcase

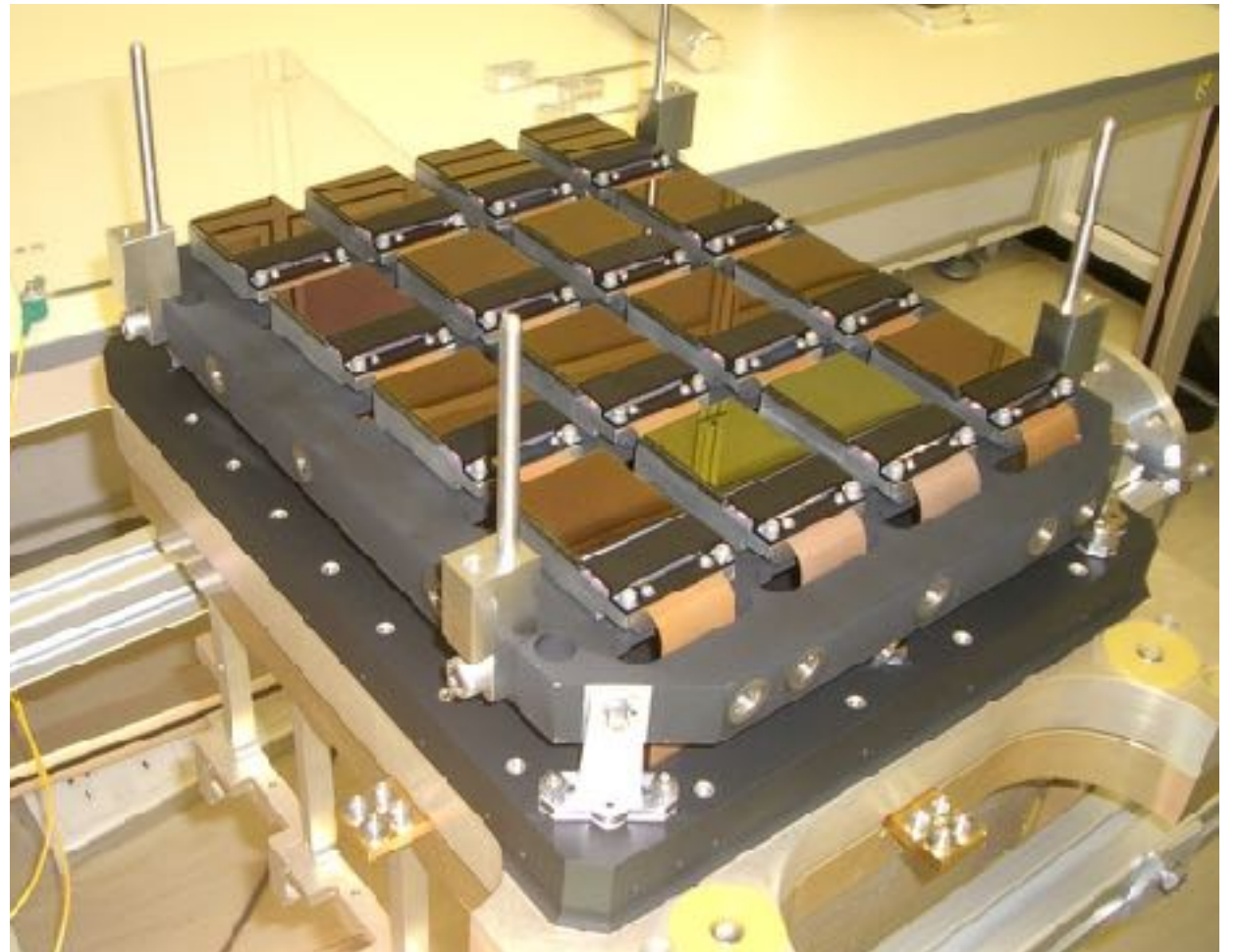


The Infrared Universe Light from 1.6 million galaxies reveals the structure of the local universe

The VISTA Camera Array

VISTA is a 4-m wide-field survey telescope, equipped with a near infrared camera (1.65 degree diameter field of view) containing 67 million pixels of mean size 0.34 arcsec and broad band filters at Z,Y,J,H,Ks and a narrow band filter at 1.18 micron.

The VISTA camera contains 16 HgCdTe VIRGO detectors and is the largest IR mosaic thus far.



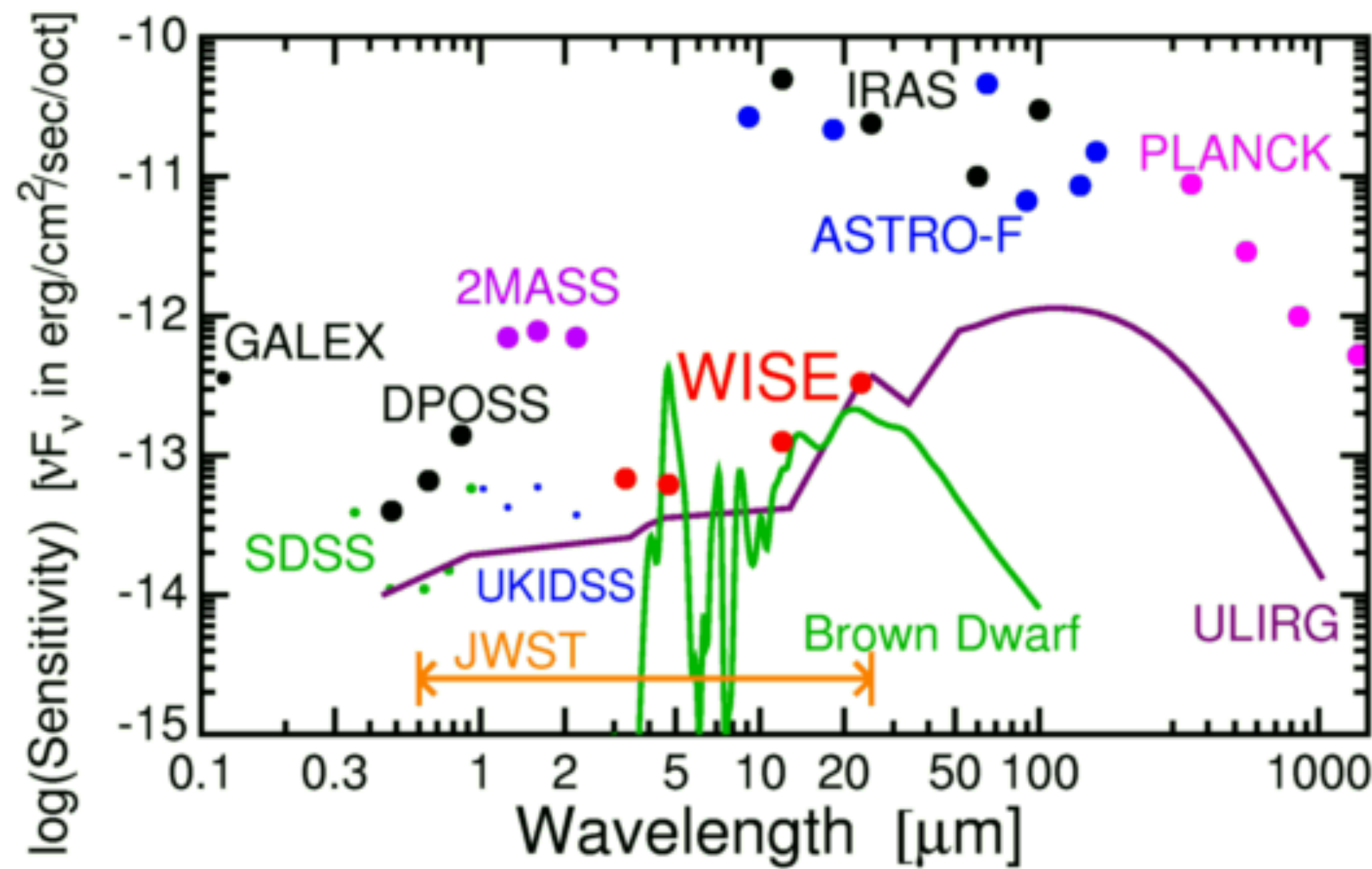
Previous IR Mission

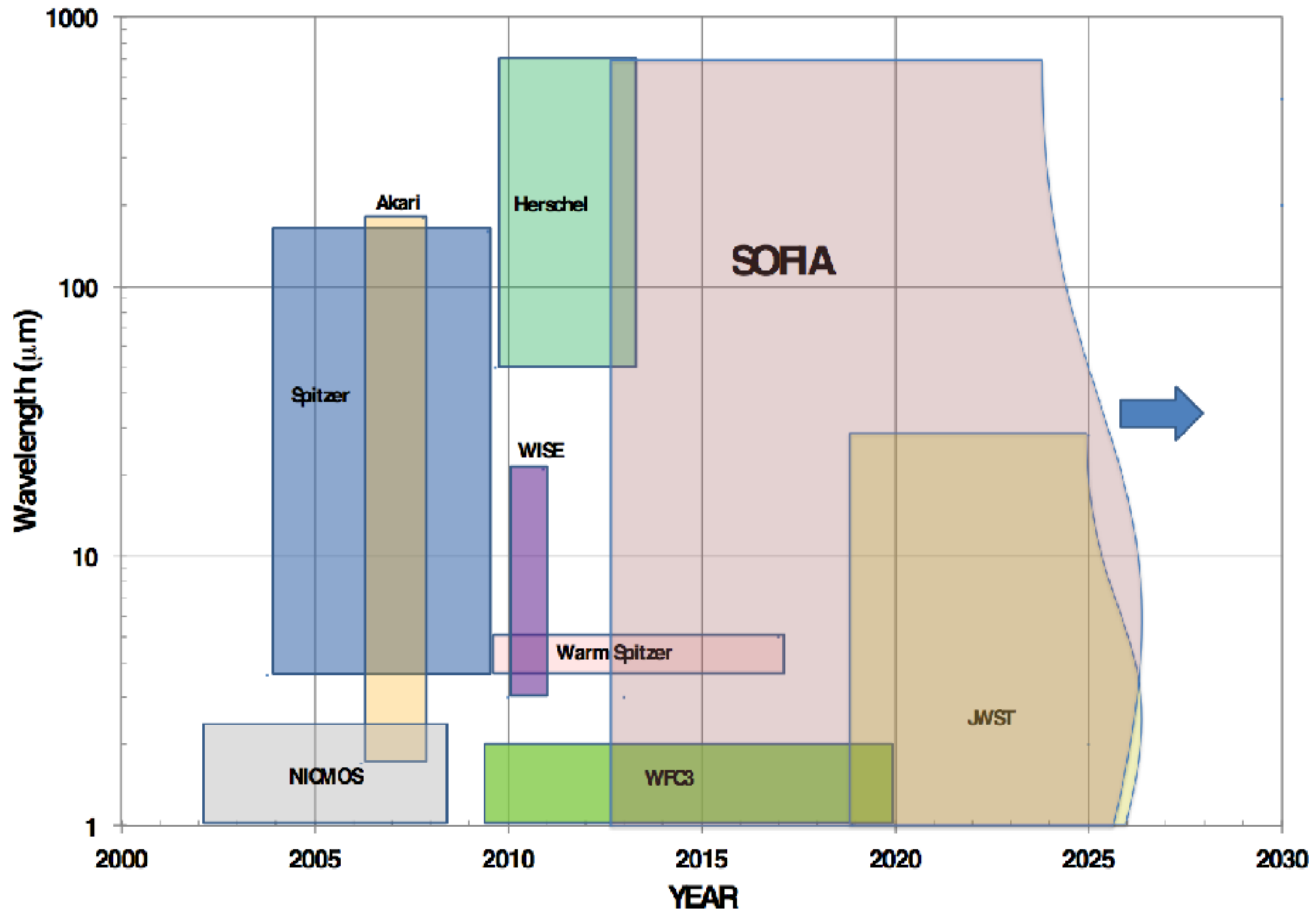


Wide Field Infrared Survey Explorer (WISE)

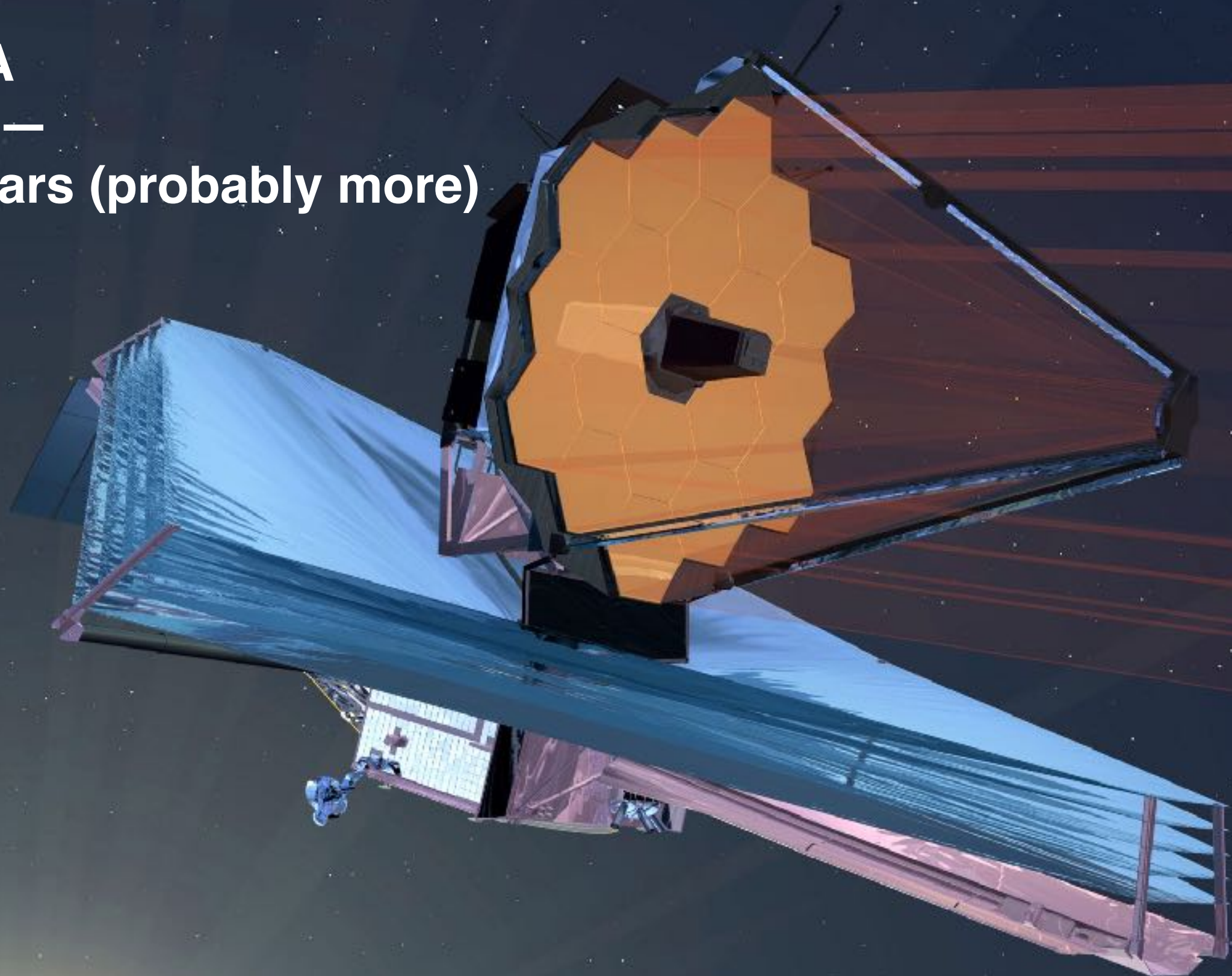


- 2009–2011
- 40cm cold telescope
- 3.4, 4.5, 12, 22 μm



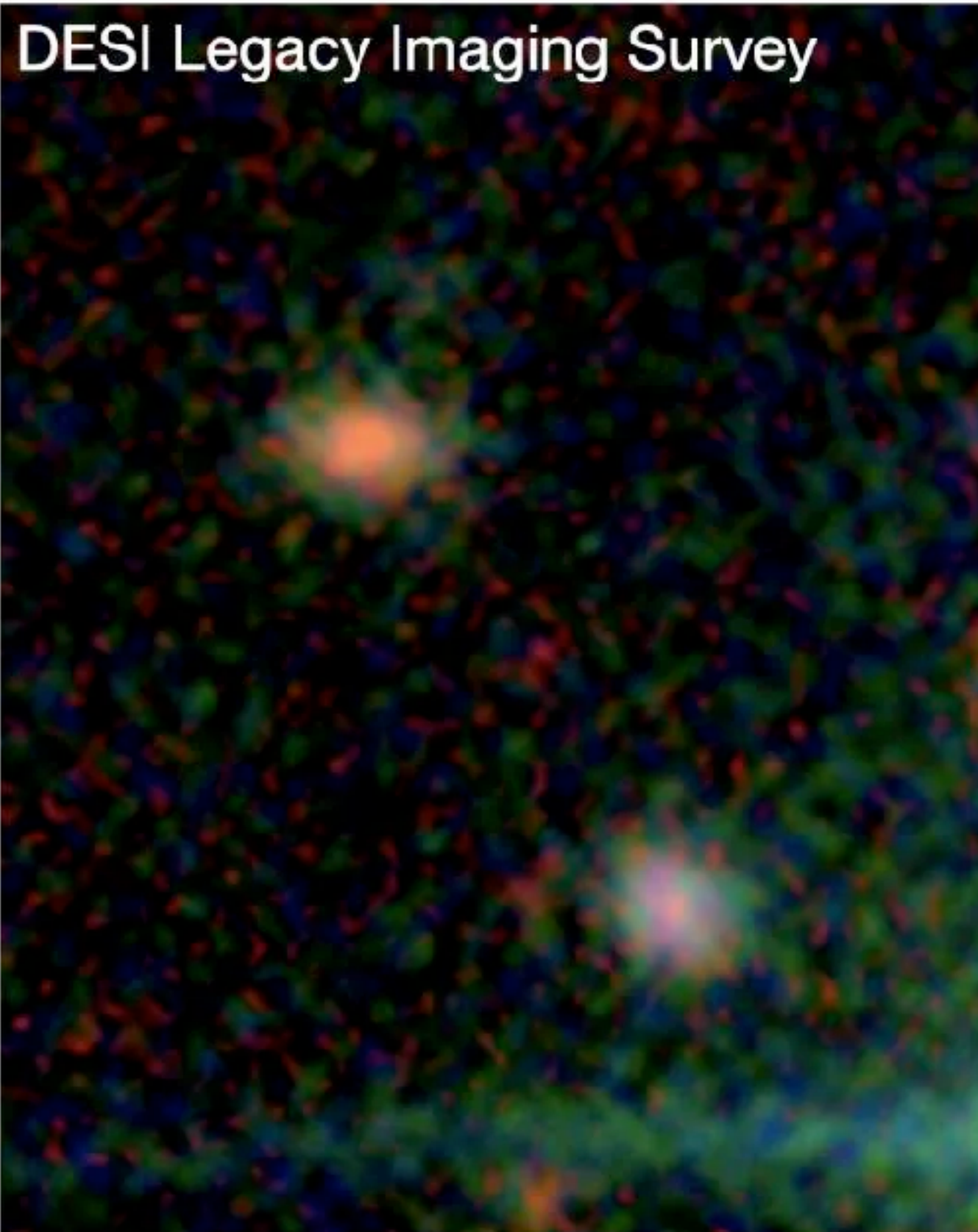


JWST
NASA
2021 –
10 years (probably more)

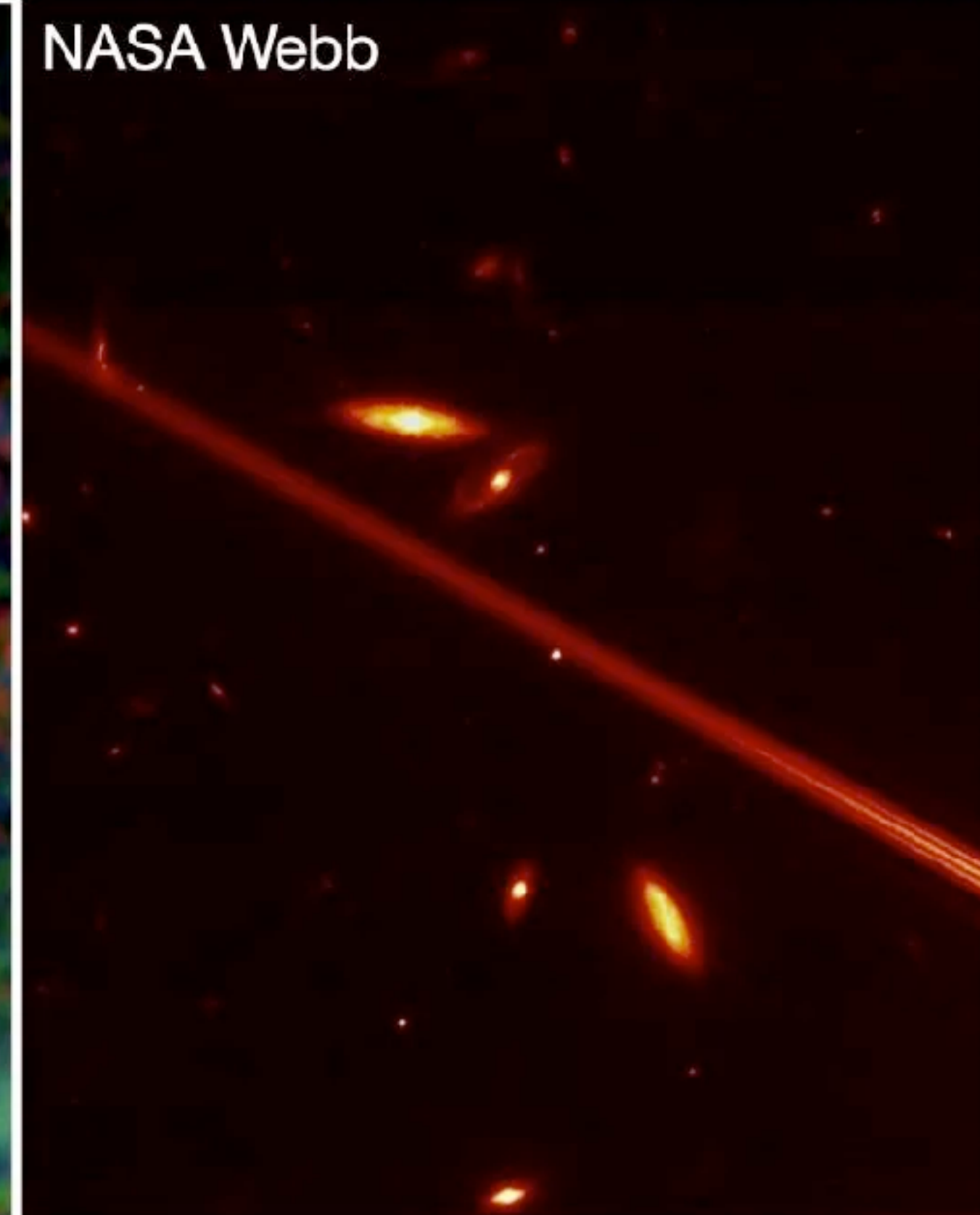


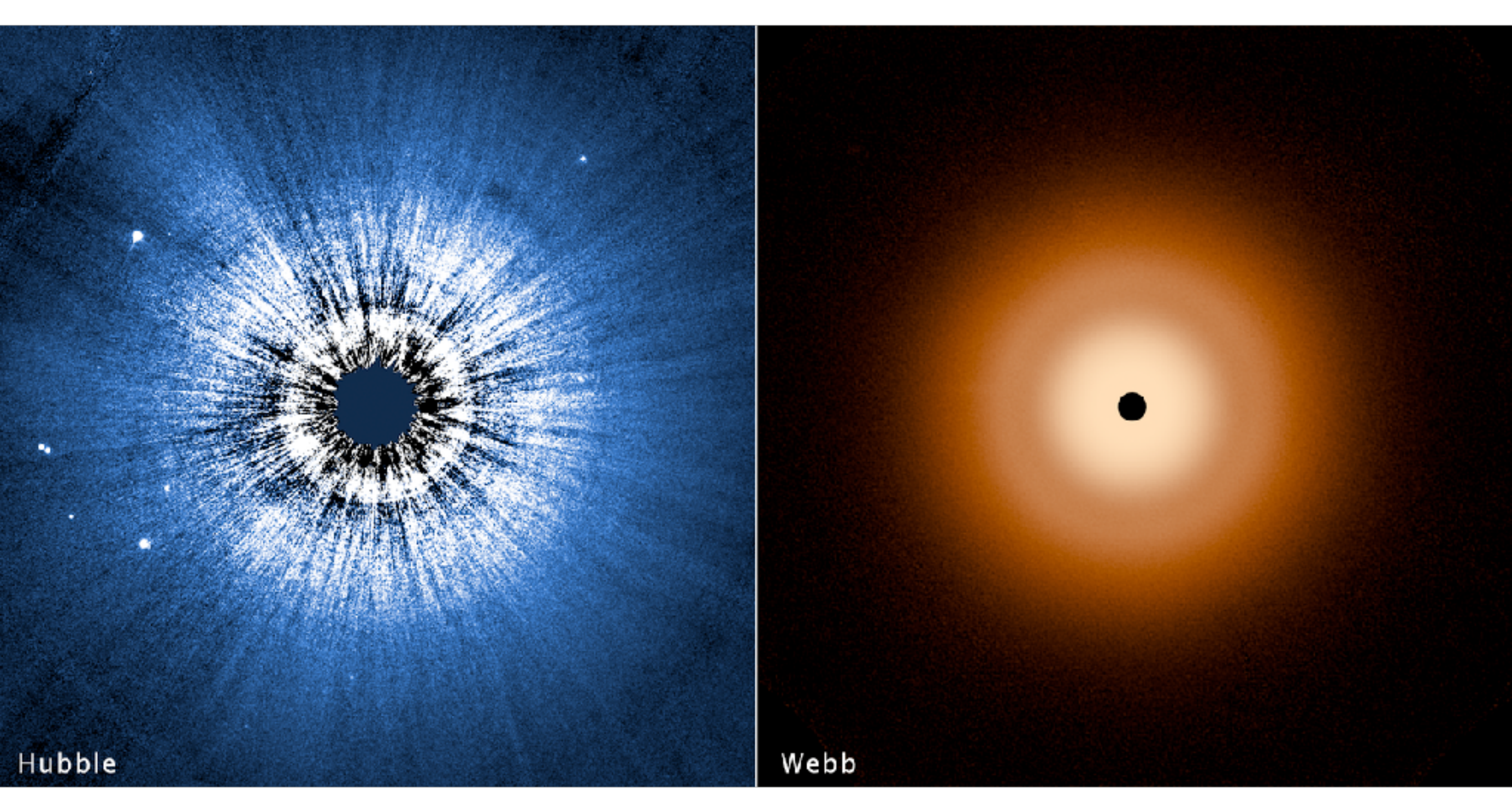
NIRCam
NIRSpec
MIRI

DESI Legacy Imaging Survey



NASA Webb





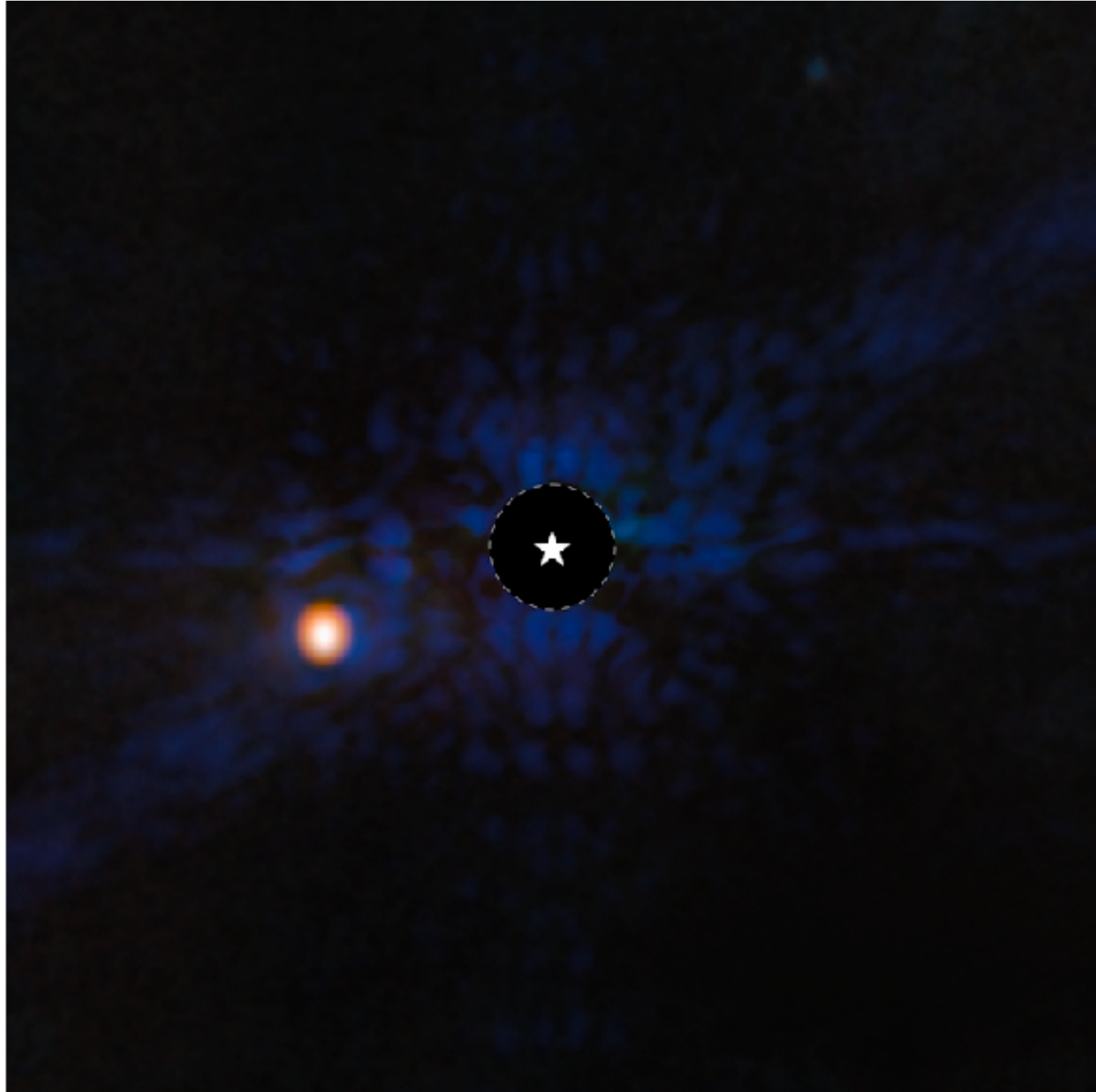
Hubble

[left]

A Hubble Space Telescope false-color view of a 100-billion-mile-wide disk of dust around the summer star Vega. Hubble detects reflected light from dust that is the size of smoke particles largely in a halo on the periphery of the disk. The disk is very smooth, with no evidence of embedded large planets. The black spot at the center blocks out the bright glow of the hot young star.

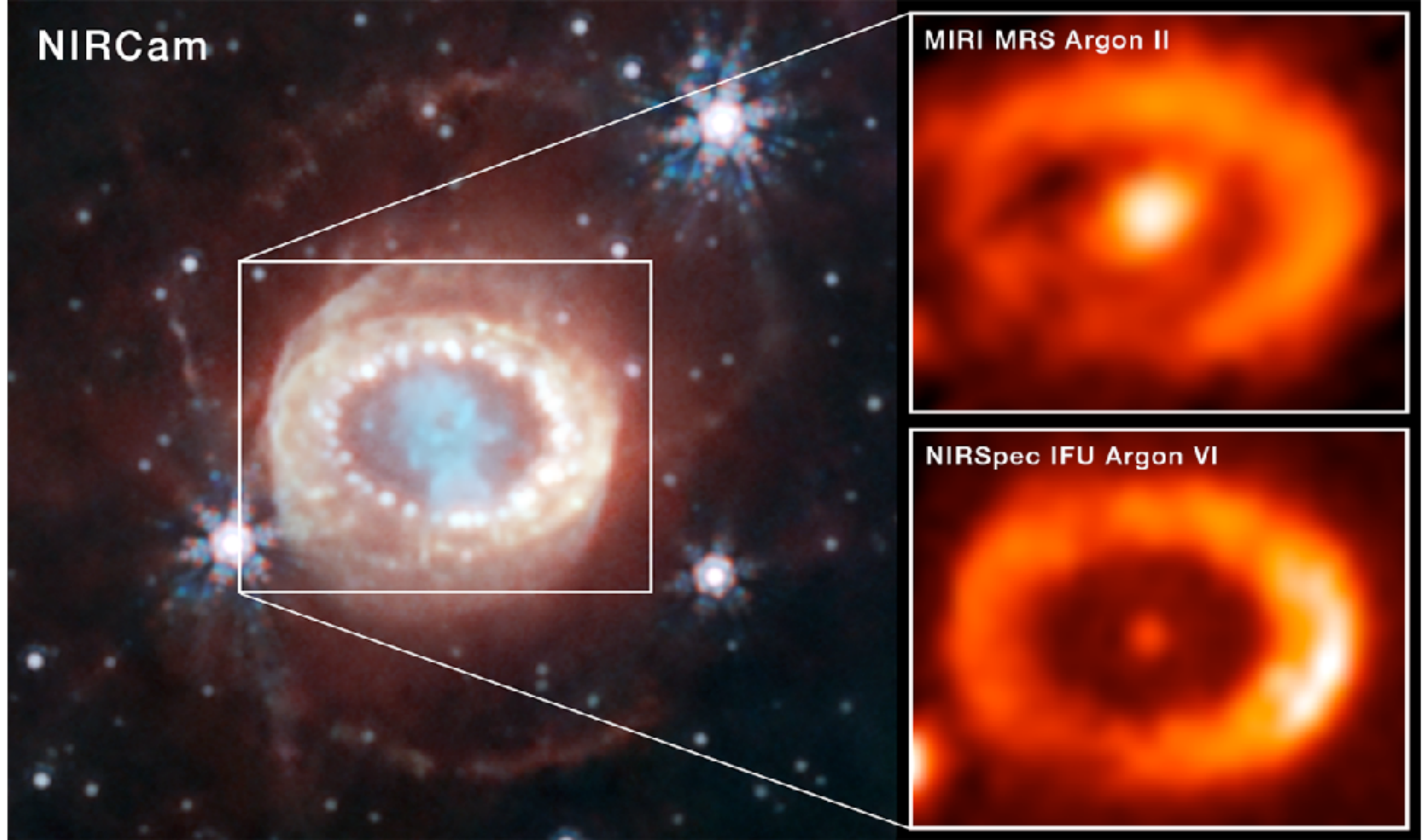
[right]

The James Webb Space Telescope resolves the glow of warm dust in a disk halo, at 23 billion miles out. The outer disk (analogous to the solar system's Kuiper Belt) extends from 7 billion miles to 15 billion miles. The inner disk extends from the inner edge of the outer disk down to close proximity to the star. There is a notable dip in surface brightness of the inner disk from approximately 3.7 to 7.2 billion miles. The black spot at the center is due to lack of data from saturation.



gas-giant exoplanet Epsilon Indi Ab with the MIRI coronagraph

NIRCam



MIRI MRS Argon II

NIRSpec IFU Argon VI



In Hubble's image, the star-filled spiral arms glow brightly in blue, and the galaxies' cores in orange. Both galaxies are covered in dark brown dust lanes, which obscures the view of IC 2163's core at left.

In Webb's image, cold dust takes center stage, casting the galaxies' arms in white. Areas where stars are still deeply embedded in the dust appear pink.

HUBBLE AND WEBB SPACE TELESCOPES

SPIRAL GALAXIES | IC 2163 + NGC 2207



16,500 LIGHT-YEARS

0.5 ARCMIN



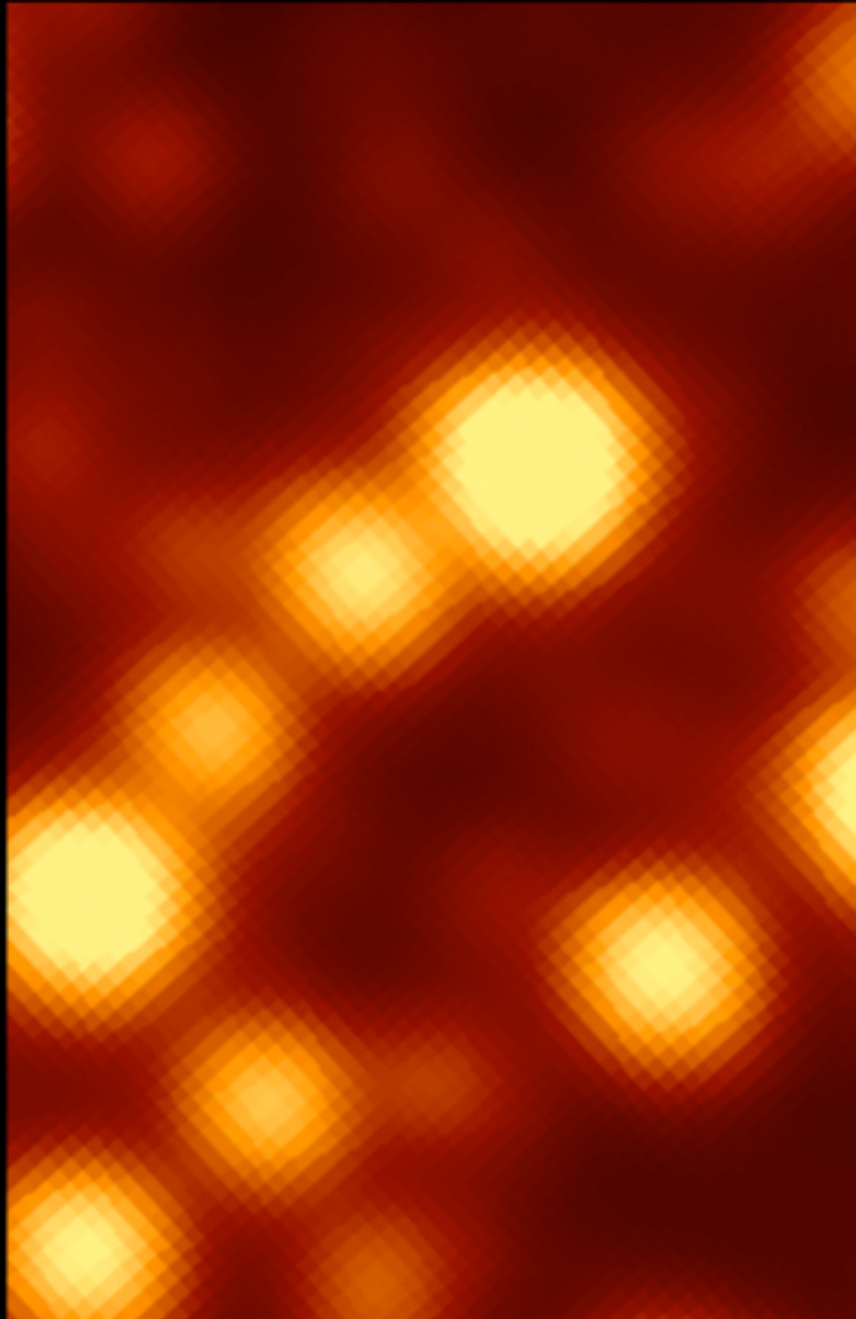
Hubble WFC3 Filters

F430W F566W F814W

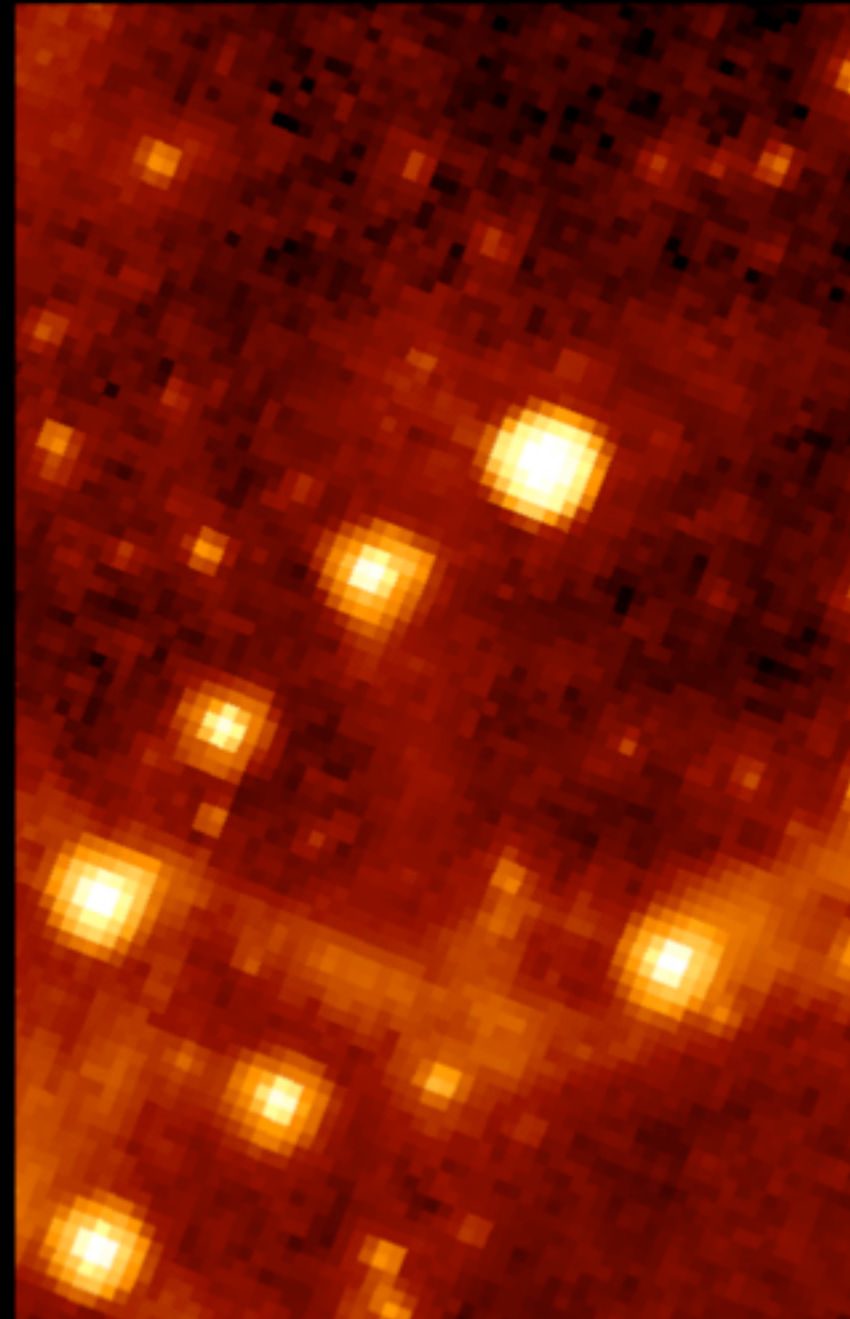
Webb MIRI Filters

F770W F1130W F1500W

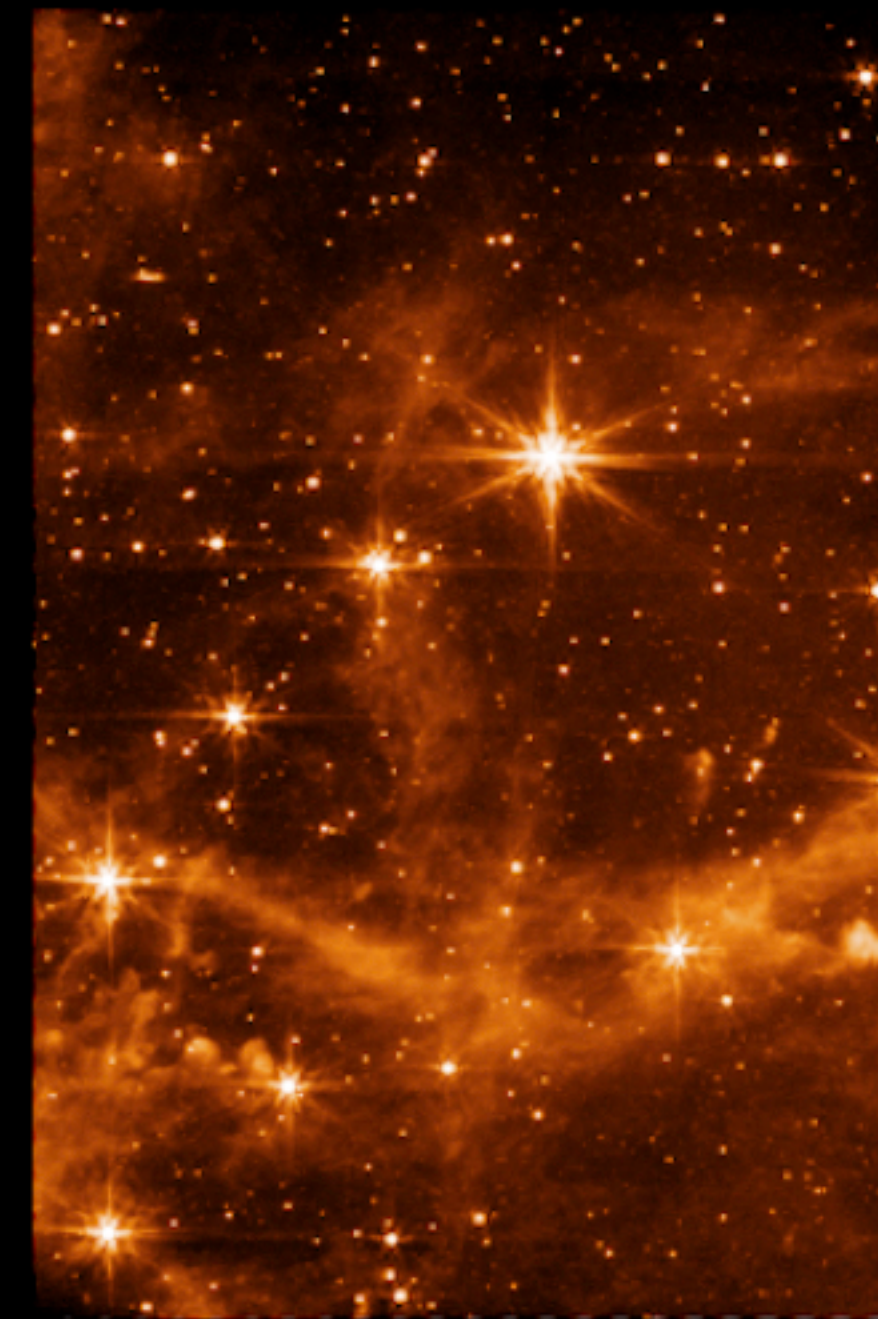
The Evolution of Infrared Space Telescopes



WISE W2 4.6 μm

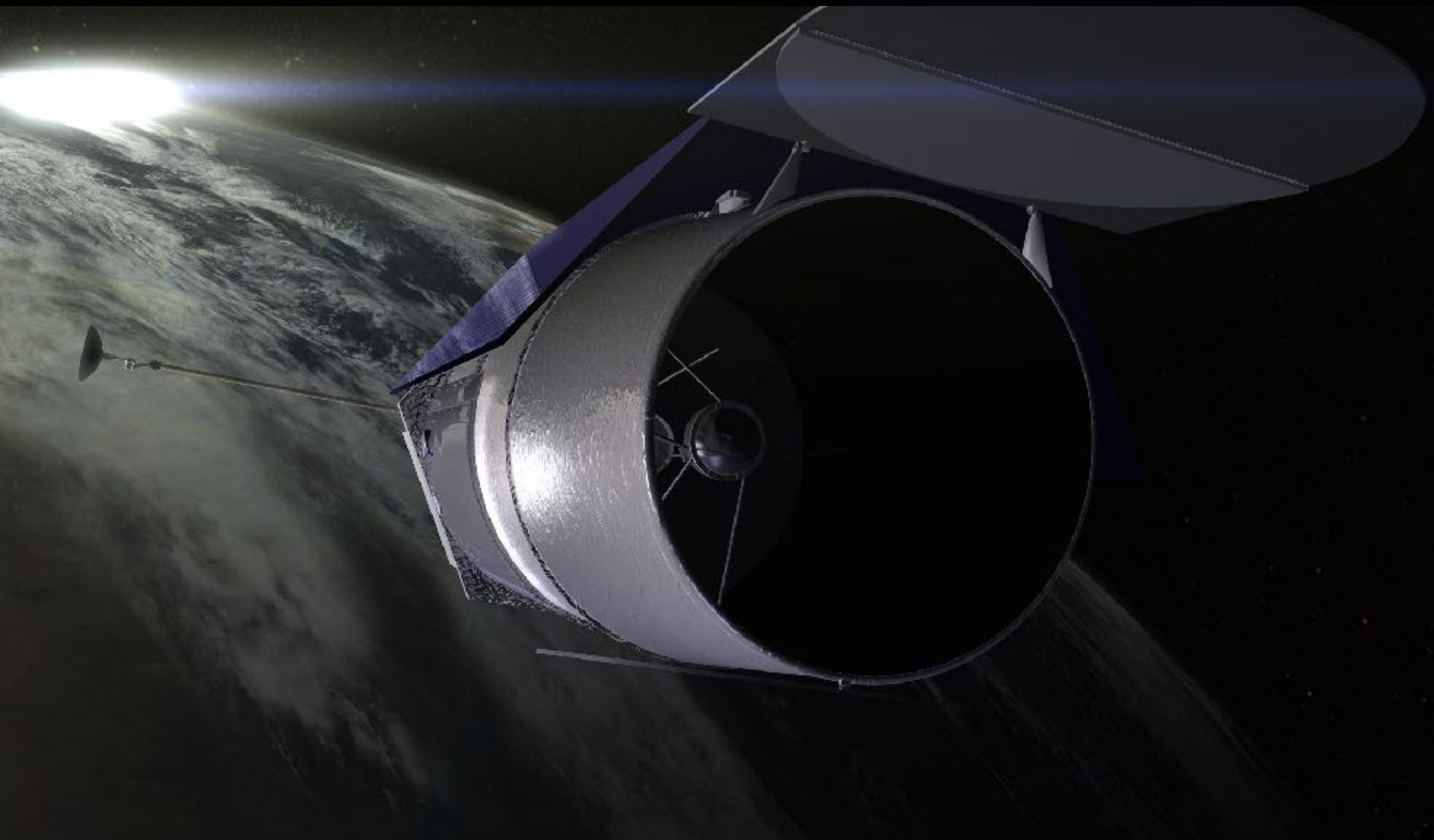


Spitzer/IRAC 8.6 μm



JWST/MIRI 7.7 μm

Nancy Grace Roman Space Telescope



Launch window opens in Late 2026 - but probably 2027

Roman WFI
Field of View



HST Field of View

- WFC3/IR
- WFC3/UVIS

JWST Field of View

- NIRCam
- MIRI

Background Sky:

Digitized Sky Survey and R. Gendler

Moon:

NASA/GSFC/ASU/Lunar Reconnaissance Orbiter



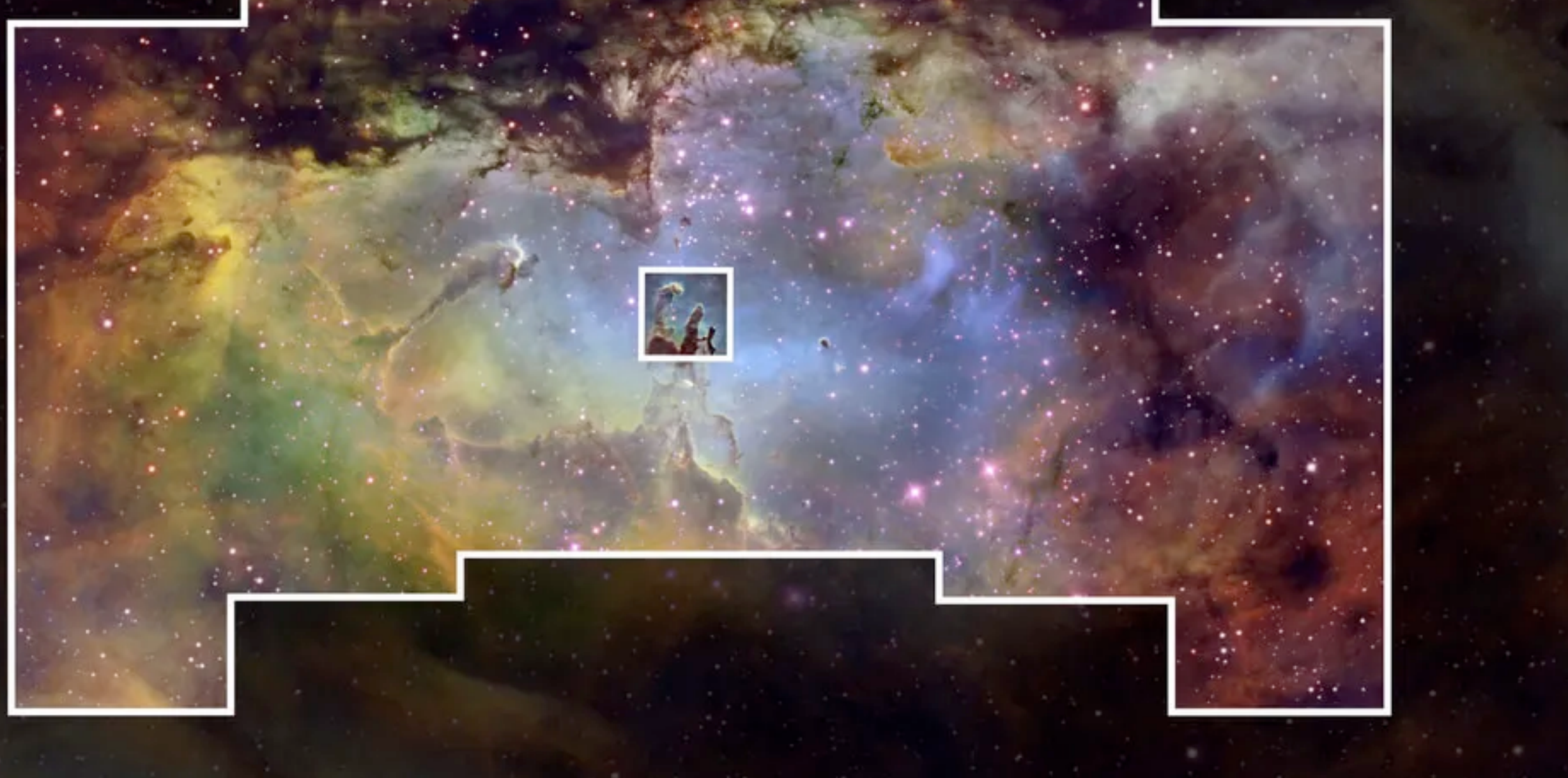
Moon to scale



20,000 light-years

6,200 parsecs

27'



Telescope	year	diameter [m]	temperature [K]	wavelength [um]	LHe [l]
IRAS	1983	0.51	2	12–100	720
ISO	1995—1998	0.6	3.4	2.4—240	2268
Spitzer	2003—2009	0.85	5.5	3.4—160	337
WIRE	1999—X	0.3	12	9—27	
Akari	2006—2011	0.68	5.5	2.5—160	2300
WISE	2009—2010	0.4	12	3.4—22	
Herschel	2009—2013	3.5	70	60—500	2400
Planck	2009—2013	1.5	56	350—3000	36,000
JWST	2021—2031	6.5	50	1—30	—
OST	2035 ??	9.2	4	30—500	—

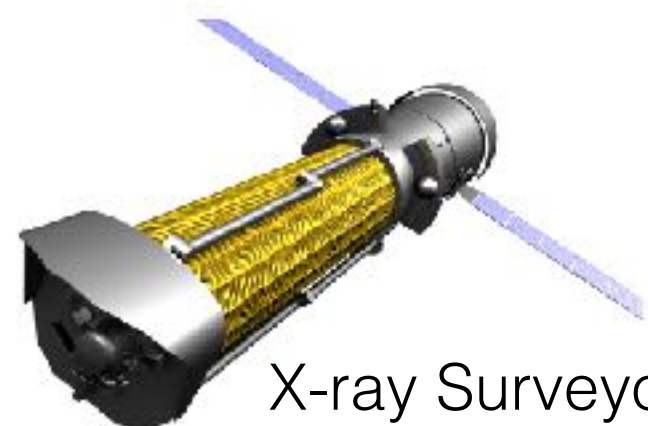
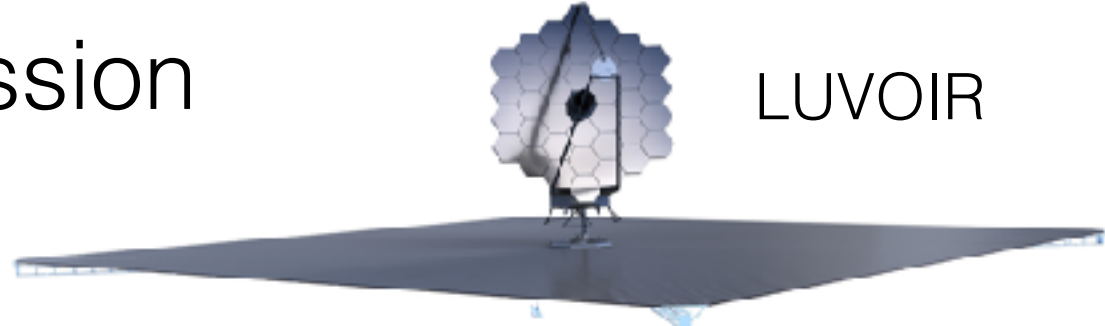
Planning for the next big NASA mission



LUVOIR

Four large mission concept studies studies were proposed for the last decadal review, but ultimately, the decadal didn't recommend any - they recommended a new hybrid approach.

- **Large ultraviolet, optical and infrared (LUVOIR) telescope. Über Hubble. 8-15m active surface mirror.**
- Origins Space Telescope (OST) aka FIR Surveyor. Über Spitzer. Cold 8-12m mirror.
- X-ray Surveyor. Über Chandra.
- **The habitable exoplanet imaging mission (HabEx).**



X-ray Surveyor



HabEx

NEW TECHNOLOGIES ENABLE NEW CAPABILITIES TO EXPLORE OUR COSMIC ORIGINS

New Technology

Space

Cold Mirror

Large Telescope

Large Detector Arrays

Integrated Spectrometers

New Capability

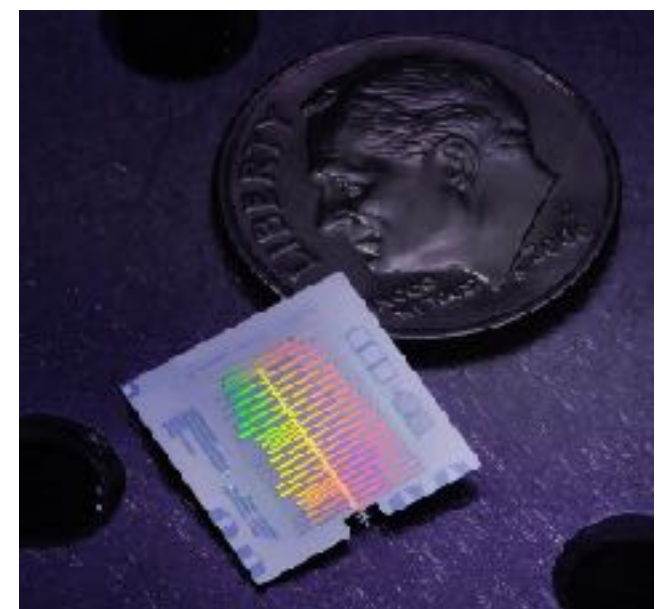
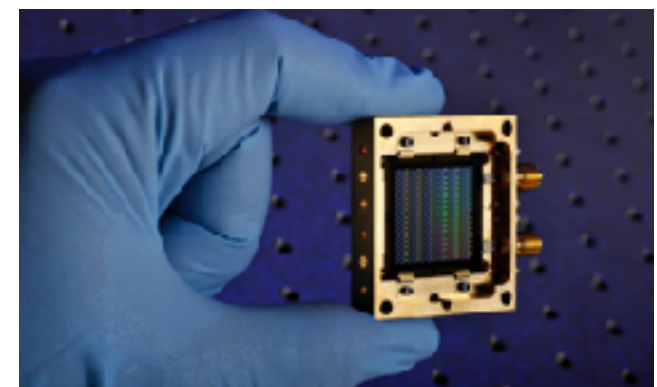
Wavelength coverage
JWST<—>ALMA

Spectroscopic line
sensitivity

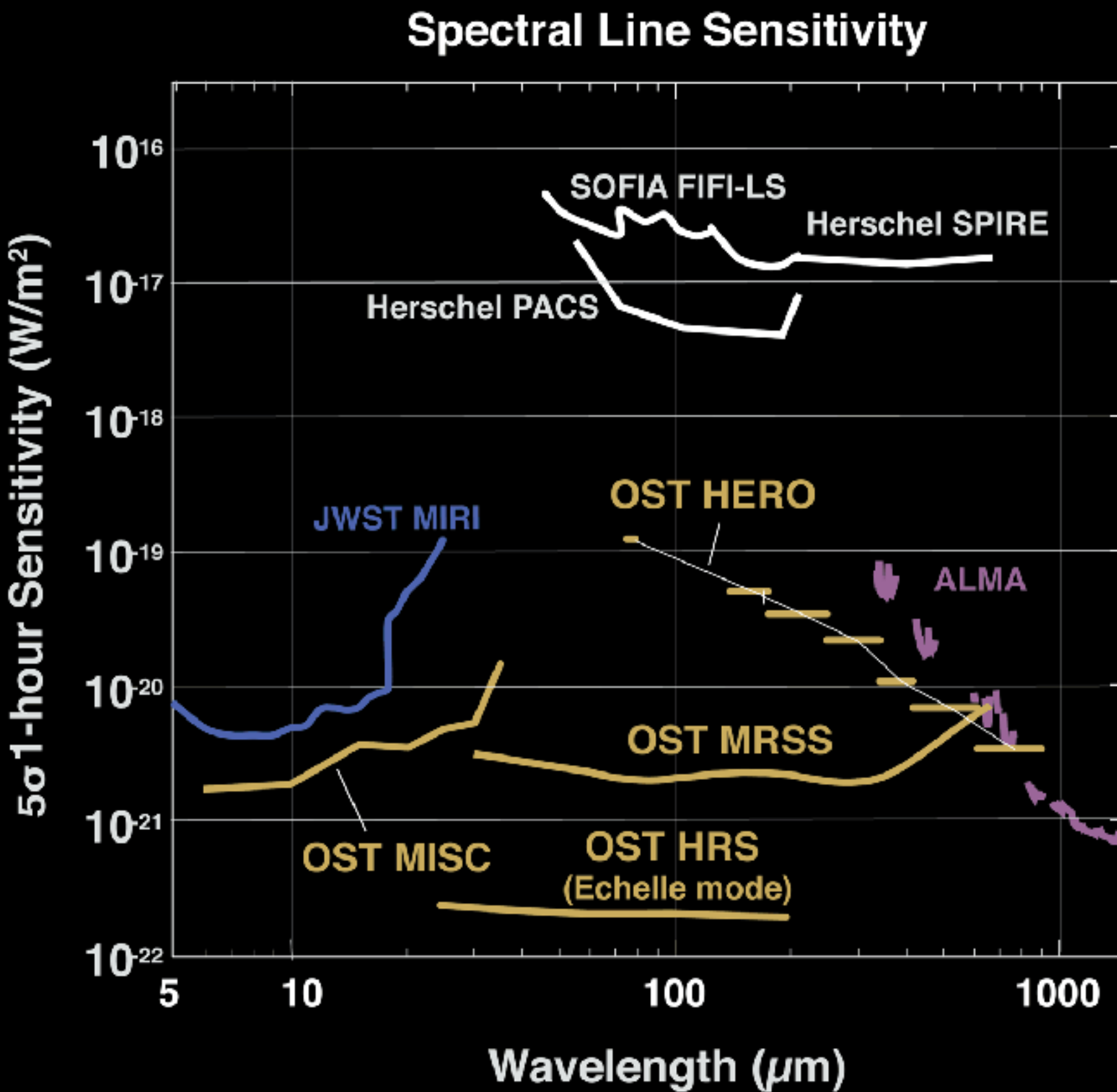
Spatial resolution and
sensitivity

Wide field imaging

3D mapping



OST Spectral Line Sensitivity



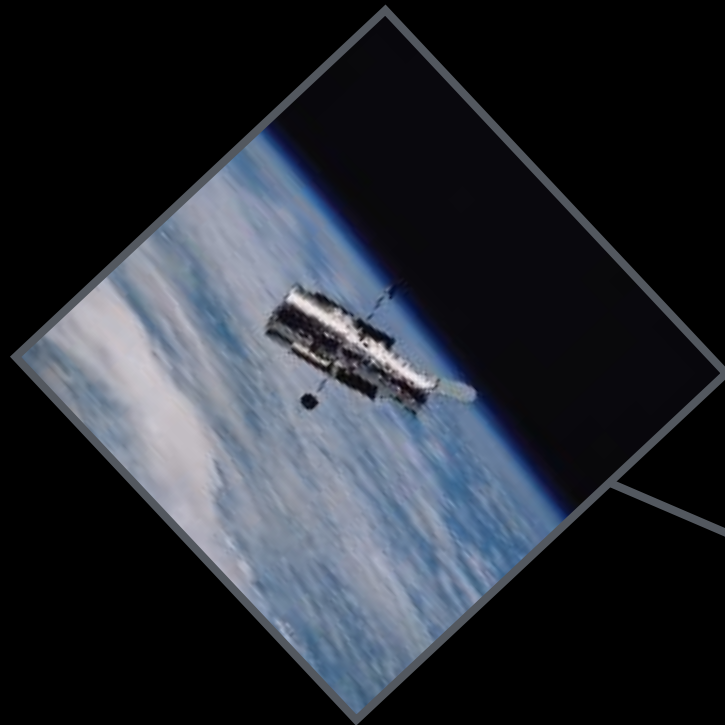
Hubble Space Telescope

1990–2018

2.4 meter

0.1–2.4 μm

260 K



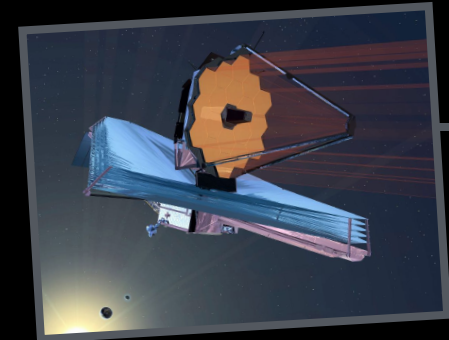
James Webb Space Telescope

2021–2031 (nominal)

6.5 meter

0.6–29 μm

50 K



Origins Space Telescope

2035–2045

~9 meter

5–660 μm

4 K

